



!!! Neurolutions
IpsiHand
Brain-Computer Interface System

Physician Information

INDICATION FOR USE

The Neurolutions Upper Extremity Rehabilitation System is indicated for use in chronic stroke patients (\geq 6 months post stroke) age 18 or older undergoing stroke rehabilitation, to facilitate muscle re-education and for maintaining or increasing range of motion in the upper extremity.

- Intended Use Environment: The Neurolutions System is designed for use in clinic or home settings as part of prescribed therapy.

CONTRAINDICATIONS

The Neurolutions System is contraindicated for use in patients having any of the following conditions:

- Severe spasticity or rigid contractures in the wrist and/or digits that would prevent the Neurolutions Handpiece from being properly fit or positioned for use.
- Skull defects due to craniotomy or craniectomy.

(1) QRS-008, QRS-012, & QRS-013; (2) Bundy DT, Souders L, Baranyai K, Leonard L, Schalk G, Coker R, Moran DW, Huskey T, Leuthardt EC. Contralesional Brain-Computer Interface Control of a Powered Exoskeleton for Motor Recovery in Chronic Stroke Survivors. *Stroke*. 2017 Jul;48(7):1908-1915. doi: 10.1161/STROKEAHA.116.016304. Epub 2017 May 26. PMID: 28550098; PMCID: PMC5482564. Contralesional Brain-Computer Interface Control of a Powered Exoskeleton for Motor Recovery in Chronic Stroke Survivors; (3) TSP-001, TSP-002, TSP-008, User Manual LBL-001(P), MKT-0003

Neuroolutions

IpsiHand

Brain-Computer Interface System



Accelerating Motor Recovery Using The Power of The Mind



**Clinically Meaningful
Improvement That Lasts¹**



**Empower Patients at All
Levels of Motor Severity²**



**Designed for Simple Set-Up
and Seamless Integration³**



**Digital Analytics &
Remote Monitoring**

INDICATION FOR USE

The Neuroolutions Upper Extremity Rehabilitation System is indicated for use in chronic stroke patients (≥ 6 months post stroke) age 18 or older undergoing stroke rehabilitation, to facilitate muscle re-education and for maintaining or increasing range of motion in the upper extremity.

- Intended Use Environment: The Neuroolutions System is designed for use in clinic or home settings as part of prescribed therapy.

CONTRAINDICATIONS

The Neuroolutions System is contraindicated for use in patients having any of the following conditions:

- Severe spasticity or rigid contractures in the wrist and/or digits that would prevent the Neuroolutions Handpiece from being properly fit or positioned for use.
- Skull defects due to craniotomy or craniectomy.

(1) QRS-008, QRS-012, & QRS-013; (2) Bundy DT, Souders L, Baranyai K, Leonard L, Schalk G, Coker R, Moran DW, Huskey T, Leuthardt EC. Contralesional Brain-Computer Interface Control of a Powered Exoskeleton for Motor Recovery in Chronic Stroke Survivors. Stroke. 2017 Jul;48(7):1908-1915. doi: 10.1161/STROKEAHA.116.016304. Epub 2017 May 26. PMID: 28550098; PMCID: PMC5482564. Contralesional Brain-Computer Interface Control of a Powered Exoskeleton for Motor Recovery in Chronic Stroke Survivors; (3) TSP-001, TSP-002, TSP-008, User Manual LBL-001(P), MKT-0003

Neuroolutions

CLINICAL@NEUOLUTIONS.COM | NEUOLUTIONS.COM

The IpsiHand Upper Extremity Rehabilitation System

uses a breakthrough **Brain Computer Interface** to detect neural activity in the unaffected cortical hemisphere.



HANDPIECE

Powered by the user's thoughts, the wireless neurobotic Handpiece moves the hand open and closed.



HEADSET

The non-invasive EEG Headset measures electrical signals from the uninjured brain hemisphere capturing the user's "intention to move" the impaired hand.

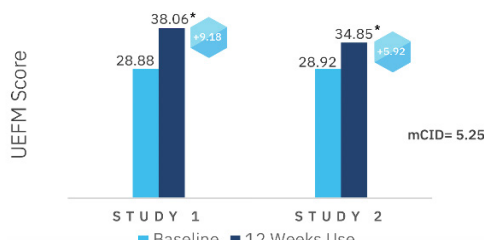


TABLET

The Tablet provides wireless interface between the Headset and Handpiece to guide the user through a therapy session.



Significant UEFM Increase from Baseline to 12 Weeks Use



Enhanced Clinical Outcomes:

- + All patients experienced improvement on the primary study outcome measures¹
- + 66.7% measured statistically and clinically meaningful improvement (mCID)²
- + All patients who met mCID maintained improvement for at least 6 months post-therapy³

System Components

- Neuroolutions Handpiece - ASY-1001
- AC/DC power supply - PRT-0032
- Mirror- To view placement of the headset on the head - PRT-0040
- Tape Measure- To assist Headset head placement - PRT-0039
- Headset - PRT-0224
- Cleaning Brush- To clean the EEG Headset's electrodes - PRT-0042
- Cleaning Solution Container for Headset electrode cleaning solution - PRT-0041
- Battery Wall Charger - PRT-0037
- Sensory Key- To aid in working sensor electrodes through the hair - PRT-0052
- Extra Battery - PRT-0038
- Tablet - ASY-0013
- AC/DC power supply - PRT-003

Note: A typical facility order includes both a right and left system.



IMPORTANT SAFETY INFORMATION

- System components contain lithium-ion batteries that MUST NOT be exposed to flame, excessive heat, or incinerated; personal injury may occur.
- Only use the Charging Adapters provided with the Neuroolutions System to recharge system components and avoid risk of shock.
- Use of the Neuroolutions System adjacent to or stacked with other equipment should be avoided because it could result in improper operation. If such use is necessary, the Neuroolutions System and the other equipment should be observed to verify that they are operating normally.
- Portable RF communications equipment (including peripherals such as antenna cables and external antennas) should be used no closer than 30 cm (12 inches) to any part of the Neuroolutions System. Otherwise, degradation of the performance of the Neuroolutions System could result.
- The Neuroolutions Handpiece enclosure may reach a maximum temperature up to 43°C during use. To reduce the risk of discomfort, you should remove the Handpiece from your hand if the device feels warm on your skin.
- Tight straps on the Handpiece may restrict your circulation. Therefore, always check that the straps are not too tight throughout your range of motion to ensure proper circulation during use.
- The Neuroolutions System should only be used on intact skin, and the System should be cleaned and disinfected regularly to minimize possible contamination and risk of infection.

* Denotes Statistical Significance; Study 1: QRS-0012; Study 2: QRS-0013; (1) QRS-008, QRS-012, & QRS-013; (2) QRS-008; (3) QRS-012 and QRS-013, pooled results



FDA Device Indication:

The Neurolutions IpsiHand Upper Extremity Rehabilitation System is indicated for use in chronic stroke patients (≥ 6 months post-stroke) age 18 or older undergoing stroke rehabilitation, to facilitate muscle re-education and for maintaining or increasing range of motion in the upper extremity.

PATIENT INFORMATION

FIRST NAME _____ LAST NAME _____

ADDRESS _____ CITY _____

STATE _____ ZIP _____

ICD-10 CODE _____ BIRTHDATE ____/____/____
MM DD YYYY

HEALTH CARE PRACTITIONER

FIRST NAME _____ LAST NAME _____

NPI NUMBER _____ EMAIL _____
NATIONAL PROVIDER IDENTIFIER 10-DIGIT NUMBER

ADDRESS _____ CITY _____

STATE _____ ZIP _____ PHONE _____

APPEAL STATUS Submitted to Insurance Will Submit to Insurance N/A

PRESCRIPTION ITEM

IpsiHand Upper Extremity Rehabilitation System

LEFT OR RIGHT SIDE

Left

Right

DATE

____/____/____
MM DD YYYY

HCP SIGNATURE

Medical Necessity and Clinical Efficacy

FDA Designation:

- **Exclusive FDA Market Authorization:** IpsiHand stands alone as the first and only non-invasive brain-computer interface (BCI) therapy to obtain FDA market authorization. It is important to highlight that **there are no comparable therapeutic alternatives** in the market for its specific indication.
-

Clinical Efficacy and Safety:

- **Superior UEFM Outcomes:** The device remarkably outperforms standard care, achieving an average improvement of **7.7 UEFM points** over 12 weeks. The minimal clinically important difference (MCID) for UEFM is +5.25, indicating significant clinical benefit.
 - **Durable and Retained Gains:** Functional improvements extend to the hand, wrist, and arm, and are retained post-therapy, signifying durable, long-term benefits.
 - **Zero Adverse Events:** Clinical studies report **no patient injury or adverse events**, solidifying its safety profile.
-

Mechanism of Action and Neuroplasticity

- **Proprietary Prosthetic Motor Circuit:** IpsiHand employs a unique prosthetic motor circuit, corroborated by functional MRI and electrophysiological studies, that effectively remodels the brain.
 - **Reset in Phase Amplitude Coupling:** The therapy induces significant changes in phase amplitude coupling between theta and gamma rhythms, directly correlating with motor recovery.
-

Patient Population and Home-Based Therapy

- **Addresses Underserved Population:** Indicated for **chronic stroke patients (≥ 6 months post-stroke) aged 18 or older**, it serves an often-neglected demographic with limited therapeutic options.
 - **Self-Administered Home Therapy:** IpsiHand offers the convenience of self-administered, home-based therapy, requiring just one-hour modules five days per week.
-

Summary of Clinical Performance Testing

The Neuroolutions System has been evaluated in 40 subjects across three separate clinical studies (described below), all of which evaluated use of the Neuroolutions system in chronic stroke survivors. All three studies were designed to determine the feasibility of recording electroencephalogram (EEG) signals from the affected and/or unaffected brain hemispheres, and to use the signals to control a computer to facilitate movement of a robotic hand orthosis (Handpiece). The results of the studies have been analyzed to determine if the Neuroolutions System can be used to positively impact rehabilitation. These three studies were open-label studies whereby a literature meta-analysis assessing usual care as well as minimal clinically important difference (MCID) benchmarks were utilized for comparison of device effectiveness in lieu of randomized control data.

Results of testing demonstrate that following 12-weeks of use of the Neuroolutions System, chronic stroke survivors showed increases in the mean change from their baseline scores on the primary outcome measure for the three respective studies. Ten of the total 40 subjects were assessed utilizing the Action Research Arm Test (ARAT) as the primary outcome measure and the mean scores exceeded the Minimal Clinically Important Difference (MCID) of 5.7 points (study QRS-0008). In the two other studies (QRS-0012 and QRS-0013), 30 of the total 40 subjects were assessed utilizing the Fugl-Meyer Upper Extremity (UEFM) assessment as the primary outcome measure. For 66.7% of these 30 subjects, mean scores exceeded the MCID of 5.25 points. Overall, ARAT data were collected on a total of 27 subjects from QRS-0008 and QRS-0012 (ARAT was a secondary measure in QRS-0012), while UEFM data were collected in 30 subjects from studies QRS-0012 and QRS-0013. The 17 subjects assessed with ARAT as a secondary measure in QRS-0012, while demonstrating some mean improvement, did not exceed MCID. No patient injury or adverse events occurred in any of the studies.

Results of Pooled Analysis: The results from 30 subjects across two studies (QRS-0012 and QRS-0013) may be validly pooled because the studies have the same primary endpoint and were conducted under nearly identical protocols (including inclusion/exclusion criteria and treatment regimen) and investigated the same version of the device in a very similar patient population (as evidenced by a comparison of the demographic data). Moreover, the primary endpoint, change in UEFM, was compared at the same timepoint, and the studies were weighted relative to their size. Based on the foregoing, a pooled analysis for UEFM, including all 30 subjects from the two studies, resulted in a mean change at 12-weeks of 7.77 points (SD of 5.041, two-sided, one-sample t-test, p-value < .0001), which exceeds the Minimal Clinically Important difference (MCID) of +5.25 points reported in the literature.

Across the two pooled clinical studies (QRS-0012 and QRS-0013), 100% (30/30) of the subjects demonstrated improvement on the primary outcome measure, UEFM. A total of 66.7% of these subjects exceeded the *minimal clinical important difference* (MCID). The MCID is the change in a treatment outcome as measured by a trained clinician and regarded as important and clinically meaningful to health professionals and patients.^{[1],[2],[3],[4]} The remaining 33.3% of the subjects, although demonstrating improvement, did not achieve the MCID.

For a cohort of 12 patients who participated in (QRS-0012), durability data was assessed at 6-months following completion of their 12-week study visit. Durability assessment of the primary and secondary outcome measures revealed these subjects maintained their level of improved functional and motor performance. This demonstrates that the motor improvements achieved with the Neuroolutions System therapy were maintained at 6-months following the last device use. However, as durability testing has not

been completed beyond 6-months, persistence of benefits beyond 6-months post device use are currently unknown.

^[1] Page, S. J., Fulk, G. D., & Boyne, P. (2012). Clinically important differences for the upper-extremity Fugl-Meyer Scale in people with minimal to moderate impairment due to chronic stroke. *Physical therapy*, 92(6), 791–798. <https://doi.org/10.2522/ptj.20110009>

^[2] Bushnell, C., Bettger, J. P., Cockroft, K. M., Cramer, S. C., Edelen, M. O., Hanley, D., Katzan, I. L., Mattke, S., Nilsen, D. M., Piquado, T., Skidmore, E. R., Wing, K., & Yenokyan, G. (2015). Chronic Stroke Outcome Measures for Motor Function Intervention Trials: Expert Panel Recommendations. *Circulation. Cardiovascular quality and outcomes* 8(6 Suppl 3), S163–S169. <https://doi.org/10.1161/CIRCOUTCOMES.115.002098>

^[3] Fugl-Meyer Assessment of Motor Recovery after Stroke. (2016, August 2). Shirley Ryan Ability Lab. <https://www.sralab.org/rehabilitation-measures/fugl-meyer-assessment-motor-recovery-after-stroke>

^[4] Teasell R, Cotoi A, Chow J, Wiener J, Iliescu A, Hussein N, Salter K. *The Stroke Rehabilitation Evidence-Based Review: 18th edition*. Canadian Stroke Network, March 2018. Chapter 20. Page 21 www.ebrsr.com

FDA NEWS RELEASE

FDA Authorizes Marketing of Device to Facilitate Muscle Rehabilitation in Stroke Patients

For Immediate Release:

April 23, 2021

Today, the U.S. Food and Drug Administration authorized marketing of a new device indicated for use in patients 18 and older undergoing stroke rehabilitation to facilitate muscle re-education and for maintaining or increasing range of motion. The Neuroolutions IpsiHand Upper Extremity Rehabilitation System (IpsiHand System) is a Brain-Computer-Interface (BCI) device that assists in rehabilitation for stroke patients with upper extremity—or hand, wrist and arm—disability.

“Thousands of stroke survivors require rehabilitation each year. Today’s authorization offers certain chronic stroke patients undergoing stroke rehabilitation an additional treatment option to help them move their hands and arms again and fills an unmet need for patients who may not have access to home-based stroke rehabilitation technologies,” said Christopher M. Loftus, M.D., acting director of the Office of Neurological and Physical Medicine Devices in the FDA’s Center for Devices and Radiological Health.

A stroke occurs when normal blood flow to the brain is interrupted. Brain cells obtain oxygen and nutrients from regular blood circulation, so when there is a blockage of blood flow to the brain caused by a clot (an ischemic stroke) or excessive bleeding in the brain due to a ruptured blood vessel (a hemorrhagic stroke), the brain cells can die from a lack of blood and oxygen. Although stroke is a brain disease, it can affect the entire body and sometimes causes long-term disability such as complete paralysis of one side of the body (hemiplegia) or one-sided weakness (hemiparesis) of the body. Stroke survivors may have problems with the simplest of daily activities, including speaking, walking, dressing, eating and using the bathroom. According to the Centers for Disease Control and Prevention (<https://www.cdc.gov/stroke/facts.htm>), someone in the United States has a stroke every 40 seconds. About 795,000 people in the U.S. have a stroke each year.

Post-stroke rehabilitation helps individuals overcome disabilities that result from stroke damage. The IpsiHand System uses non-invasive electroencephalography (EEG) electrodes instead of using an implanted electrode or other invasive feature to record brain activity. The EEG data is then wirelessly conveyed to a tablet for analysis of the intended muscle movement

(intended motor function) and a signal is sent to a wireless electronic hand brace, which in turn moves the patient's hand. The device aims to help stroke patients improve grasping. The device is prescription-only and may be used as part of rehabilitation therapy.

The FDA assessed the safety and effectiveness of the IpsiHand System device through clinical data submitted by the company, including an unblinded study of 40 patients over a 12-week trial. All participants demonstrated motor function improvement with the device over the trial. Adverse events reported included minor fatigue and discomfort and temporary skin redness.

The IpsiHand System device should not be used by patients with severe spasticity or rigid contractures in the wrist and/or fingers that would prevent the electronic hand brace from being properly fit or positioned for use or those with skull defects due to craniotomy or craniectomy.

The IpsiHand System device was granted [Breakthrough Device \(/medical-devices/how-study-and-market-your-device/breakthrough-devices-program\)](#) designation, which is a process designed to expedite the development and review of devices that may provide for more effective treatment or diagnosis of life-threatening or irreversibly debilitating diseases or conditions.

The FDA reviewed the IpsiHand System device through the [De Novo \(/medical-devices/premarket-submissions-selecting-and-preparing-correct-submission/de-novo-classification-request\)](#) premarket review pathway, a regulatory pathway for low- to moderate-risk devices of a new type. Along with this authorization, the FDA is establishing special controls for devices of this type, including requirements related to labeling and performance testing. When met, the special controls, along with general controls, provide reasonable assurance of safety and effectiveness for devices of this type. This action creates a new regulatory classification, which means that subsequent devices of the same type with the same intended use may go through the FDA's 510(k) premarket process, whereby devices can obtain clearance by demonstrating substantial equivalence to a predicate device.

The FDA granted marketing authorization of the Neuroolutions IpsiHand Upper Extremity Rehabilitation System to Neuroolutions, Inc.

The FDA, an agency within the U.S. Department of Health and Human Services, protects the public health by assuring the safety, effectiveness, and security of human and veterinary drugs, vaccines and other biological products for human use, and medical devices. The agency also is responsible for the safety and security of our nation's food supply, cosmetics, dietary supplements, products that give off electronic radiation, and for regulating tobacco products.

Related Information

- [FDA: Breakthrough Devices Program \(/medical-devices/how-study-and-market-your-device/breakthrough-devices-program\)](/medical-devices/how-study-and-market-your-device/breakthrough-devices-program).
- [FDA: De Novo Classification Request \(/medical-devices/premarket-submissions-selecting-and-preparing-correct-submission/de-novo-classification-request\)](/medical-devices/premarket-submissions-selecting-and-preparing-correct-submission/de-novo-classification-request).
- [CDC: Stroke Facts \(https://www.cdc.gov/stroke/facts.htm\)](https://www.cdc.gov/stroke/facts.htm).
- [National Institute of Neurological Disorders and Stroke: Stroke Information Page \(https://www.ninds.nih.gov/Disorders/All-Disorders/Stroke-Information-Page\)](https://www.ninds.nih.gov/Disorders/All-Disorders/Stroke-Information-Page).

###

Inquiries

Media:

✉ [Shirley Simson \(mailto:Shirley.Simson@fda.hhs.gov\)](mailto:Shirley.Simson@fda.hhs.gov)

☎ 202-597-4230

Consumer:

☎ 888-INFO-FDA

🔗 [More Press Announcements \(/news-events/newsroom/press-announcements\)](/news-events/newsroom/press-announcements)



Motor Network Reorganization Induced in Chronic Stroke Patients with the Use of a Contralesionally-Controlled Brain Computer Interface

Joseph B. Humphries, Daniela J. S. Mattos, Jerrel Rutlin, Andy G. S. Daniel, Kathleen Rybczynski, Theresa Notestine, Joshua S. Shimony, Harold Burton, Alexandre Carter & Eric C. Leuthardt

To cite this article: Joseph B. Humphries, Daniela J. S. Mattos, Jerrel Rutlin, Andy G. S. Daniel, Kathleen Rybczynski, Theresa Notestine, Joshua S. Shimony, Harold Burton, Alexandre Carter & Eric C. Leuthardt (2022) Motor Network Reorganization Induced in Chronic Stroke Patients with the Use of a Contralesionally-Controlled Brain Computer Interface, *Brain-Computer Interfaces*, 9:3, 179-192, DOI: [10.1080/2326263X.2022.2057757](https://doi.org/10.1080/2326263X.2022.2057757)

To link to this article: <https://doi.org/10.1080/2326263X.2022.2057757>



© 2022 The Author(s). Published by Informa UK Limited, trading as Taylor & Francis Group.



[View supplementary material](#)



Published online: 01 Jul 2022.



[Submit your article to this journal](#)



Article views: 651



[View related articles](#)



[View Crossmark data](#)

Motor Network Reorganization Induced in Chronic Stroke Patients with the Use of a Contralesionally-Controlled Brain Computer Interface

Joseph B. Humphries^a, Daniela J. S. Mattos^b, Jerrel Rutlin^c, Andy G. S. Daniel^a, Kathleen Rybczynski^d, Theresa Notestine^d, Joshua S. Shimony^e, Harold Burton^e, Alexandre Carter^b and Eric C. Leuthardt^{a,d,e,f*}

^aDepartments of Neurosurgery, Washington University in St. Louis, St. Louis, MO, USA; ^bNeurology, Washington University in St. Louis, St. Louis, MO, USA; ^cMallinckrodt Institute of Radiology, Washington University in St. Louis, St. Louis, MO, USA; ^dNeurosurgery, Washington University in St. Louis, St. Louis, MO, USA; ^eNeuroscience, Washington University in St. Louis, St. Louis, MO, USA; ^fMechanical Engineering and Materials Science, Washington University in St. Louis, St. Louis, MO, USA

ABSTRACT

Upper extremity weakness in chronic stroke remains a problem not fully addressed by current therapies. Brain–computer interfaces (BCIs) engaging the unaffected hemisphere are a promising therapy that are entering clinical application, but the mechanism underlying recovery is not well understood. We used resting state functional MRI to assess the impact a contralesionally driven EEG BCI therapy had on motor system functional organization. Patients used a therapeutic BCI for 12 weeks at home. We acquired resting-state fMRI scans and motor function data before and after the therapy period. Changes in functional connectivity (FC) strength between motor network regions of interest (ROIs) and the topographic extent of FC to specific ROIs were analyzed. Most patients achieved clinically significant improvement. Motor FC strength and topographic extent decreased following BCI therapy. Motor recovery correlated with reductions in motor FC strength across the entire motor network. These findings suggest BCI-mediated interventions may reverse pathologic strengthening of dysfunctional network interactions.

ARTICLE HISTORY

Received 12 July 2021
Accepted 20 March 2022

KEYWORDS



Rehabilitation; stroke; brain–computer interface; functional MRI; motor network

1. Introduction


Stroke causes adult disability in approximately 800,000 adults annually in the United States [1]. Unilateral upper motor weakness, known as hemiparesis, occurs in 77% of new stroke cases [2]. Hemiparesis frequently persists into the chronic stage of stroke; 65% of chronic stroke patients report reduced motor function 6 months after stroke [3,4]. Patients rarely obtain substantial motor improvement 3 months after a stroke, with residual motor deficits effectively becoming permanent [5–11]. Behavioral adaptations instead of spontaneous recovery generally underlie subsequent improvements [9]. Recent innovations in rehabilitation techniques, however, offer new opportunities for motor recovery, even in the chronic stage.

The efficacy of brain–computer interfaces (BCIs) for post-stroke motor rehabilitation has been demonstrated with a variety of designs [12]. However, there is a lack of consensus regarding the neurophysiological mechanisms driving recovery through BCI [13–16], which necessitated further study. Functional recovery was previously shown in a severely impaired chronic stroke

population treated with a BCI system using signals from the contralesional motor cortex [17]. The former study used cortical EEG signals to control a robotic hand orthosis. Additionally, the efficacy of BCI on motor recovery was linked to changes in EEG activity in motor regions within frequencies used for BCI [17]. Given that this contralesional BCI system, known as the IpsiHand (Neuroolutions, Santa Cruz CA), recently received FDA market authorization and will be applied to stroke populations, understanding the mechanism of its clinical benefit is of high importance. Power fluctuations in alpha (8–12 Hz) and beta (13–25 Hz) frequencies are observed in motor cortex during motor activity [18,19]. These frequencies are also used for BCI control [17]. We therefore hypothesized BCI may have affected neural circuitry to facilitate motor recovery via experience-dependent plasticity. However, previously recorded EEG signals only assess broad cortical regions with limited anatomic specificity. Here, we used functional MR imaging to study whether BCI therapy affected functional connectivity organization in the motor cortex and cerebellum.

CONTACT Eric C. Leuthardt  leuthardt@wustl.edu  Department of Neurological Surgery, Washington University in St. Louis, 660 S. Euclid Avenue, Campus Box 807, St. Louis, MO 63110, USA

*Drs. Carter and Leuthardt contributed equally to this project.

 Supplemental data for this article can be accessed online at <https://doi.org/10.1080/2326263X.2022.2057757>

© 2022 The Author(s). Published by Informa UK Limited, trading as Taylor & Francis Group.

This is an Open Access article distributed under the terms of the Creative Commons Attribution-NonCommercial-NoDerivatives License (<http://creativecommons.org/licenses/by-nc-nd/4.0/>), which permits non-commercial re-use, distribution, and reproduction in any medium, provided the original work is properly cited, and is not altered, transformed, or built upon in any way.

Networks of correlated spontaneous brain activity during rest have been extensively described using functional MRI (fMRI) [20–22]. Strokes disrupt ‘functional connectivity’ networks [23–26]. Furthermore, the extent of network disruption correlated with stroke-induced impairments in multiple behavioral domains [23,25–27]. Strokes altered network modularity, typically by a decrease and then a partial recovery in association with behavioral improvements [25,28,29]. Connectivity changes between specific regions have also been implicated in stroke recovery [30–32]. Further, performance on motor function assessment tasks after a stroke was reduced with disrupted interhemispheric motor network connectivity [24,33]. Thus, recovery from stroke induced by BCI might involve changes in resting-state functional connectivity (rsFC).

The objective of the current study was to determine whether an EEG-driven BCI controlled by motor signals from the unaffected hemisphere reorganized brain networks for motor control. Based on previous reports linking motor network organization with post-stroke motor function, we hypothesized that motor recovery achieved during BCI therapy would change motor network connectivity, and that these rsFC changes in motor systems would correlate with the strength of recovery. Increases in interhemispheric connectivity, and decreases in intrahemispheric connectivity have previously been reported during stroke recovery [24,25,30,33–35]. Consequently, we hypothesized motor recovery via BCI would lead to similar patterns of change in inter- and intrahemispheric rsFC. The unexpected findings in this study suggest a potential novel recovery mechanism associated with BCI induced recovery in chronic stroke.

2. Materials and methods

2.1. Patient demographics

Eight enrolled patients had an upper limb hemiparesis (Median upper extremity portion of the Fugl-Meyer Assessment (UEFM) = 21.75) at least 6 months

post-stroke. Exclusion criteria included evidence of memory loss, severe aphasia, joint contractures in the upper limb, unilateral neglect, or an inability to generate a consistent BCI control signal. A complete list of inclusion and exclusion criteria is available in the supplemental material. Table 1 details patient demographic information. Most patients showed a moderate or severe motor impairment, although two patients showed a mild impairment. Every patient provided written informed consent before data collection.

2.2. EEG screening

Patients performed an EEG screening task to identify a brain signal associated with motor imagery of the affected hand from the contralesional hemisphere (i.e. the BCI control feature). Patients had to generate the motor imagery EEG signal consistently for the BCI therapy task. Initially, patients rested quietly for approximately 7 minutes during recordings of baseline EEG activity. Patients then performed a series of paired trials of quiet rest and imagined movement of their left, right, or both hands at the same time. Trial duration was 8 seconds with an inter-trial interval of 3 seconds. A single EEG screening session included acquisition of approximately 45 trials of rest and each type of imagined hand motion. Patients had to avoid moving or talking during EEG recordings. Screenings paused automatically for patients to rest in absence of a specific task at 25% completion intervals for the full duration of the screening. Each patient performed at least two screening sessions. A third session was necessary when detected feature frequencies were erratic or EEG signal quality was low in a prior session. Excluded patients had low-quality EEG data in all screening sessions, showed no reliable feature frequency, or could not regularly perform the BCI task.

Table 1. Demographic information.

Patient ID	Age (y)	Time Post-Stroke (mo.)	Gender	Lesion Location	Affected Limb	UEFM Baseline	UEFM Final	UEFM Change
1	55	183	F	L SMC	R	56	64	8
2	55	54	F	L BG, Thal	R	41	48	7
3	60	119	M	R BG, CST, L Thal	L	25.5	30	4.5
4	56	34	M	L BG, CST	R	19.5	25	5.5
5	68	46	M	L BG, Thal, CST	R	14.5	22	7.5
6	74	26	F	R BG, CST	L	12	21	9
7	63	71	M	L BG, CST, R BG	R	21.5	32	10.5
8	38	70	M	R BG, Thal, CST	L	22	31	9
Median	58	62				21.75	30.5	7.75

SMC: Somatomotor Cortex, BG: Basal Ganglia, Thal: Thalamus, CST: Corticospinal Tract.

2.3. BCI feature frequency

Control of the BCI device was through a 1 Hz wide feature frequency distinctly identified from EEG screening data in each patient. Stroke disrupts normal cortical oscillations in sensorimotor frequencies [36,37]. A patient-specific feature frequency approach was therefore implemented to lessen the impact of stroke-induced changes in the sensorimotor rhythm, which is classically used to control motor BCIs. The band-limited power of the feature frequency determined whether the orthosis opened (decreased power) or closed (increased power) during BCI therapy. A detailed description of BCI control signal processing is available in the supplemental material. A measure of the variance in each feature frequency from each patient was its coefficient of determination (R^2), calculated from the difference in quiet rest and impaired hand imagery task states in each screening session. Negative R^2 values indicated a power decrease during motor imagery relative to rest. Selected from each patient were feature frequencies with the largest negative R^2 value within mu or beta frequency bands (8–25 Hz) dependably produced across screening sessions.

2.4. Intervention protocol

The study timeline started with screening sessions over 1–2 weeks, followed by pre-therapy motor assessments and resting-state fMRI (Figure 1(a)). Next, patients trained to use the BCI device. They subsequently received a complete set of equipment to use at home. Patients then performed 12 weeks of home BCI therapy sessions, when they used the equipment for 1 hour per day, 5 days per week. The assigned therapy sessions totaled 60 hours. Although all patients were assigned the same amount of BCI therapy, usage varied among patients. Therapy dosage for BCI patients was estimated by summing the number of runs with at least 10% accuracy on both movement imagery and rest trials. Five BCI runs were approximately one hour of therapy. Patients either performed the therapy and device setup alone or with a caretaker based on their specific needs and living situation. Members of the research team were available via phone and e-mail to assist with technical issues. Excluded from the study were patients unable to use the BCI device. Patients had to enter their usage on a provided tracking sheet, which assisted them in documenting therapy times and any problems experienced with the equipment. Clinicians assessed motor function

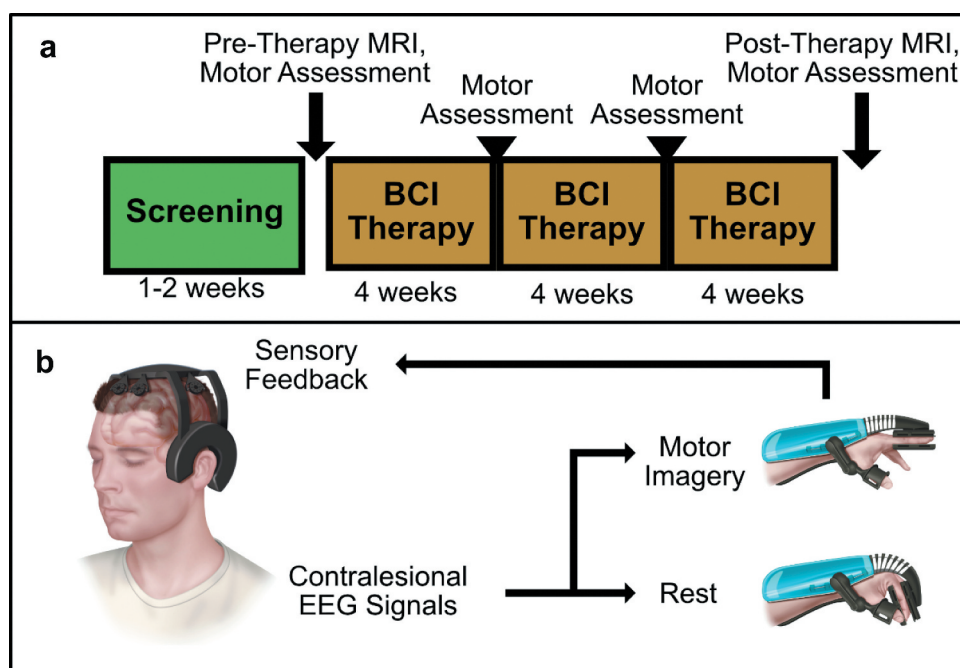


Figure 1. BCI Intervention protocol and system design overview. (a) Protocol Timeline. Screening for EEG feature frequency and inclusion and exclusion criteria occur over several sessions in a 1–2 week period. Following screening, patients undergo an MRI scan and motor assessments before receiving their BCI device. Patients perform BCI therapy for 12 weeks at home, returning every 4 weeks for motor assessments. A final MRI scan and motor assessment is performed after 12 weeks of therapy. (b) BCI System Design.

once per month (Figure 1(a)). After 12 weeks of BCI therapy, patients received a post-therapy motor assessment and second resting-state fMRI scan. Patients in the comparison group received intensive physical therapy in an 8-week task-specific training program.

2.5. BCI system design

Components of the BCI system included a motorized hand orthosis and wireless EEG headset (Wearable Sensing, San Diego, CA) with dry, active electrodes (Figure 1(b)). A Windows tablet connected via bluetooth to the EEG headset to record signals from the electrodes. A local Wi-Fi network generated within the orthosis supported communications between the tablet and a computer within the orthosis. The computer controlling orthosis received commands to open or close the hand via the tablet through these communications.

BCI therapy sessions involved multiple steps: (1) Patients put on the BCI headset and hand orthosis, turned on system components, and confirmed correct communications through a series of automated test outputs. The index and middle fingers of the affected limb were placed into padded braces where they could be flexed and extended with the orthosis. The motor and electronics in the orthosis were contained inside the device and rested on the forearm of the affected limb. After powering on the system components, the BCI control software loaded onto the tablet checked for connections to the headset and orthosis. Upon confirmation of these connections, the software proceeded to signal quality assessment. (2) Next, EEG signal quality assessments involved comparing low amplitude rest signals to noisy signals activated by jaw clenches. Patients were prompted to rest and clench their jaws, each for 5 seconds. Raw signals were displayed to the patients during this process, and they were trained to identify the characteristic noise expected during clenching. Following the rest and clench states, an electrode map was displayed with colors (green, yellow, and red) denoting signal quality at each electrode site. Quality was assessed by measuring the difference in signal power between rest and clench states, as a jaw clench typically results in significantly higher signal power. When signals were too noisy, patients could improve electrode connections by manually adjusting the headset and electrodes to facilitate contact with the scalp, rotating electrodes to push through hair, and waiting for a gradual decline in dry electrode impedance. Therapy did not proceed until signal quality improved with a subsequent assessment. (3) Patients began the BCI therapy task following a one-minute recording of an at-

rest signal and eight repetitions each of 8-second-long quiet rest and motor imagery trials. These recordings enabled threshold adjustments for orthosis control for each session. During therapy, patients received a cue to remain quietly at rest or perform vivid motor imagery of their affected hand. Band-limited power of the feature frequency was extracted from the contralesional EEG signal during therapy. The hand orthosis opened in a 3-point grip (Figure 1(b), upper right) after power of the feature frequency dropped below the threshold. The orthosis remained closed at higher feature frequency power levels (Figure 1(b), lower right). Patients received an instruction to attempt opening the orthosis by thinking about moving during motor imagery trials, and kept the hand closed by clearing their thoughts during rest trials. Patients thereby received proprioceptive and visual sensory feedback from the orthosis based on the EEG signals they generated. Individual trials lasted 8 seconds followed by a 3-second inter-trial interval.

2.6. Motor function assessment

The upper extremity portion of the Fugl-Meyer Assessment functioned as the primary motor outcome due to its wide use and high inter- and intra-rater reliability [38–40]. UEFM is a 66-point measurement of reaching and grasping ability with several hand orientations and ranges of motion. Secondary outcomes included grip strength, Motricity Index, Modified Ashworth Scale (MAS), and Arm Motor Ability Test (AMAT) [41–43]. Motor function assessment to establish a stable baseline occurred twice before commencing therapy. Baseline motor function was the average of two assessments (pre_1 and pre_2). Further assessments occurred at 4-week intervals during therapy, and at 6-months post-therapy completion. Calculation of motor improvement followed the formula:

$$UEFM_{post} - \frac{UEFM_{pre1} + UEFM_{pre2}}{2},$$

that is, the post-therapy motor function score minus the average of the baseline motor function scores. Occupational and physical therapists assessed motor function.

2.7. MRI acquisition protocol

MRI scans with a Siemens Prisma 3 T scanner included structural images from T1-weighted MP-RAGE, T2-weighted fast spin echo, and fluid attenuation inversion recovery (FLAIR) sequences. Scanning sessions occurred within 2 weeks of initiating and completing

the 12-week therapy protocol. Capture of BOLD signals for resting-state data utilized a 64-channel head coil and a gradient echo EPI sequence (voxel size = $2.4 \times 2.4 \times 2.4$ mm; TR = 1070 ms; TE = 30 ms; flip angle = 70° ; multi-band factor 4). Each of three, approximately 7-minute scans collected 400 frames of resting-state functional MRI data, for a total of 1200 frames over 21 minutes. We acquired distortion maps immediately prior to each resting-state BOLD scan.

Comparison group MRI scans included similar T1- and T2-weighted structural images with a Siemens TRIO 3 T scanner. Resting state BOLD data acquisition included the following parameters: 4 mm isotropic voxels; TR = 2000 ms; TE = 27 ms; 12 channel head coil; 4 scans with 128 frames each.

2.8. MRI preprocessing

A previously described pipeline preprocessed all functional MRI data [44]. The 4dfp suite (4dfp.readthedocs.io) of preprocessing steps comprised slice-time correction, removal of odd-even slice intensity differences, rigid body motion correction, affine transformation to a $(3 \text{ mm})^3$ atlas space, spatial smoothing with a 6 mm FWHM Gaussian kernel, voxelwise linear detrending, and a temporal low pass filter (0.1 Hz cutoff). Freesurfer software performed cortical surface segmentation. Regression of nuisance waveforms, derived from motion correction timeseries, CSF signal, white matter signal, and the whole brain ('global') signal, reduced spurious variance [45,46]. High-motion frames were removed from the analysis [44]. Fisher z-transforms were applied to Pearson correlation coefficients prior to statistical analysis.

2.9. Seed-based functional connectivity calculations

Analysis of preprocessed MRI data utilized MATLAB (MathWorks, Natick, MA) unless otherwise noted. Cortical regions previously implicated in motor control served as *a priori* regions of interest (ROIs). These included the hand region of bilateral primary dorsal motor cortex (M1), dorsal premotor area (PMA), and supplementary motor area (SMA). We used Neurosynth [47] for all cortical ROI coordinates. Peak Z-scores for each ROI served as centers for 8 mm diameter spheres. Extracted mean BOLD timeseries were from each ROI. Generation of two aggregate cerebellum (CBL) ROIs were from somatomotor regions in anterior CBL lobules. Separately averaged left and right CBL somatomotor regions formed the

basis of left and right CBL mean timeseries [48]. Then, labeling these left- and right-side timeseries as contralesional and ipsilesional was relative to the left/right stroke brain location. Cerebellar laterality was in correspondence to motor network membership (i.e. left cerebellum and right primary motor cortex were in the same functional hemisphere). Excluded ROIs overlaid the stroke lesion. Analyses were of functional connectivity, defined as the Pearson correlation of paired mean ROI timeseries and between select ROIs and all other voxels in the brain. Pre- and post-therapy connectivity differences indicated changes in functional connectivity.

2.10. Functional connectivity analyses

A twofold focus of the functional connectivity analysis was: 1) define changes in cortical and subcortical connectivity topography and 2) define alterations in magnitude of connectivity in known motor network ROIs. For network topography, primary analyses performed on fMRI data included voxel-based functional connectivity between ROI in contralesional M1, ipsilesional M1, contralesional CBL, and ipsilesional CBL and the rest of the brain. Findings assessed connectivity changes at specific ROIs following BCI therapy. We examined only statistically significant functional connectivity maps by applying a threshold of $z = 0.3$. Obtained maps were from pre- and post-therapy timepoints. Counts of suprathreshold voxels in each connectivity map tracked spatial distributions for pre- and post-therapy MRI scans. Voxel counts were from the whole brain and each hemisphere. Wilcoxon signed-rank tests compared pre- and post-therapy timepoints for whole-brain voxel counts. Timepoints here refers to MRI scans at baseline before any therapy (pre-therapy) and after 12 weeks of BCI therapy (post-therapy). Suprathreshold voxel counts for each patient and ROI evaluated relationships between functional topography plasticity and motor recovery. The subtraction of pre- from post-therapy voxel counts quantified changes. Spearman rank correlations estimated the relationship between motor recovery and change in number of suprathreshold voxels.

Evaluations of motor network connectivity changes following therapy relied on assessments of network strength through pairwise functional connectivity (FC) measurements between ROIs. Median adjacency matrices generated from Pearson correlation coefficients between each ROI pair visualized FC

strength in the pre-therapy state as well as changes in FC following therapy. Adjacency matrices were converted into circular graphs for visualization using the Python NetworkX package [49]. Circular graph nodes were per ROI. Color of edges (lines) connecting nodes mark the z-score value of Pearson correlations (i.e. connectivity strength).

Pairwise connectivity measurements were grouped into the following subsets: all motor ROI pairs, inter-hemispheric ROI pairs contralesional intrahemispheric pairs, and ipsilesional intrahemispheric pairs. Interhemispheric ROI pairs indicated FC strengths between contra- and ipsilesional ROIs. For each ROI pair within these groupings, FC strengths across all cases were combined into distributions showing the proportion of each FC strength value at pre- and post-therapy timepoints. Similarly, distributions of all FC z-values for each ROI pair and per patient showed individual differences in changed FC strengths between pre- and post BCI therapy. Wilcoxon signed-rank tests assessed differences between pre- and post-therapy FC strength distributions relative to the number of correlation z-scores of a given magnitude. The formula listed below estimated the Wilcoxon signed-rank effect sizes:

$$r = Z/\sqrt{N},$$

with r the effect size, Z the signed-rank test Z-statistic, and N the sample size. The Spearman rank correlation between Wilcoxon effect sizes and increases in UEFM scores examined the relationships between FC change and motor recovery.

3. Results

3.1. Motor rehabilitation

All BCI patients showed an increase in UEFM score after 12 weeks of contralesional BCI therapy. Clinically meaningful recovery occurred in seven of the eight patients who reached a minimal clinically important difference (MCID) threshold of at least a 5.2 point score increase [50]. Median increase in UEFM score was 7.25. Figure 2 illustrates progressive longitudinal motor recovery from baseline in each case. Most patients passed the clinically significant threshold by 8 weeks. Patients 1 and 2 showed similar UEFM improvement to other subjects despite having a much milder baseline impairment. Wilcoxon signed-rank tests also found significant improvement ($p < 0.05$) in grip strength, Motricity Index score, and AMAT scores (see Supplemental Material for more detail). Median changes included increased grip strength (3.75 pounds, $p = 0.0234$), Motricity Index (2 points, $p = 0.0156$), and AMAT (5 points, $p = 0.0156$). The Modified Ashworth Scale, a measure of spasticity, showed median changes of 0 at the elbow and 0.125 at the wrist. No MCID comparisons were available for these measures. Individual changes in secondary outcomes are detailed in Table S1.

3.2. BCI performance

Patients generally used their BCI systems effectively, achieving median move and rest success rates of 78.5% and 35%, respectively. A definition of

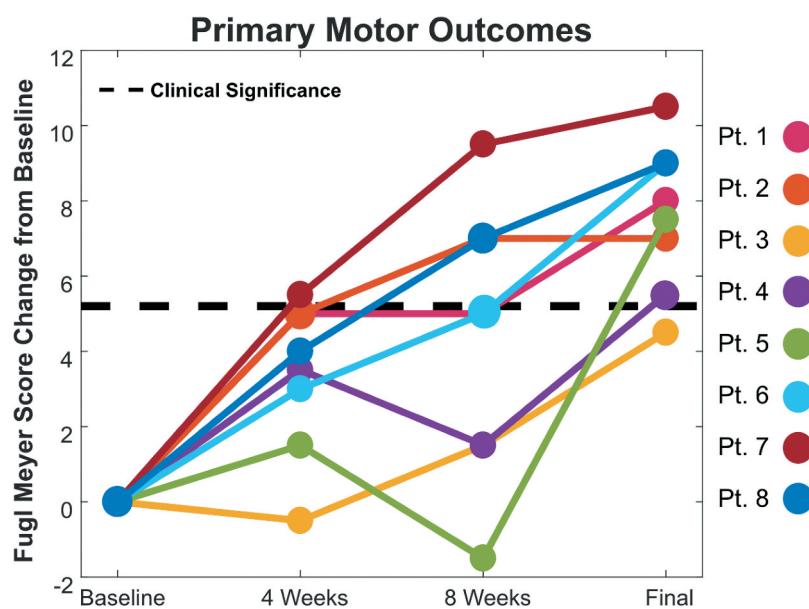


Figure 2. Longitudinal BCI primary motor outcomes. Longitudinal change in UEFM score from baseline. Each patient represented as a different line color. Dotted black line indicates minimal clinically important difference of 5.2 points on the UEFM.

Table 2. BCI performance data.

Subject	Move Success Rate (%)	Rest Success Rate (%)	Move Error (SS)	Rest Error (SS)	R^2	Total Sessions	Total Trials	Feature Frequency (Hz)
1	84	15	3.7	2.7	0.089	47	6120	21
2	49	48	3.9	4.1	0.102	62	9660	15
3	34	60	2.8	2.8	0.089	19	2790	19
4	92	23	3.6	3.8	0.256	50	8250	15
5	73	37	3.1	3.2	0.239	61	9750	16
6	31	62	4.7	4.9	0.128	29	3690	11
7	96	33	18.5	4.1	4.145	86	9420	10
8	91	22	18.5	3.3	3.341	26	3090	18

SS: Sum of Squares, R^2 : Coefficient of Determination, Bold denotes updated hardware algorithm which changes estimation of error and R^2 .

a successful trial was reaching the BCI activation threshold for at least 1 second for move trials or staying under the activation threshold for the entire trial duration for rest trials. Most patients showed greater success rates with movement imagery trials due to restrictive criteria for success on rest trials. Although we accepted feature frequencies in both alpha (8–12 Hz) and beta (13–25 Hz) bands, six out of eight patients had beta feature frequencies. This preference for beta frequencies is consistent with previous studies of ipsilateral motor electrophysiology in which there are stronger spectral power changes in the beta band than in the mu (also known as alpha) band during ipsilateral movement [51].

Table 2 contains BCI performance data including feature frequencies, trial success rates, signal error (Sum of Squares), and coefficients of determination (R^2).

3.3. Spatial distributions of voxel-based functional connectivity in select ROIs

BCI therapy-induced changes in spatial connectivity patterns in contralesional and ipsilesional primary motor cortex and cerebellum from pre- and post-therapy in group average functional connectivity maps ($z > 0.3$), as shown in Figure 3. Qualitatively, contralesional and ipsilesional M1 (Figure 3(a,b)) and cerebellar

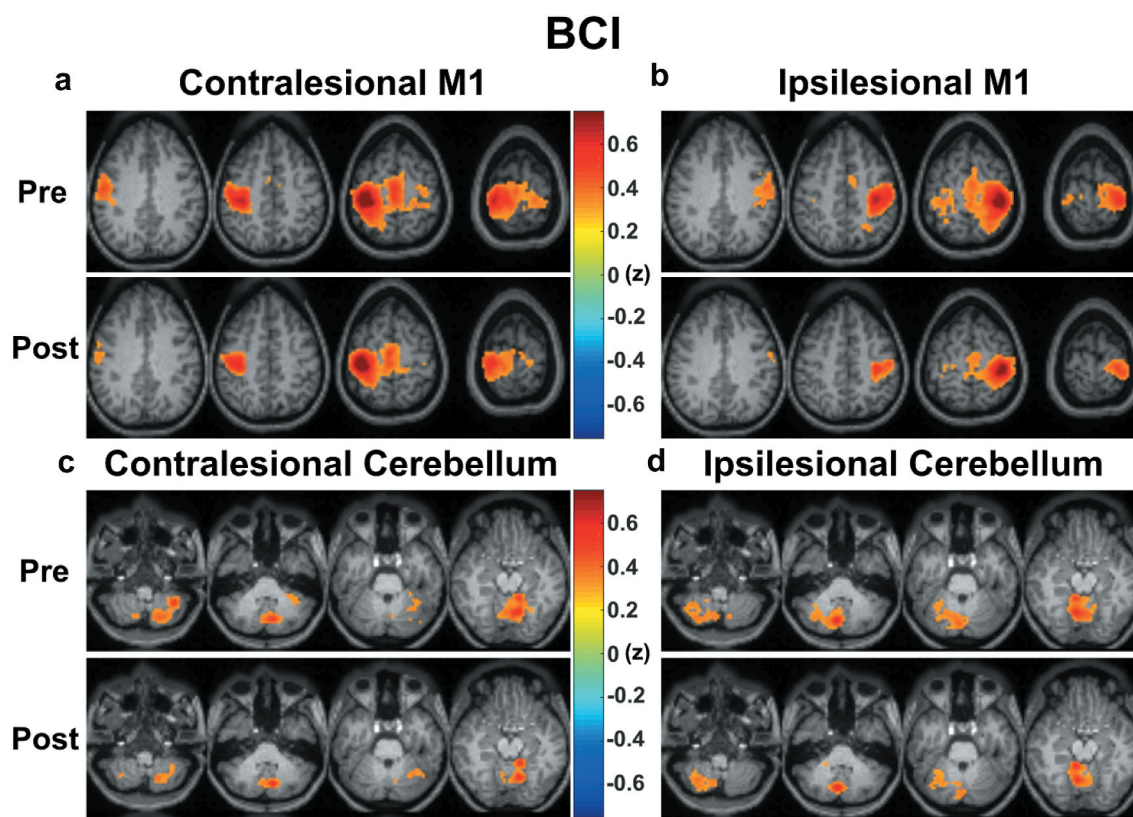


Figure 3. Spatial connectivity distributions change following BCI Therapy. Pre- and post-therapy maps of group average voxelwise functional connectivity ($z > 0.3$) are shown for contralesional M1 (a), ipsilesional M1 (b), contralesional cerebellum (c), and ipsilesional cerebellum (d). Pre-therapy maps are shown above their post-therapy equivalents.

(Figure 3(c,d)) ROIs showed decreased spatial distributions functional connectivity voxels post therapy (Figure 3(a–d)). Smaller extents of functional connectivity appeared especially in ipsilesional M1 (Figure 3(b)) and contralesional cerebellum (Figure 3(c)).

Quantitatively, suprathreshold voxel counts significantly decreased for ipsilesional M1 following BCI therapy (Figure 4, Wilcoxon signed-rank test, $p = 0.0156$). Suprathreshold voxel count changes were normalized to the matching baseline for each patient and region. Box-and-whisker plots of pre- and post-therapy counts of voxels surpassing the functional connectivity statistical significance threshold ($z > 0.3$) show decreased variance following BCI therapy (Figure S4). No statistically significant correlations were observed between voxel count changes and motor recovery (Figure S5).

3.4. ROI-ROI and interhemispheric connectivity

Circular graph representations show median functional connectivity strengths pre-therapy for contra- and ipsilesional ROIs, based on z -scores of Pearson correlations between paired ROI nodes (Figure 5(a)). Strong connectivity strengths ($z > 0.6$) characterized links between cortical motor ROI with connections located entirely contralesional or ipsilesional and

most interhemispheric links (Figure 5(a)). Relatively weaker connectivity strengths ($z < 0.5$) occurred between interhemispheric CBL and motor ROIs (e.g. cSMA to iPMA or iM1; cM1 to iM1 or iPMA). Generally, many nodes showed connectivity above the threshold to other motor ROIs, an expected feature of the motor network. All suprathreshold connectivity changes in BCI patients were negative from pre- to post-therapy timepoints, regardless of whether paired ROIs were contralesional, ipsilesional, or interhemispheric. (Figure 5 (b)). Not shown are median connectivity changes of $|z| < 0.1$.

Functional connectivity strength in BCI patients was significantly lower post-therapy compared to pre-therapy. Normalized distributions of functional connectivity strengths pre- and post-therapy are shown in Figure 6. The analysis included all ROI pairs regardless of a threshold of $z > 0.3$ for results shown in Figure 5. A Wilcoxon signed-rank test found statistically significant decreases from pre- to post-therapy timepoints across all motor ROIs and patients ($p = 1 \times 10^{-6}$), all interhemispheric motor ROI ($p = 0.006$), all ipsilesional intrahemispheric ROI pairs (Figure 6(d), $p = 0.003$), but not any contralesional intrahemispheric ROI pairs (Figure 6(c), $p = 0.071$). These results showed

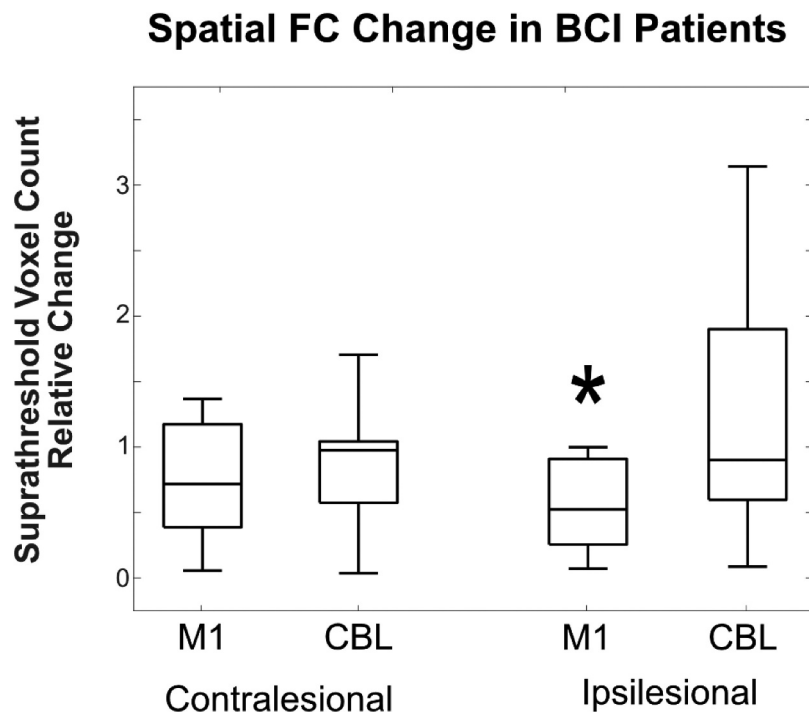


Figure 4. Normalized voxel count changes in select ROIs. Difference relative to baseline for the number of voxels with statistically significant functional connectivity ($z > 0.3$) to contralesional and ipsilesional primary motor cortex (M1) and cerebellum (CBL) in chronic stroke patients pre- and post-therapy. Box-and-whisker plots indicate median values. Value of 1 indicates no change. The ipsilesional M1 region showed a statistically significant reduction in number of suprathreshold voxels compared to the pre-therapy timepoint with a Wilcoxon signed-rank test ($p = 0.0156$).

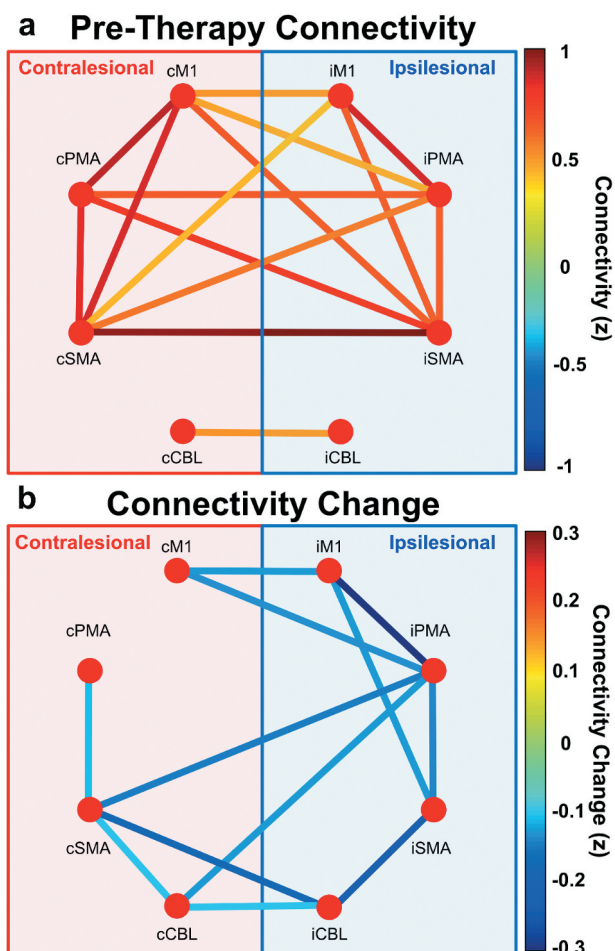


Figure 5. Functional connectivity changes in motor regions. (a) Median pre-therapy functional connectivity between motor ROI pairs in BCI patients. Primary motor, premotor, supplementary motor, and cerebellar ROIs used. Each node marks an ROI with a prefix specifying laterality (e.g. cSMA is contralateral supplementary motor area). Nodes in red and blue background areas are contralateral and ipsilateral ROIs, respectively. Line color indicates connectivity strength. Threshold of $z = 0.3$ applied to connectivity graph. (b) Median change in connectivity from pre-therapy to post-therapy timepoints (post – pre) in BCI patients. Threshold of $z = 0.1$ applied to connectivity graph.

contralateral BCI therapy significantly decreased motor network connectivity strength, regardless of hemisphere in relation to stroke location.

A key issue was whether motor recovery corresponded with decreases in motor connectivity. A nonparametric rank correlation analysis sorted patients by change in FC strength and extent of motor recovery. The analysis found that larger decreases in motor FC strength correlated with greater motor recovery (Figure 7(a) $r = 0.77$, $p = 0.033$). These significant findings indicated motor recovery through contralateral BCI therapy resulted in decreased overall motor intra-network functional connectivity. No other ROI sets showed connectivity changes correlated with recovery (Figure 7(b–d)).

4. Discussion

Upper extremity motor function improved in a chronic stroke population following 12 weeks of training with a noninvasive, contralaterally controlled brain–computer interface. Decreases in functional connectivity strength and topography in motor cortex ROIs were concurrent with upper limb motor improvements. Reductions in topographic connectivity to ipsilateral primary motor cortex correlated with recovery. Motor recovery levels were also significantly correlated with a reduction in functional connectivity strength. These findings suggest that contralateral BCI-induced motor function improvement in chronic stroke patients may be partially driven by widespread decreases in motor network functional connectivity.

Of particular importance was finding contralateral BCI therapy effectively enabled recovery for chronic hemiparesis. Chronic hemiparetic stroke patients usually experience poor motor recovery after 3 months post-stroke [5–9]. Studied patients were at a median of 62 months post-stroke. Nevertheless, 7 out of 8 patients made clinically significant improvements in upper limb motor function following contralateral BCI therapy. Ipsilateral BCI therapy for both acute and chronic hemiparesis has been previously implemented in a variety of configurations [12]. Robotic orthoses, electrical stimulation, and visual imagery feedback have all been used successfully in combination with ipsilateral BCI systems across several studies [12,13,16,52–55]. The current contralaterally driven BCI therapy method and intervention protocol replicated BCI-mediated recovery reported previously, thus confirming motor recovery with contralateral BCI therapy [17]. Critically, patients achieved motor improvement using BCI in a home therapy setting, with patients or their caretakers operating the BCI system. Others have recently noted the practical challenges of implementing BCI therapy in a clinical setting and suggested home-based therapy as a potential solution [54,56]. The current BCI approach advantageously expanded a therapy method previously confined to in-person clinical settings.

Acquisition of noninvasive functional neuroimaging concurrent with BCI therapy additionally revealed unexpected motor network changes during rehabilitation. Decreases in motor network functional connectivity strength suggest different network dynamics occur during recovery in chronic stroke compared to (sub)acute stroke. Typically, acutely injured networks characteristically showed increased intra- and decreased interhemispheric resting-state FC strength [24,25,30,33–35]. Task-based BOLD

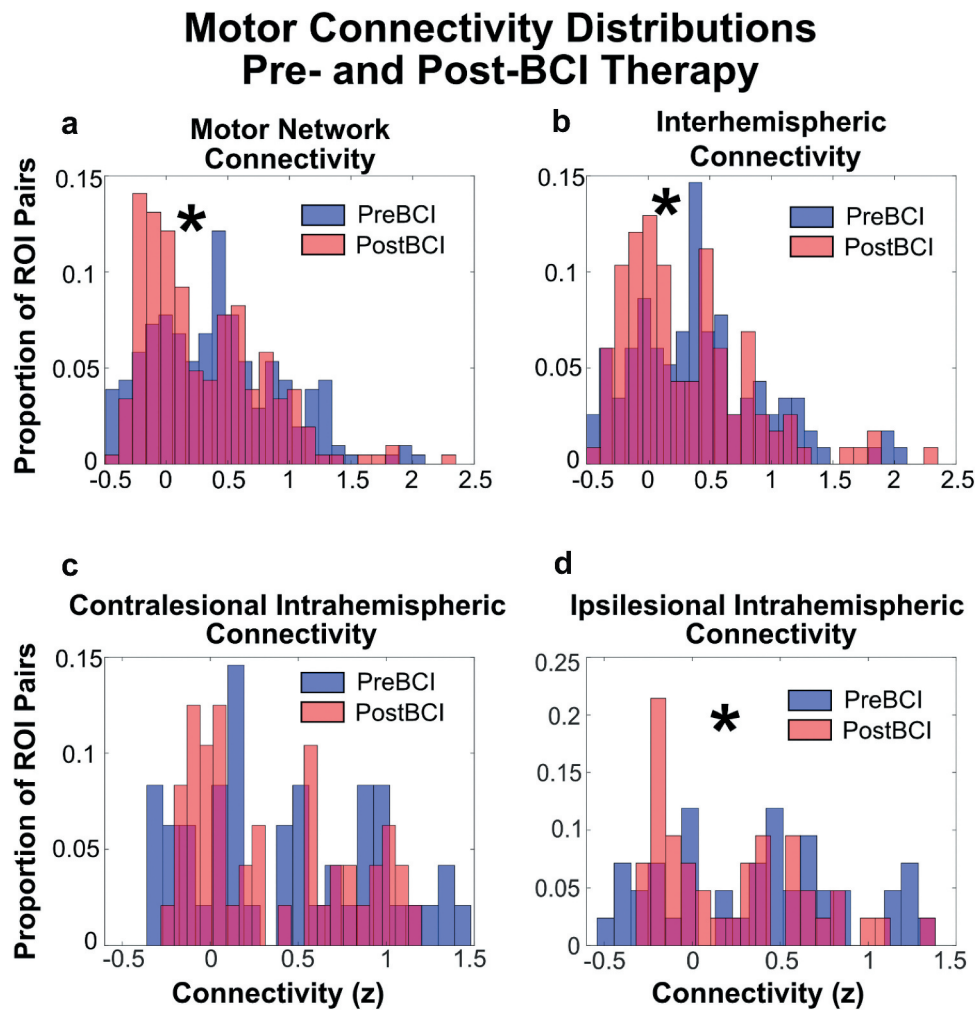


Figure 6. Motor connectivity decreases following BCI rehabilitation. Histograms constructed from motor ROI sets across all BCI patients at pre-therapy (blue) and post-therapy (red) timepoints. Overlapping histograms shown in purple. Histograms displays the normalized distribution of Z-transformed functional connectivity. ROI sets include all motor ROI pairs (a), interhemispheric ROI pairs (b), contralateral intra-hemispheric ROI pairs (c), and ipsilesional intra-hemispheric ROI pairs (d). Decreased post-therapy motor FC is statistically significant via Wilcoxon signed-rank test for full motor ROI set ($p = 1 \times 10^{-6}$), interhemispheric ROI set ($p = 0.006$), and ipsilesional intra-hemispheric ROI set ($p = 0.003$). Contralateral intra-hemispheric connectivity decreased, but this change was not statistically significant ($p = 0.071$).

activations during motor tasks also became lateralized toward the contralateral hemisphere [57]. With functional recovery in the subacute stage, brain function gradually reverted toward the pre-stroke state with increased interhemispheric connectivity and a return of ipsilesional cortical activation during a motor task [16,29,30,32,34,57,58]. Functional organization with more successful behavioral recovery resembled that of a healthy brain [29,30,32,58]. In contrast, contralaterally driven BCI therapy resulted in broadly decreased motor network intra- and interhemispheric connectivity strength. The findings also were not an epiphenomenon given a significant correlation between connectivity change and motor recovery.

Contralaterally driven BCI rehabilitation in chronic stroke may operate by affecting inhibitory circuit activity through experience-dependent plasticity. Mouse models of stroke recovery have indicated that experience-dependent plasticity may be important for stroke recovery. Studies in whisker barrel cortex suggest a possible model in which loss of incoming sensory input (e.g. removal of a whisker) resulted in robust alteration in the activity, connectivity, and structure of neural circuits [59]. Loss of input to a deprived barrel column precipitated a loss of inhibitory firing in that column. Unmasked horizontal excitatory connections possibly provoked expanded adjacent receptive fields serviced from neighboring columns linked to intact whiskers. These changes

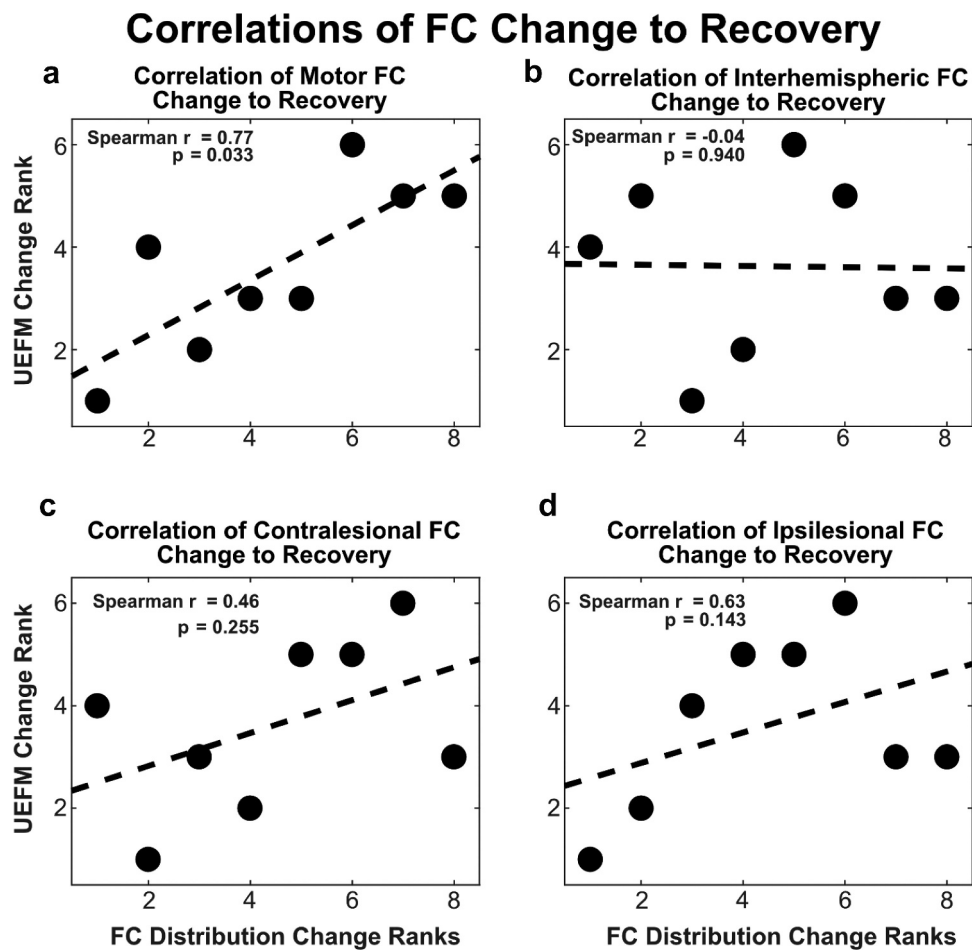


Figure 7. Correlation between connectivity change and BCI motor recovery. Spearman correlations between motor ROI connectivity change and motor recovery. Data represented in ranked form. The dotted line represents a least-squares regression fit onto the ranked data. Connectivity change in four ROI sets measured as shown in Figure 5. The correlation between connectivity change in all motor ROIs and motor recovery was statistically significant.

might be a consequent pathologic expansion of local connectivity [60]. Similar changes in cortical topographical maps arose from peripheral loss in nonhuman primates [61,62]. A possible mechanism affecting these network changes might be injury-induced downregulation of inhibitory circuits [62–64], allowing increased neural activity via *preexisting* thalamocortical and intracortical connectivity as opposed to *de novo* sprouting [65–67]. Similarly, provoked increases in intracortical connectivity might occur following stroke-mediated white matter transections in human cortex [68]. Consequently, chronic loss of motor output from stroke might pathologically diminish inhibitory activity, resulting in a net increase in maladaptive connectivity of the remaining motor network. This connectivity increase probably does not represent a compensatory mechanism, but rather a long-term pathologic end point of an injury. Thus, a consistent engagement of thalamocortical inhibitory motor rhythms with BCI usage may reverse this chronic

state of maladaptive, decreased inhibitory activity [18]. A consequence of the reversal could be the observed reduced motor functional connectivity, which may result from restored inhibitory activity. Further, enhanced inhibition might lead to increased functional specialization within the motor network, consistent with current findings of reduced nodal connectivity and diminished topographic distributions of connectivity (most notably in ipsilesional M1).

Ipsilesional primary motor cortex in BCI patients was the only ROI that showed a statistically significant change in suprathreshold voxels. Previous studies into motor network connectivity following acute stroke typically reported positive associations between ipsilesional M1 connectivity or activity and motor recovery – this does not match the presented findings [16,24,32,57]. While we observed no correlations between the degree of motor recovery and the change in ipsilesional M1 connectivity extent, there was an observed increase in a patient population achieving clinically significant recovery. The discrepancy may be due

to the specific design of the BCI device used for therapy. By promoting contralesional activity during therapy, activity-dependent plasticity may have altered functionally relevant ipsilesional activity. Extensive contralesional BCI use potentially resulted in reduced ipsilesional M1 connectivity specifically, in addition to the general decrease in motor network connectivity.

The current findings of BCI effects on motor recovery and decreased motor network connectivity indicate the importance of further optimization of BCI-mediated therapies. Previously, Bundy et al. demonstrated functional recovery correlated with patient accuracies of BCI control [17]. Thus, enhancing the personalization of BCI control to best facilitate patients' ability to control BCI therapy devices may be important for effective therapy [69]. The described methods used for BCI control in this study were relatively simple. The BCI system was controlled by the signal from a single electrode and a 1-Hz wide EEG frequency band associated with motor imagery. More elaborate control algorithms reliant on different EEG features may enhance rehabilitative effects. Further, other methods of feedback could include functional electric stimulation or virtual representations of a paretic hand moving [12,13,52,70–73]. In particular, the current feedback was only through proprioceptive sensation from moving the hand. Abundant evidence showed robotic manipulation of an affected limb has provided substantive benefit [12,13,52,70–72]. Designing an optimal feedback regimen to best affect identified motor network changes will require further research, possibly piloted initially in an animal model.

4.1. Limitations

We executed a small, non-randomized, prospective study, which constrained the impact of these findings. The small sample size also constrained statistical testing to less powerful non-parametric tests, which may unreliably detect results from small effect sizes. Two BCI patients had multiple-stroke lesions, which may have further affected motor connectivity. However, we assumed these patients achieved full recovery from non-motor deficits due to our strict inclusion and exclusion criteria. Despite additional stroke effects in these cases, seven of eight patients showed clinically significant upper motor recovery after BCI therapy, which coincided with decreased in motor network connectivity.

5. Conclusion

Chronic stroke patients used a contralesionally controlled BCI system to achieve clinically significant upper motor recovery. Motor recovery was coincident

with decreases in resting-state functional connectivity among motor ROIs. These findings are notably different from those in the subacute stage of stroke. Future studies need to explore the influence of BCI as a therapy for strokes affecting motor behavior.

Acknowledgments

The authors thank the study participants for their time and effort, and thank Kristina Zinn, Xin Hong, and Catherine Lang for providing the physical therapy data they worked to acquire.

Disclosure statement

Dr. Leuthardt owns stock in Neuroolutions, Inner Cosmos, and Sora Neuroscience. Washington University owns stock in Neuroolutions. Other authors report no conflicts. The funders had no role in study design, data collection and analysis, decision to publish, or preparation of the manuscript.

Funding

This work was supported by NIH R21NS102696 (Leuthardt and Carter) and NIH P41-EB018783.

References

- [1] Virani SS, Alonso A, Benjamin EJ, et al. Heart disease and stroke statistics—2020 update: a report from the American Heart Association. *Circulation*. 2020;141:E139–E596.
- [2] Lawrence ES, Coshall C, Dundas R, et al. Estimates of the prevalence of acute stroke impairments and disability in a multiethnic population. *Stroke*. 2001;32(6):1279–1284.
- [3] Sunderland A, Tinson D, Bradley L, et al. Arm function after stroke. An evaluation of grip strength as a measure of recovery and a prognostic indicator. *J Neurol Neurosurg Psychiatry*. 1989;52(11):1267–1272.
- [4] Wade DT, Langton-Hewer R, Wood VA, et al. The hemiplegic arm after stroke: measurement and recovery. *J Neurol Neurosurg Psychiatry*. 1983;46(6):521–524.
- [5] Duncan PW, Goldstein LB, Matchar D, et al. Measurement of motor recovery after stroke. *Stroke*. 1992;23(8):1084–1089.
- [6] Jorgensen HS, Nakayama H, Raaschou HO, et al. Outcome and time course of recovery in stroke. Part II: time course of recovery. The Copenhagen stroke study. *Arch Phys Med Rehab*. 1995;76(5):406–412.
- [7] Lloyd-Jones D, Adams R, Carnethon M, et al. Heart disease and stroke statistics - 2009 update. A report from the American heart association statistics committee and stroke statistics subcommittee. *Circulation*. 2009;119(3):480–486.

- [8] Hatem SM, Saussez G, Della Faille M, et al. Rehabilitation of motor function after stroke: a multiple systematic review focused on techniques to stimulate upper extremity recovery. *Front Hum Neurosci.* 2016;10:442.
- [9] Kwakkel G, Kollen B, Lindeman E. Understanding the pattern of functional recovery after stroke: facts and theories. *Restor Neurol Neurosci.* 2004;22(3-5):281-299.
- [10] Krakauer JW. Motor learning: its relevance to stroke recovery and neurorehabilitation. *Curr Opin Neurol.* 2006;19(1):84-90.
- [11] Langhorne P, Bernhardt J, Kwakkel G. Stroke rehabilitation. *Lancet.* 2011;377(9778):1693-1702.
- [12] Cervera MA, Soekadar SR, Ushiba J, et al. Brain-computer interfaces for post-stroke motor rehabilitation: a meta-analysis. *Ann Clin Transl Neurol.* 2018;5(5):651-663.
- [13] Biasucci A, Leeb R, Iturrate I, et al. Brain-actuated functional electrical stimulation elicits lasting arm motor recovery after stroke. *Nat Commun.* 2018;9(1):1-13.
- [14] Pichiorri F, Morone G, Petti M, et al. Brain-computer interface boosts motor imagery practice during stroke recovery. *Ann Neurol.* 2015;77(5):851-865.
- [15] Várkuti B, Guan C, Pan Y, et al. Resting state changes in functional connectivity correlate with movement recovery for BCI and robot-assisted upper-extremity training after stroke. *Neurorehabil Neural Repair.* 2013;27(1):53-62.
- [16] Ramos-Murguialday A, Broetz D, Rea M, et al. Brain-machine interface in chronic stroke rehabilitation: a controlled study. *Ann Neurol.* 2013;74(1):100-108.
- [17] Bundy DT, Souders L, Baranyai K, et al. Contralateral brain-computer interface control of a powered exoskeleton for motor recovery in chronic stroke survivors. *Stroke.* 2017;48(7):1908-1915.
- [18] Pfurtscheller G, Stancák A, Neuper C. Event-related synchronization (ERS) in the alpha band - An electrophysiological correlate of cortical idling: a review. *Int J Psychophysiol.* 1996;24(1-2):39-46.
- [19] Pfurtscheller G. Central beta rhythm during sensorimotor activities in man. *Electroencephalogr Clin Neurophysiol.* Published online 1981. DOI: [10.1016/0013-4694\(81\)90139-5](https://doi.org/10.1016/0013-4694(81)90139-5).
- [20] Biswal B, Yetkin FZ, Haughton VM, et al. Functional connectivity in the motor cortex of resting human brain using echo-planar MRI. *Magn Reson Med.* 1995;34(4):537-541.
- [21] van den Heuvel MP, Hulshoff Pol HE. Exploring the brain network: a review on resting-state fMRI functional connectivity. *Eur Neuropsychopharmacol.* 2010;20(8):519-534.
- [22] Smitha KA, Akhil Raja K, Arun KM, et al. Resting state fMRI: a review on methods in resting state connectivity analysis and resting state networks. *Neuroradiol J.* 2017;30(4):305-317.
- [23] He BJ, Snyder AZ, Vincent JL, et al. Breakdown of functional connectivity in frontoparietal networks underlies behavioral deficits in spatial neglect. *Neuron.* 2007;53(6):905-918.
- [24] Carter AR, Astafiev SV, Lang CE, et al. Resting inter-hemispheric functional magnetic resonance imaging connectivity predicts performance after stroke. *Ann Neurol.* 2010;67(3):365-375.
- [25] Siegel JS, Ramsey LE, Snyder AZ, et al. Disruptions of network connectivity predict impairment in multiple behavioral domains after stroke. *Proc Natl Acad Sci U S A.* 2016;113(30):E4367-76.
- [26] Baldassarre A, Ramsey L, Hacker CL, et al. Large-scale changes in network interactions as a physiological signature of spatial neglect. *Brain.* 2014;137(12):3267-3283.
- [27] Ramsey LE, Siegel JS, Baldassarre A, et al. Normalization of network connectivity in hemispatial neglect recovery. *Ann Neurol.* 2016;80(1):127-141.
- [28] Gratton C, Nomura EM, Pérez F, et al. Focal brain lesions to critical locations cause widespread disruption of the modular organization of the brain. *J Cogn Neurosci.* 2012;24(6):1275-1285.
- [29] Siegel JS, Seitzman BA, Ramsey LE, et al. Re-emergence of modular brain networks in stroke recovery. *Cortex.* 2018;101:44-59.
- [30] Fan Y, Wu C, Liu H, et al. Neuroplastic changes in resting-state functional connectivity after stroke rehabilitation. *Front Hum Neurosci.* 2015;9(OCT):546.
- [31] Park C, Chang WH, Ohn SH, et al. Longitudinal changes of resting-state functional connectivity during motor recovery after stroke. *Stroke.* 2011;42(5):1357-1362.
- [32] Golestani AM, Tymchuk S, Demchuk A, et al. Longitudinal evaluation of resting-state fMRI after acute stroke with hemiparesis. *Neurorehabil Neural Repair.* 2013;27(2):153-163.
- [33] Lin LY, Ramsey L, Metcalf NV, et al. Stronger prediction of motor recovery and outcome post-stroke by cortico-spinal tract integrity than functional connectivity. *Boltze J, ed. PLoS One.* 2018;13(8):e0202504.
- [34] Baldassarre A, Ramsey LE, Siegel JS, et al. Brain connectivity and neurological disorders after stroke. *Curr Opin Neurol.* 2016;29(6):706-713.
- [35] Siegel JS, Mitra A, Laumann TO, et al. Data quality influences observed links between functional connectivity and behavior. *Cereb Cortex.* 2017;27(9):4492-4502.
- [36] Rossiter HE, Boudrias M-H, Ward NS. Do movement-related beta oscillations change after stroke? *J Neurophysiol.* 2014;112(9):2053-2058.
- [37] Westlake KP, Hinkley LB, Bucci M, et al. Resting state α -band functional connectivity and recovery after stroke. *Exp Neurol.* 2012;237(1):160-169.
- [38] Sanford J, Moreland J, Swanson LR, et al. Reliability of the Fugl-Meyer assessment for testing motor performance in patients following stroke. *Phys Ther.* 1993;73(7):447-454.
- [39] Sullivan KJ, Tilson JK, Cen SY, et al. Fugl-Meyer assessment of sensorimotor function after stroke: standardized training procedure for clinical practice and clinical trials. *Stroke.* 2011;42(2):427-432.
- [40] Gladstone DJ, Danells CJ, Black SE. The Fugl-Meyer assessment of motor recovery after stroke: a critical review of its measurement properties. *Neurorehabil Neural Repair.* 2002;16(3):232-240.

- [41] Collin C, Wade D. Assessing motor impairment after stroke: a pilot reliability study. *J Neurol Neurosurg Psychiatry*. 1990;53(7):576.
- [42] Kopp B, Kunkel A, Flor H, et al. The Arm Motor Ability Test: reliability, validity, and sensitivity to change of an instrument for assessing disabilities in activities of daily living. *Arch Phys Med Rehabil*. 1997;78(6):615–620.
- [43] Bohannon RW, Smith MB. Interrater reliability of a modified Ashworth scale of muscle spasticity. *Phys Ther*. 1987;67(2):206–207.
- [44] Power JD, Mitra A, Laumann TO, et al. Methods to detect, characterize, and remove motion artifact in resting state fMRI. *Neuroimage*. 2014;84:320–341.
- [45] Fox MD, Zhang D, Snyder AZ, et al. The global signal and observed anticorrelated resting state brain networks. *J Neurophysiol*. 2009;101(6):3270–3283.
- [46] Power JD, Plitt M, Laumann TO, et al. Sources and implications of whole-brain fMRI signals in humans. *Neuroimage*. 2017;146:609–625.
- [47] Yarkoni T, Poldrack RA, Nichols TE, et al. Large-scale automated synthesis of human functional neuroimaging data. *Nat Methods*. 2011;8(8):665–670.
- [48] Seitzman BA, Gratton C, Marek S, et al. A set of functionally-defined brain regions with improved representation of the subcortex and cerebellum. *Neuroimage*. 2020;206:116290.
- [49] Hagberg AA, Swart PJ, Schult DA. Exploring network structure, dynamics, and function using networkx. *Proc 7th Python Sci Conf (SciPy 2008)*. Published online August 2008.:11–15.
- [50] Page SJ, Fulk GD, Boyne P. Clinically important differences for the upper-extremity Fugl-Meyer scale in people with minimal to moderate impairment due to chronic stroke. *Phys Ther*. 2012;92(6):791–798.
- [51] Bundy DT, Szrama N, Pahwa M, et al. Unilateral, Three-dimensional Arm Movement Kinematics are Encoded in Ipsilateral Human Cortex. *J Neurosci*. Published online October 8, 2018:0015–0018. DOI:10.1523/JNEUROSCI.0015-18.2018.
- [52] Ono T, Shindo K, Kawashima K, et al. Brain-computer interface with somatosensory feedback improves functional recovery from severe hemiplegia due to chronic stroke. *Front Neuroeng*. 2014;7(July):19.
- [53] Mukaino M, Ono T, Shindo K, et al. Efficacy of brain-computer interface-driven neuromuscular electrical stimulation for chronic paresis after stroke. *J Rehabil Med*. 2014;46(4):378–382.
- [54] Coscia M, Wessel MJ, Chaudary U, et al. Neurotechnology-aided interventions for upper limb motor rehabilitation in severe chronic stroke. *Brain*. 2019;142(8):2182–2197.
- [55] Carvalho R, Dias N, Cerqueira JJ. Brain-machine interface of upper limb recovery in stroke patients rehabilitation: a systematic review. *Physiother Res Int*. 2019;24(2):e1764.
- [56] Simon C, Bolton DAE, Kennedy NC, et al. Challenges and opportunities for the future of brain-computer interface in neurorehabilitation. *Front Neurosci*. 2021;15:814.
- [57] Cramer SC, Nelles G, Benson RR, et al. A functional MRI study of subjects recovered from hemiparetic stroke. *Stroke*. 1997;28(12):2518–2527.
- [58] van Meer MPA, van der Marel K, Wang K, et al. Recovery of sensorimotor function after experimental stroke correlates with restoration of resting-state inter-hemispheric functional connectivity. *J Neurosci*. 2010;30(11):3964–3972.
- [59] Kraft AW, Bauer AQ, Culver JP, et al. Sensory deprivation after focal ischemia in mice accelerates brain remapping and improves functional recovery through Arc-dependent synaptic plasticity. *Sci Transl Med*. 2018;10(426):31.
- [60] Kathleen Kelly M, Carvell GE, Kodger JM, et al. Sensory loss by selected whisker removal produces immediate disinhibition in the somatosensory cortex of behaving rats. *J Neurosci*. 1999;19(20):9117–9125.
- [61] Manger PR, Woods TM, Jones EG. Plasticity of the somatosensory cortical map in macaque monkeys after chronic partial amputation of a digit. *Proc R Soc B Biol Sci*. 1996;263(1372):933–939.
- [62] Jones EG. Cortical and subcortical contributions to activity-dependent plasticity in primate somatosensory cortex. *Annu Rev Neurosci*. 2000;23:1–37.
- [63] Hendry SHC, Jones EG. Reduction in number of immunostained GABAergic neurones in deprived-eye dominance columns of monkey area 17. *Nature*. 1986;320(6064):750–753.
- [64] Hendry SHC, Fuchs J, DeBlas AL, et al. Distribution and plasticity of immunocytochemically localized GABAA receptors in adult monkey visual cortex. *J Neurosci*. 1990;10(7):2438–2450.
- [65] DeFelipe J, Conley M, Jones EG. Long-range focal collateralization of axons arising from corticocortical cells in monkey sensory-motor cortex. *J Neurosci*. 1986;6(12):3749–3766.
- [66] Rausell E, Bickford L, Manger PR, et al. Extensive divergence and convergence in the thalamocortical projection to monkey somatosensory cortex. *J Neurosci*. 1998;18(11):4216–4232.
- [67] Rausell E, Jones EG. Extent of intracortical arborization of thalamocortical axons as a determinant of representational plasticity in monkey somatic sensory cortex. *J Neurosci*. 1995;15(6):4270–4288.
- [68] Hawasli AH, Kim DH, Ledbetter NM, et al. Influence of white and gray matter connections on endogenous human cortical oscillations. *Front Hum Neurosci*. 2016;10:10.
- [69] Raffin E, Hummel FC. Restoring motor functions after stroke: multiple approaches and opportunities. *Neuroscientist*. 2018;24(4):400–416.
- [70] Soekadar SR, Birbaumer N, Slutzky MW, et al. Brain-machine interfaces in neurorehabilitation of stroke. *Neurobiol Dis*. 2015;83:172–179.
- [71] Young BM, Williams J, Prabhakaran V. BCI-FES: could a new rehabilitation device hold fresh promise for stroke patients? *Expert Rev Med Devices*. 2014;11(6):537–539.
- [72] Foong R, Tang N, Chew E, et al. Assessment of the efficacy of EEG-Based MI-BCI with visual feedback and EEG correlates of mental fatigue for upper-limb stroke rehabilitation. *IEEE Trans Biomed Eng*. 2020;67(3):786–795.
- [73] López-Larraz E, Sarasola-Sanz A, Irastorza-Landa N, et al. Brain-machine interfaces for rehabilitation in stroke: a review. *NeuroRehabilitation*. 2018;43(1):77–97.

BRAIN COMMUNICATIONS

Theta–gamma coupling as a cortical biomarker of brain–computer interface-mediated motor recovery in chronic stroke

Nabi Rustamov,^{1,2} Joseph Humphries,³ Alexandre Carter⁴ and Eric C. Leuthardt^{1,2,3,5,6}

Chronic stroke patients with upper-limb motor disabilities are now beginning to see treatment options that were not previously available. To date, the two options recently approved by the United States Food and Drug Administration include vagus nerve stimulation and brain–computer interface therapy. While the mechanisms for vagus nerve stimulation have been well defined, the mechanisms underlying brain–computer interface-driven motor rehabilitation are largely unknown. Given that cross-frequency coupling has been associated with a wide variety of higher-order functions involved in learning and memory, we hypothesized this rhythm-specific mechanism would correlate with the functional improvements effected by a brain–computer interface. This study investigated whether the motor improvements in chronic stroke patients induced with a brain–computer interface therapy are associated with alterations in phase–amplitude coupling, a type of cross-frequency coupling. Seventeen chronic hemiparetic stroke patients used a robotic hand orthosis controlled with contralesional motor cortical signals measured with EEG. Patients regularly performed a therapeutic brain–computer interface task for 12 weeks. Resting-state EEG recordings and motor function data were acquired before initiating brain–computer interface therapy and once every 4 weeks after the therapy. Changes in phase–amplitude coupling values were assessed and correlated with motor function improvements. To establish whether coupling between two different frequency bands was more functionally important than either of those rhythms alone, we calculated power spectra as well. We found that theta–gamma coupling was enhanced bilaterally at the motor areas and showed significant correlations across brain–computer interface therapy sessions. Importantly, an increase in theta–gamma coupling positively correlated with motor recovery over the course of rehabilitation. The sources of theta–gamma coupling increase following brain–computer interface therapy were mostly located in the hand regions of the primary motor cortex on the left and right cerebral hemispheres. Beta–gamma coupling decreased bilaterally at the frontal areas following the therapy, but these effects did not correlate with motor recovery. Alpha–gamma coupling was not altered by brain–computer interface therapy. Power spectra did not change significantly over the course of the brain–computer interface therapy. The significant functional improvement in chronic stroke patients induced by brain–computer interface therapy was strongly correlated with increased theta–gamma coupling in bihemispheric motor regions. These findings support the notion that specific cross-frequency coupling dynamics in the brain likely play a mechanistic role in mediating motor recovery in the chronic phase of stroke recovery.

1 Department of Neurological Surgery, Washington University School of Medicine, St Louis, MO, USA

2 Center for Innovation in Neuroscience and Technology, Washington University School of Medicine, St Louis, MO, USA

3 Department of Biomedical Engineering, Washington University in St Louis, St Louis, MO, USA

4 Department of Neurology, Washington University in St Louis, St Louis, MO, USA

5 Department of Neuroscience, Washington University School of Medicine, St Louis, MO, USA

6 Department of Mechanical Engineering and Materials Science, Washington University in St Louis, St Louis, MO, USA

Correspondence to: Eric C. Leuthardt, MD
FNAI Department of Neurological Surgery
Washington University School of Medicine
660 S. Euclid Avenue

Received September 22, 2021. Revised March 19, 2022. Accepted May 23, 2022. Advance access publication May 25, 2022

© The Author(s) 2022. Published by Oxford University Press on behalf of the Guarantors of Brain.

This is an Open Access article distributed under the terms of the Creative Commons Attribution License (<https://creativecommons.org/licenses/by/4.0/>), which permits unrestricted reuse, distribution, and reproduction in any medium, provided the original work is properly cited.

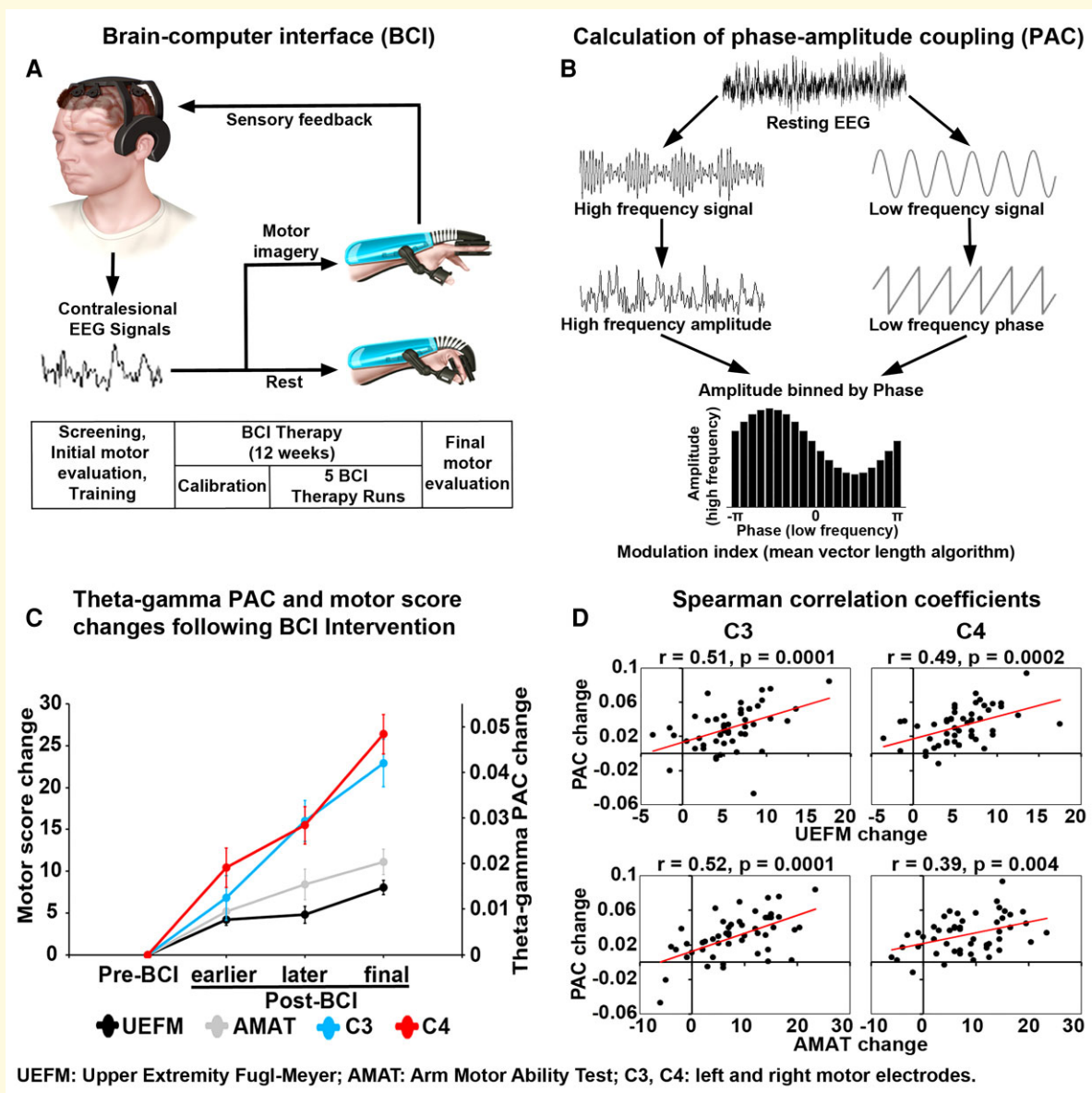
Campus Box 8057 St Louis, MO 63110, USA
E-mail: leuthardte@wustl.edu

Correspondence may also be addressed to: Nabi Rustamov, MD, PhD
Department of Neurological Surgery
Washington University School of Medicine
520 S. Euclid Avenue
St Louis, MO 63110, USA
E-mail: rustamov.nabi@wustl.edu

Keywords: chronic stroke rehabilitation; brain-computer interface; theta-gamma coupling

Abbreviations: AMAT = Arm Motor Ability Test; BCI = brain-computer interface; CFC = cross-frequency coupling; FIR = finite impulse response; GABA = gamma-aminobutyric acid; M1 = primary motor cortex; MAS = modified Ashworth Scale; MCID = minimal clinically significant difference; MVL = mean vector length; PAC = phase-amplitude coupling; PSD = power spectral densities; SEM = standard error of mean; tACS = transcranial alternating current stimulation; UEFM = upper extremity Fugl-Meyer

Graphical Abstract



Introduction

About two-thirds of stroke patients suffering from hemiparesis are still unable to fully use their affected limb 6 months after stroke.^{1–3} Motor recovery usually plateaus at 3 months post-stroke, and residual motor deficits ultimately become permanent.^{4–8} Trials of increased rehabilitation therapy dose or brain stimulation therapies have not been effective.^{9–11} Developing new treatments for stroke rehabilitation remains a research priority. Vagus nerve stimulation therapy combined with movement training has been shown to help achieve improvement in upper-limb motor recovery in patients with chronic stroke,^{12–14} possibly through cholinergic and monoaminergic modulation of motor cortex neurons.^{15,16} Moreover, studies using neuroprosthetic strategies for stroke rehabilitation have shown that functional improvements can be achieved even in the chronic stage.^{17–21} One approach is the application of a brain–computer interface (BCI)-controlled robotic hand orthosis using EEG signals from the contralesional motor cortex.^{22–24} Contralesionally controlled BCI therapy has been shown to facilitate motor rehabilitation in severely impaired chronic stroke patients.²³ However, the mechanisms underlying BCI-driven motor rehabilitation are poorly understood. Defining changes in cortical electrophysiology with motor recovery in the chronic phase of stroke will better elucidate the mechanisms promoting motor learning and facilitate further refinement of motor rehabilitation strategies.

Previous studies have supported the role of the contralesional hemisphere in post-stroke recovery. Functional MRI (fMRI) studies of stroke patients have shown that increased contralesional activity is associated with improved motor function.^{25,26} The use of the uninjured motor cortex as the control signal for BCI rehabilitation further demonstrated the beneficial role of the unaffected hemisphere in motor recovery.²³ Conversely, several studies have shown that the reduction of the contralesional motor cortical activity enhances motor function in the affected limb of hemiparetic stroke patients, which suggests that the contralesional hemisphere impedes recovery.^{27–30} Taken together, there is increasing support that the unaffected motor cortex plays a role in motor recovery, but underlying physiological mechanisms require further clarification. In previous work in animal models, there has been substantial evidence that M1 plays a role in the acquisition of motor skills.^{31–33} In humans, the cortical physiology associated with motor learning in M1 is more limited.^{34,35} This physiology in the setting of chronic stroke is even more scarce (see Katak *et al.*³⁶ for a review).

Coupling between different frequency bands may be a potential mechanism for motor learning. Traditionally, neural oscillations have been divided into specific frequency bands and studied according to their spectral features alone.^{37,38} Higher-frequency oscillations (>70 Hz), known as gamma rhythms, are thought to represent local cortical ensembles.^{39,40} Narrow bands under 30 Hz, such as theta (4–7 Hz), alpha (8–12 Hz) and beta rhythms (13–29 Hz), have been posited to

represent modulatory circuits associated with deeper grey structures such as the thalamus and hippocampus.^{41–43} In the recent years, there is growing interest in exploring more complex properties of neural oscillations, such as synchronization between the phase of low-frequency oscillations and the amplitude of higher-frequency oscillations, i.e. phase–amplitude coupling (PAC), a type of cross-frequency coupling (CFC).^{44–48} It has been suggested that PAC reflects the regulation of high-frequency local oscillation by a larger network oscillating at lower frequencies.⁴⁹ PAC has been associated with a wide variety of higher-order functions involved in learning and memory,^{50–54} attention,^{55,56} nociception,^{57,58} motor and visuomotor tasks.^{59–64} The mechanisms underlying learning have been most extensively studied in the hippocampus, where theta–gamma PAC has been hypothesized as a key learning-related mechanism.^{46,54,65–67} It has been determined that theta–gamma PAC also plays a similar role in learning throughout the neocortical regions.^{49,68} As in the hippocampus, M1 gamma oscillations are modulated by theta activity through PAC.⁶⁹ In a preliminary study, enhancement of theta–gamma PAC via transcranial alternating current stimulation (tACS) over M1 during learning of motor skills resulted in a significant improvement in motor skill acquisition.⁷⁰ This implies a potential role of theta–gamma PAC in motor skill learning but requires further investigation.

In this study, we sought to evaluate in chronic stroke patients whether BCI therapy-induced motor improvement is associated with alterations in PAC between gamma and lower frequencies. Contralesionally controlled BCI training used cortical signals related to affected hand motor imagery, recorded from the unaffected hemisphere, to control the affected hand via a powered hand exoskeleton. Resting-state EEG recordings of patients with chronic stroke were examined throughout a 12-week period of BCI training. Given the prior evidence showing the potential implications of theta–gamma PAC in motor learning, we hypothesized that theta–gamma PAC will be primarily changed with BCI intervention and that these changes over motor areas will correlate with the magnitude of motor recovery. As in prior studies, chronic stroke patients achieved a clinically significant motor recovery following BCI therapy.^{22–24} Here, we found a significant increase in theta–gamma PAC over motor areas which positively correlated with these functional improvements. These findings highlight an important role of theta–gamma PAC enhancement in the facilitation of motor improvement which may represent a key underlying mechanism for motor learning with the use of a BCI therapy in chronic stroke patients.

Materials and methods

Study population

Seventeen chronic stroke patients with upper-limb hemiparesis completed the full course of BCI therapy for 12 weeks. The inclusion criteria were the following: stroke at least 6 months prior confirmed by neurologist or medical records;

Table 1 Patient demographics and primary motor assessment scores (mean \pm SEM)

Age (years)	Time since stroke (months)	BCI usage (h)	Lesion side: hemisphere	Gender	Baseline UEFM	Final UEFM	UEFM change
54.7 (2.9)	65.7 (15.5)	41.7 (5.2)	L/6 R	7 f/10 m	33.3 (3.5)	41.4 (3.4)	8.03 (0.9)

BCI, brain-computer interface; f, female; L, left; m, male; R, right; SEM, standard error of mean; UEFM, upper extremity Fugl-Meyer assessment.

intact cognitive ability quantified by a score of 0–1 on Items 1b and 1c (cognition) of the NIH Stroke Scale; unilateral upper extremity weakness; ability to provide informed consent; full passive range of motion of the affected elbow, wrist and digits and normal sensation (tactile and proprioceptive) in the affected upper extremity. The exclusion criteria were the following: severe visual impairment; cognitive impairment (8 or more on the Short Blessed Test); Botox injections in the affected upper extremity for spasticity management in the prior 3 months; severe aphasia, ataxia or unilateral neglect; severe psychiatric disorders such as schizophrenia or pre-stroke bipolar disorder; concurrent participation in other stroke studies. All patients suffered a first-time stroke at least 6 months prior to this study. Patient demographics are shown in Table 1 (see the ‘Results’ section). Motor function outcomes were primarily assessed with the upper extremity Fugl-Meyer (UEFM) assessment, which has been validated in a stroke patient population and has high reliability.^{71–73} Secondary motor function outcomes were measured using the Arm Motor Ability Test (AMAT), motricity index (MI), modified Ashworth Scale (MAS) at the wrist and elbow and grip strength. This study was approved by the Institutional Review Board of Washington University School of Medicine in St Louis. The data in this study were pooled across two pre-registered studies (NCT04338971 and NCT03611855) with identical research protocols. Before data collection, all patients gave written informed consent according to the Declaration of Helsinki.

BCI system design

The BCI system and intervention protocol have been designed as we previously described.²³ The system consisted of a robotic hand orthosis, EEG amplifier and wireless EEG cap with six active electrodes (US Food and Drug Administration-authorized IpsiHand Upper Extremity Rehabilitation System, Neuroolutions, Santa Cruz, CA, USA) (Fig. 1A, top panels). A touchscreen tablet was connected via Bluetooth to the EEG headset to record signals from the brain. The local Wi-Fi network supported communication between the tablet and orthosis. The tablet guided patients through BCI tasks and translated spectral power changes into orthosis control to open and close it in a 3-finger pinch grip. For the BCI task, patients were instructed to open the orthosis with motor imagery of the affected hand or to keep the orthosis closed by resting quietly. The orthosis opened and closed in response to changes in the power of the patient-specific control signal. Subjects who could partially move their affected arm were instructed to allow passive movements by the orthotic device.

Intervention protocol

The diagram of the BCI intervention timeline is shown in Fig. 1A (bottom panels). Patients were first tested for the inclusion and exclusion criteria and the ability to perform the BCI task. The exclusion criteria included severe aphasia, joint contractures in the upper limb, unilateral neglect or inability to generate a consistent BCI control signal. During EEG screening session prior to therapy implementation, patients were instructed to perform a series of rest and motor imagery trials. The 1 Hz width frequency band with spectral power modulation best corresponding to the difference between rest and motor trials was selected as the BCI device control signal. The selected control signal was always within the mu (8–12 Hz) or beta (13–29 Hz) canonical frequency band and remained consistent for each patient throughout BCI therapy. Patients with identifiable feature frequency consistent over two EEG screenings were included in the study. Patients were evaluated for baseline motor function before initiating the therapy by physical and occupational therapists. In addition to the UEFM, secondary motor function outcome measures using the AMAT, MI, MAS at the wrist and elbow and grip strength were also acquired. Research team members then trained patients in the use of the BCI system. Patients were instructed to use the device 1 h/day, 5 days/week, for a total of 12 weeks. BCI performance data per patient are provided in Supplementary Table 1. Clinicians assessed motor function once every 4 weeks. After 12 weeks of BCI therapy, patients underwent a final post-therapy motor assessment.

A session of BCI therapy took ~1 h to complete and consisted of one calibration period and five BCI therapy runs. Pre-therapy calibration was implemented for data quality assurance and for detecting motor imagery activity during the BCI task. During calibration, patients rested quietly and then completed a series of task blocks and rest trials. During task blocks, patients were instructed to imagine moving their affected hand. The orthosis did not move during calibration. Following calibration, patients started BCI therapy runs. Each run consisted of 30 motor imagery and 30 rest trials. The trial order was randomized, and 3 s of ‘fidget’ periods were included between each 8 s trial. A ‘fidget’ periods encouraged patients to blink or make physical adjustments. After the completion of the BCI therapy run, the system paused to allow patients to rest before continuing with their therapy. Resting-state EEG data from pre-task calibration sessions were saved to a remote server for further analysis.

In order to further validate the clinical and electrophysiological effects of BCI intervention, future sham-controlled

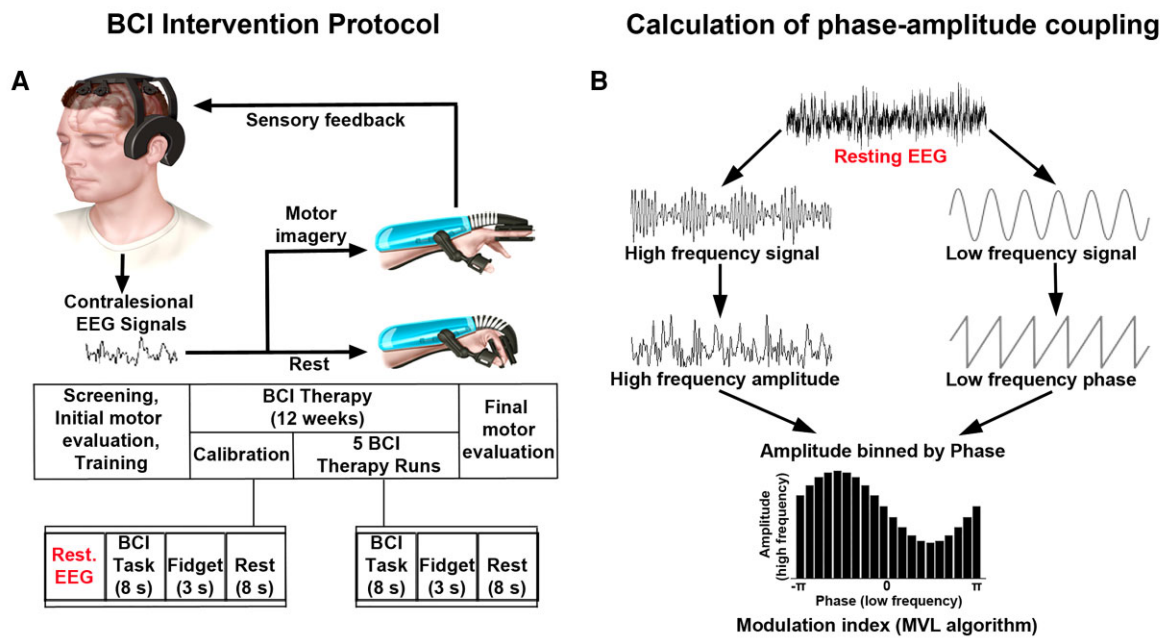


Figure 1 Experimental design and EEG processing. **(A)** BCI intervention protocol. (Top panels) BCI system design. Patients performed motor imagery tasks. Contralateral EEG signals were translated into commands to open or close the orthosis, which then provided proprioceptive sensory feedback to the patient as they performed motor imagery tasks. (Bottom panels) Intervention timeline. Patients were screened for the ability to perform the BCI task. Following screening, eligible patients underwent motor assessments before initiating the BCI therapy. Daily BCI therapy sessions included one calibration period (extended rest, alternating motor imagery and rest trials) and five BCI therapy runs (motor imagery and rest trials with active orthosis). Fidget periods were included between trials encouraging patients to blink or make physical adjustments. Motor assessments were performed every 4 weeks. Final EEG recording and motor assessment data were acquired after 12 weeks of therapy. **(B)** Data processing schematic for calculating PAC. The raw EEG signal was bandpass filtered in the lower (theta, alpha or beta) frequency range (right), and in the higher (high gamma) frequency range (left). Then, the complex analytic form of each signal was obtained using the Hilbert transform. The phase (angle of analytic signal) and power (amplitude of analytic signal) information was extracted from the lower- and higher-frequency signals, respectively. The coupling between phase and amplitude was then quantified using MVL algorithm to produce a modulation index values.

studies comparing the effects of active BCI with those observed with a sham BCI intervention are warranted. Sham BCI may consist in delivering a constant signal not coupled to the brain activity from the scalp EEG to mimic active BCI while keeping participants blind to the intervention. To rule out the possible efficacy of the sham intervention, the significance of changes in the clinical and electrophysiological outcomes between the BCI training group and the sham group should be assessed.

EEG recording and processing

EEG was recorded by means of six wireless dry electrodes (F3, F4, C3, C4, P3 and P4) mounted on the EEG headset in an International 10–20 System (Neuroolutions, Santa Cruz, CA, USA). EEG was sampled at 300 Hz with a ground electrode placed on the forehead. The electrode impedance was kept below 10 k Ω . The raw EEG data were preprocessed in a MATLAB environment (Mathworks, Natick, MA, USA). EEG data collected during the pre-therapy calibration rest period were prepared for analysis across four stages of the BCI therapy runs. These stages were Pre-BCI (before initiating

the therapy), earlier Post-BCI (4th week), later Post-BCI (8th week) and final Post-BCI (12th week). Resting-state EEG data for each condition were 5 min long. For each condition, continuous EEG recording was bandpass filtered between 1 and 100 Hz using a finite impulse response (FIR) filter. To remove environmental noise, 60 Hz notch filter was applied. EEG was screened for extreme values, as well as for infrequent and un-stereotyped artefacts. For further artefact attenuation, Infomax independent component analysis was applied.⁷⁴ Independent components found to reflect eye blinks, lateral eye movements, muscle-related and cardiac artefacts were removed from the data. EEG data were common average re-referenced. Frequency bands were defined as follows: theta, 4–7 Hz; alpha, 8–12 Hz; beta, 13–29 Hz; gamma, 65–100 Hz.³⁸

Power spectral density

The power spectral density (PSD) was calculated for each condition using Welch's method.⁷⁵ The input signal was segmented into 50% overlapping sections each with the duration of 2 s. Each segment was windowed with a Hamming

window that is the same length as the segment. A fast Fourier transform was applied to the windowed data. The periodogram of each windowed segment was averaged to form the spectrum estimate from 1 to 100 Hz. PSD values were then averaged across frequency bands and participants. The averaged data for Post-BCI runs were contrasted with Pre-BCI baseline.

A high gamma band was typically defined as cortical oscillations above 60 Hz.^{76–78} However, scalp EEG was found to effectively record high gamma activity up to 100 Hz.^{48,79–83} On the other hand, notch filtering (60 Hz) can possibly affect cortical oscillations at the neighbouring frequencies. That is why broadband gamma⁸⁴ was defined between 65 and 100 Hz.⁸⁵

Time–frequency analysis was additionally performed to support the idea that high gamma oscillations can be detected using scalp EEG. This analysis allowed visualizing resting high gamma cortical oscillations and their potential modulation by the BCI intervention. EEG was filtered offline using an FIR bandpass filter from 65 to 100 Hz. Data were segmented into 5 s epochs. A Morlet wavelet convolution was computed using the channel time–frequency option.^{81,82} Thirty-five linearly spaced frequencies were computed between 65 and 100 Hz. For each patient, time–frequency data were averaged across all epochs per condition. The grand average time–frequency maps were obtained by averaging data across patients (see [Supplementary Fig. 1A](#), *top* panels). High gamma oscillations were then averaged across 65–100 Hz to visualize a single high gamma frequency wave (see [Supplementary Fig. 1A](#), *bottom* panels).

Phase–amplitude coupling

To calculate PAC, first, the raw signal was bandpass filtered in the frequency bands of interest ([Fig. 1B](#)). A Hilbert transform was then applied to obtain the complex-valued analytic signal. Estimates of low-frequency phase and high-frequency amplitude were extracted from the low- and high-frequency filtered analytic signal, respectively. The coupling between low-frequency phase and high-frequency amplitude was quantified using the mean vector length (MVL) approach, originally described in Canolty *et al.*⁶⁹ PAC values were computed between phases of theta/alpha/beta frequency bands (4–7, 8–12 or 13–29 Hz) and amplitudes of the high gamma frequency band (65–100 Hz). Theta-, alpha- and beta-gamma PACs were compared between conditions. MVL approach allows us to estimate whether the power at high frequencies fluctuates systematically with the phase of the low frequency, i.e. PAC.

To rule out the possible effects of filtering on PAC results, we conducted additional analyses using neighbouring electrodes to generate the lower and higher-frequency signals to compute PAC. Neighbouring central (C3 and C4) and frontal (F3 and F4) electrodes were used for cross-electrode theta/alpha-high gamma and beta-high gamma PAC calculations, respectively.

As a complimentary tool, Canolty maps were calculated to visualize the high gamma power and theta–gamma PAC.⁶⁹ The phase troughs of the low frequency were specified at the theta frequency band (5 Hz). A time window of 1 s was extracted around each of these troughs. A time–frequency decomposition of these short epochs was performed. The power of all the time–frequency maps was averaged to obtain the final Canolty maps (see [Supplementary Fig. 1B](#)). This approach allowed us to visualize whether the power at high frequencies fluctuated systematically with the phase of the low frequency, i.e. PAC.

Localizing electrodes to the cortical surface for theta–gamma PAC

Cortical sources of statistically significant theta–gamma PAC increase during motor recovery relative to Pre-BCI baseline were estimated in order to spatially characterize this effect. The forward model was calculated using the Open-MEEG Boundary Element Method⁸⁶ on the cortical surface of a template MNI brain (colin27 atlas). A noise covariance matrix was estimated from the preprocessed EEG data. Cortical source activation was calculated with a constrained inverse model of EEG sources using the weighted minimum norm current estimation⁸⁷ and mapped to a distributed source model consisting of 15 002 elementary current dipoles. Theta–gamma PAC was computed on the source using the MVL method. We then applied voxelwise non-parametric permutation tests on PAC source space.

Statistical analyses

Differences in the mean PAC values were examined in a repeated-measures ANOVA with within-subjects factors *Stage* (main factor with four levels: Pre-BCI, earlier, later and final Post-BCI—see the ‘EEG recording and processing’ section) \times *Electrode* (F3, F4, C3, C4, P3 and P4). In case of significant interaction *Stage* \times *Electrode* indicating an overall difference between conditions with regard to PAC as a function of the electrode, we ran separate ANOVAs for each electrode. Planned contrasts were then used to test *a priori* hypotheses and decompose the significant effects of BCI intervention. Changes in PSD values and motor assessment scores across BCI therapy runs were also assessed by repeated-measures ANOVA. All statistical tests were two-tailed with a significance level of 0.05, and the *P*-values were adjusted using a Bonferroni correction.

For the theta–gamma PAC source, under the null hypothesis of no difference between the two conditions, each point in space per subject was randomly permuted between conditions (final Post-BCI versus Pre-BCI) and the resulting data were used to compute a permutation *t*-statistic spatiotemporal map for PAC.^{88–90} Repeating this permutation procedure 1000 times, using Monte Carlo random sampling, enabled us to estimate the empirical distribution of the *t*-statistic at each voxel, and thus convert the original data into a *P*-value statistical map. Lastly, to control for multiple comparisons across all voxels,

the P -values were adjusted using a Bonferroni correction. The significant values with $P \leq 0.05$ were retained, while values with $P > 0.05$ were set to zero.

Correlation analyses were conducted between PAC values across BCI therapy runs to test synchrony between time series data. We used a non-parametric Spearman rank correlation to avoid imposing a model assuming a linear relation between variables.^{91,92} Correlations were also calculated between motor assessment scores and electrophysiological findings. Significance thresholds were set at $P \leq 0.05$. It is worth noting that correlations were assessed for the statistically significant EEG effects (theta–gamma PAC increase at the C3 and C4 electrodes; beta–gamma PAC decrease at the F3 and F4 electrodes following BCI treatment). PAC values were averaged for electrodes showing significant effects, creating one value per electrode, subject and condition. The differences in PAC and motor assessment scores relative to the Pre-BCI baseline were computed, and correlation coefficients were calculated by comparing PAC and motor score changes across four stages of the BCI therapy runs.

Data availability

The data will be made available upon reasonable request to the corresponding author.

Results

Motor rehabilitation

Following 12 weeks of contralesionally controlled BCI therapy, all chronic stroke patients showed an increase in UEFM score which served as a primary motor outcome assessment tool. Patients achieved a mean increase of 8.03 points in UEFM (Table 1). This increase implies clinically meaningful motor recovery surpassing the minimal clinically significant difference (MCID) threshold of 5.25 points score increase.⁹³ Overall, 14 out of the 17 patients reached the MCID.

Figure 2A shows the mean primary and secondary motor assessment scores across four stages of the BCI therapy runs (Pre-BCI, earlier, later and final Post-BCI). Motor scores were examined in an ANOVA with within-subjects factor *Stage* (1)–(4) (see the ‘Statistical analyses’ section).

UEFM: the main effect of the stage proved significant, $F(3,48) = 38.11$, $P < 0.001$, indicating that UEFM scores changed across stages of BCI therapy runs. The first Helmert contrast compared motor scores during Pre-BCI with those during Post-BCI runs, revealing a significant difference for each contrast (Pre-BCI versus earlier, later or final Post-BCI, $P = 0.002$, 0.009 and 0.000003 , respectively). The second and third Helmert contrasts compared Post-BCI runs with one another: earlier versus later or final Post-BCI, and later versus final Post-BCI, respectively, revealing significant differences in contrasts with final Post-BCI (earlier versus final Post-BCI and later versus final Post-BCI, $P = 0.0008$ and 0.002 , respectively).

AMAT: the main effect of the stage proved significant, $F(3,48) = 16.15$, $P < 0.001$, indicating that AMAT scores changed across stages of BCI therapy runs. The first Helmert contrast revealed a significant difference between Pre-BCI versus Post-BCI runs (Pre-BCI versus earlier, later or final Post-BCI, $P = 0.01$, 0.002 and 0.0001 , respectively). The second Helmert contrast revealed a significant difference between earlier versus final Post-BCI ($P = 0.03$). The third Helmert contrast did not yield significant results (later versus final Post-BCI, $P = 0.08$).

Motricity index: the main effect of the stage proved significant, $F(3,48) = 18.71$, $P < 0.001$, indicating that MI scores changed across stages of BCI therapy runs. The first Helmert contrast revealed a significant difference between Pre-BCI versus Post-BCI runs (Pre-BCI versus earlier, later or final Post-BCI, $P = 0.007$, 0.002 and 0.0001 , respectively). The second and third Helmert contrasts were not significant (earlier versus later or final Post-BCI, $P = 0.94$ and 0.14 , respectively; later versus final Post-BCI, $P = 0.08$).

Grip, elbow MAS, wrist MAS: the main effect of the stage did not prove significant, $F(3,48) = 2.19$, 0.19 and 0.87 , $P = 0.12$, 0.90 and 0.46 , respectively, excluding significant changes in these motor assessment scores with the use of a BCI therapy.

EEG effects

Modulation of PAC

Theta–gamma PAC. Figure 2B shows the mean theta–gamma PAC values across four stages of the BCI therapy runs (Pre-BCI, earlier, later and final Post-BCI) separately for each electrode (also see Figs 3A and 4, top panels). PACs were examined in an ANOVA with within-subjects factors *Stage* (1)–(4) \times *Electrode* (1)–(6) (see the ‘Statistical analyses’ section). The main effect of the stage, $F(3,240) = 16.48$, $P < 0.001$, and interaction *Stage* \times *Electrode*, $F(3,240) = 17.61$, $P < 0.001$, were significant, indicating an overall difference between stages with regard to PACs as a function of the electrode. We conducted separate ANOVAs for each electrode.

C3 electrode: the main effect of the stage proved significant, $F(3,48) = 27.23$, $P < 0.001$, indicating that PAC values changed across stages of BCI therapy runs. The first Helmert contrast revealed a significant difference between Pre-BCI versus later or final Post-BCI ($P = 0.0004$ and 0.00002 , respectively), while Pre-BCI versus earlier Post-BCI contrast was not significant ($P = 0.13$). The second Helmert contrast revealed a significant difference between earlier versus later or final Post-BCI ($P = 0.02$ and $P = 0.001$, respectively). The third Helmert contrast did not yield significant results (later versus final Post-BCI, $P = 0.16$).

C4 electrode: the main effect of the stage proved significant, $F(3,48) = 35.44$, $P < 0.001$, indicating that PAC values changed across stages of BCI therapy runs. The first Helmert contrast revealed a significant difference between Pre-BCI versus later or final Post-BCI ($P = 0.0002$ and 0.000003 , respectively), while Pre-BCI versus earlier Post-BCI contrast was not significant ($P = 0.09$). The second and third Helmert contrasts revealed a significant difference between

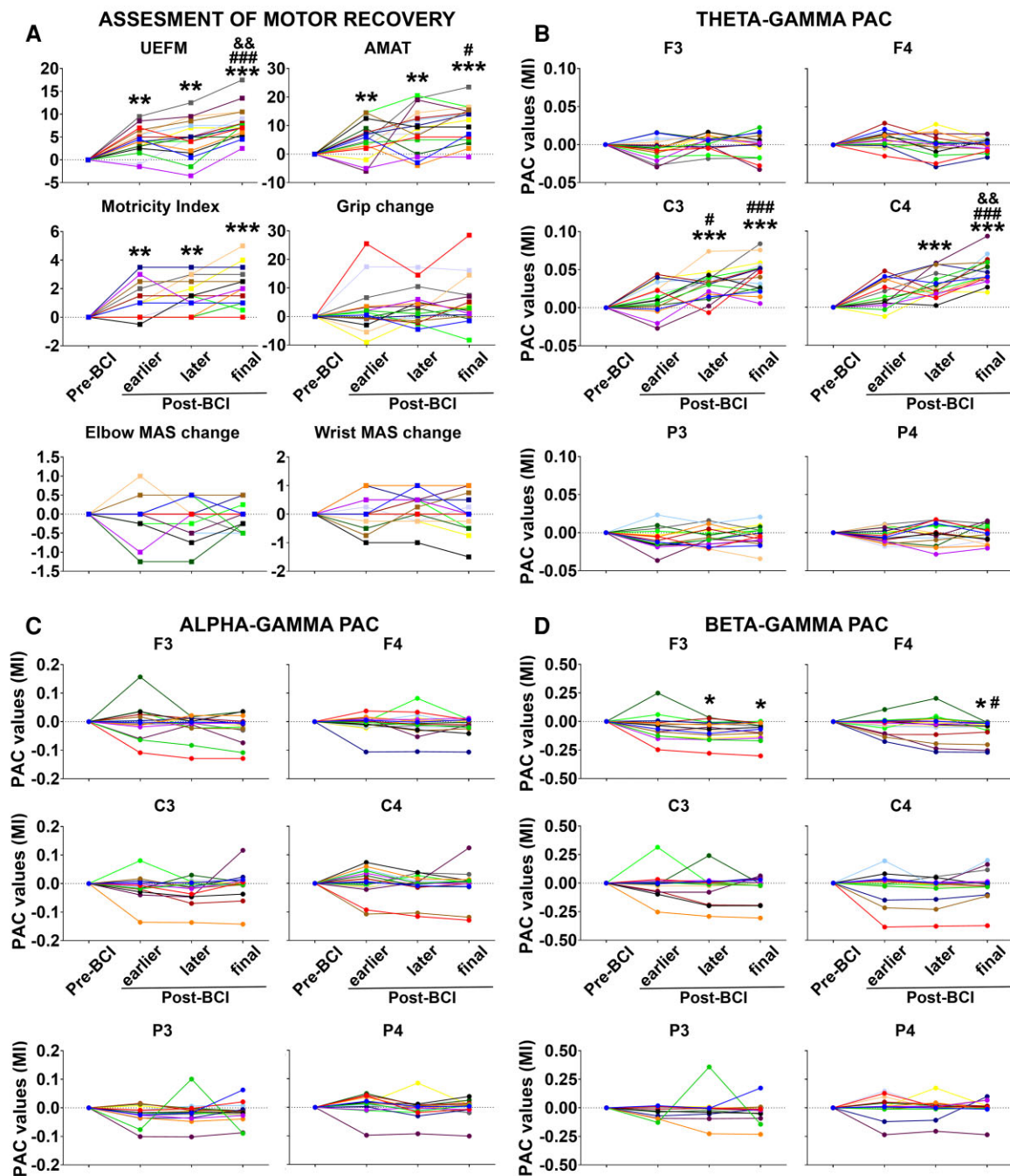
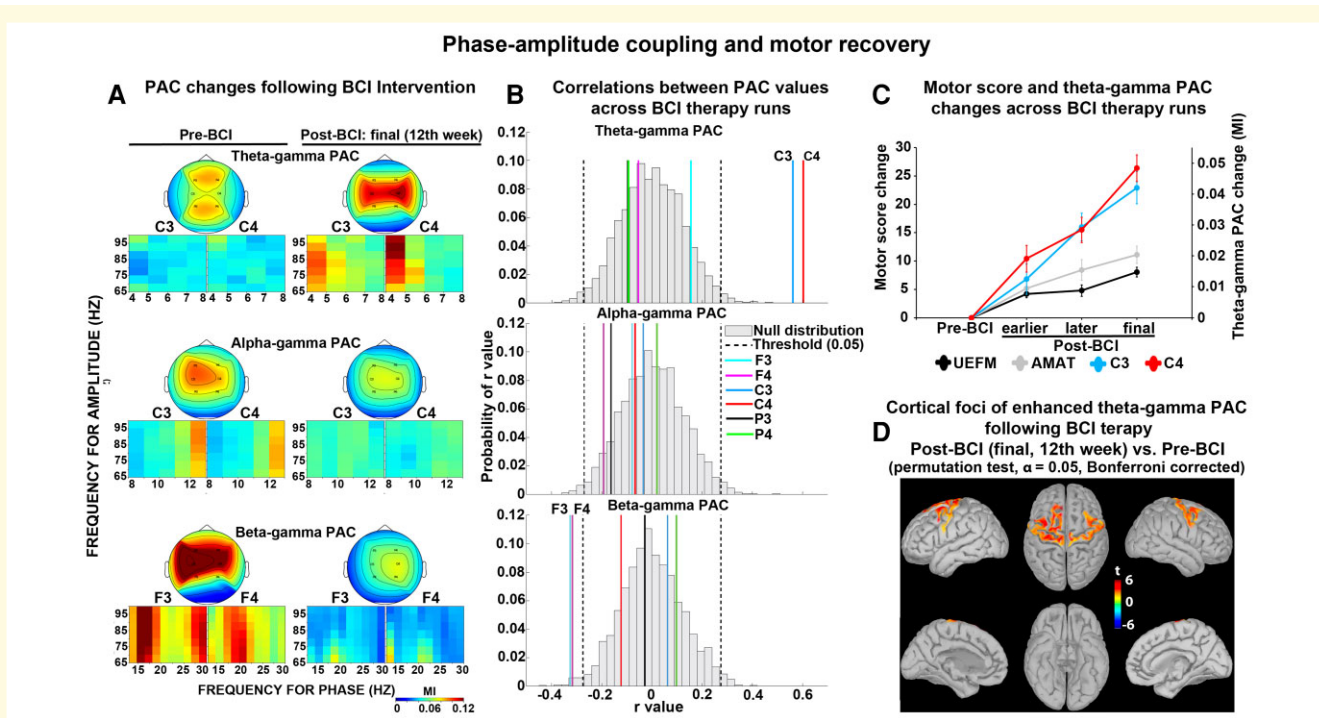


Figure 2 Mean motor assessment scores and PAC values. (A) Longitudinal changes in motor assessment scores from baseline through 12 weeks of BCI intervention. Each motor assessment tool represented as a separate graph. Y-axis, motor score; X-axis, stages of BCI therapy runs. UEFM, upper extremity Fugl-Meyer; AMAT, Arm Motor Ability Test; MAS, modified Ashworth Scale. (B–D) Theta-, alpha- and beta-gamma PAC values, respectively, across BCI therapy runs. PAC values (mean \pm SEM) for each electrode from baseline through 12 weeks of BCI intervention. Y-axis, PAC value; X-axis, stages of BCI therapy runs. Patients were depicted in 17 different colours. Significance levels were based on the pairwise comparisons in ANOVA ($N = 17$; Bonferroni corrected). * ** and *** symbols: $P \leq 0.05$, 0.01 and 0.001 for Pre-BCI versus earlier, later or final Post-BCI contrasts; # and ### symbols: $P \leq 0.05$ and 0.001 for earlier versus later or earlier versus final Post-BCI contrasts; && symbol: $P \leq 0.01$ for later versus final Post-BCI contrasts; MI, modulation index; Pre-BCI: before initiating therapy; earlier Post-BCI, 4th week; later Post-BCI, 8th week; final Post-BCI, 12th week.

earlier or later versus final Post-BCI ($P = 0.001$ and 0.002 , respectively), while the earlier versus later Post-BCI comparison did not prove significant ($P = 0.28$).

These effects have largely been replicated when electrodes over the motor region were grouped together based on lesion side (see [Supplementary Fig. 2A](#), left panels) indicating



enhancement of theta-gamma PAC over both ipsilesional and contralesional motor cortices following BCI intervention.

F3, F4, P3 and P4 electrodes: the main effect of the stage did not prove significant, $F(3,48) = 2.47, 2.36, 3.01$ and 0.69 , and $P = 0.07, 0.08, 0.06$ and 0.57 , respectively, indicating that PACs at these electrodes were not significantly modulated with the use of a BCI therapy.

Alpha-gamma PAC. The same confirmatory ANOVA (see theta-gamma PAC results) was applied to examine possible alpha-gamma PAC modulation across BCI therapy runs (Fig. 2C, also see Figs 3A and 4, middle panels). In the *Stage \times Electrode* ANOVA, the main effect of the stage, $F(3,240) = 1.34$, $P = 0.22$, and interaction *Stage \times Electrode*, $F(3,240) = 1.06$, $P = 0.39$, did not prove significant. These findings indicate that BCI therapy did not have significant effects on alpha-gamma PAC at any electrode. The lack of alpha-gamma PAC effects was not dependent on the lesion side (see Supplementary Fig. 2A, middle panels).

Beta-gamma PAC. In the same confirmatory ANOVA (see theta-gamma PAC results), the main effect of the stage,

$F(3,240) = 0.59$, $P = 0.62$, was not significant but interaction *Stage \times Electrode*, $F(3,240) = 2.13$, $P = 0.04$, proved significant, indicating an overall difference between stages with regard to PACs as a function of electrode (Fig. 2D, also see Figs 3A and 4, bottom panels). We conducted separate ANOVAs for each electrode.

F3 electrode: the main effect of the stage proved significant, $F(3,48) = 5.28$, $P = 0.001$, indicating that PAC values changed across stages of the BCI therapy runs. The first Helmert contrast revealed a significant difference between Pre-BCI versus later or final Post-BCI ($P = 0.03$ and 0.01 , respectively), while Pre-BCI versus earlier Post-BCI contrast was not significant ($P = 0.93$). The second and third Helmert contrasts did not reveal significant differences between Post-BCI runs (earlier versus later or final Post-BCI, $P = 0.34$ and 0.41 , respectively; later versus final Post-BCI, $P = 0.92$).

F4 electrode: the main effect of the stage proved significant, $F(3,48) = 4.48$, $P = 0.007$, indicating that PAC values changed across stages of the BCI therapy runs. The first Helmert contrast revealed a significant difference between Pre-BCI versus final Post-BCI ($P = 0.03$), while Pre-BCI versus earlier or later

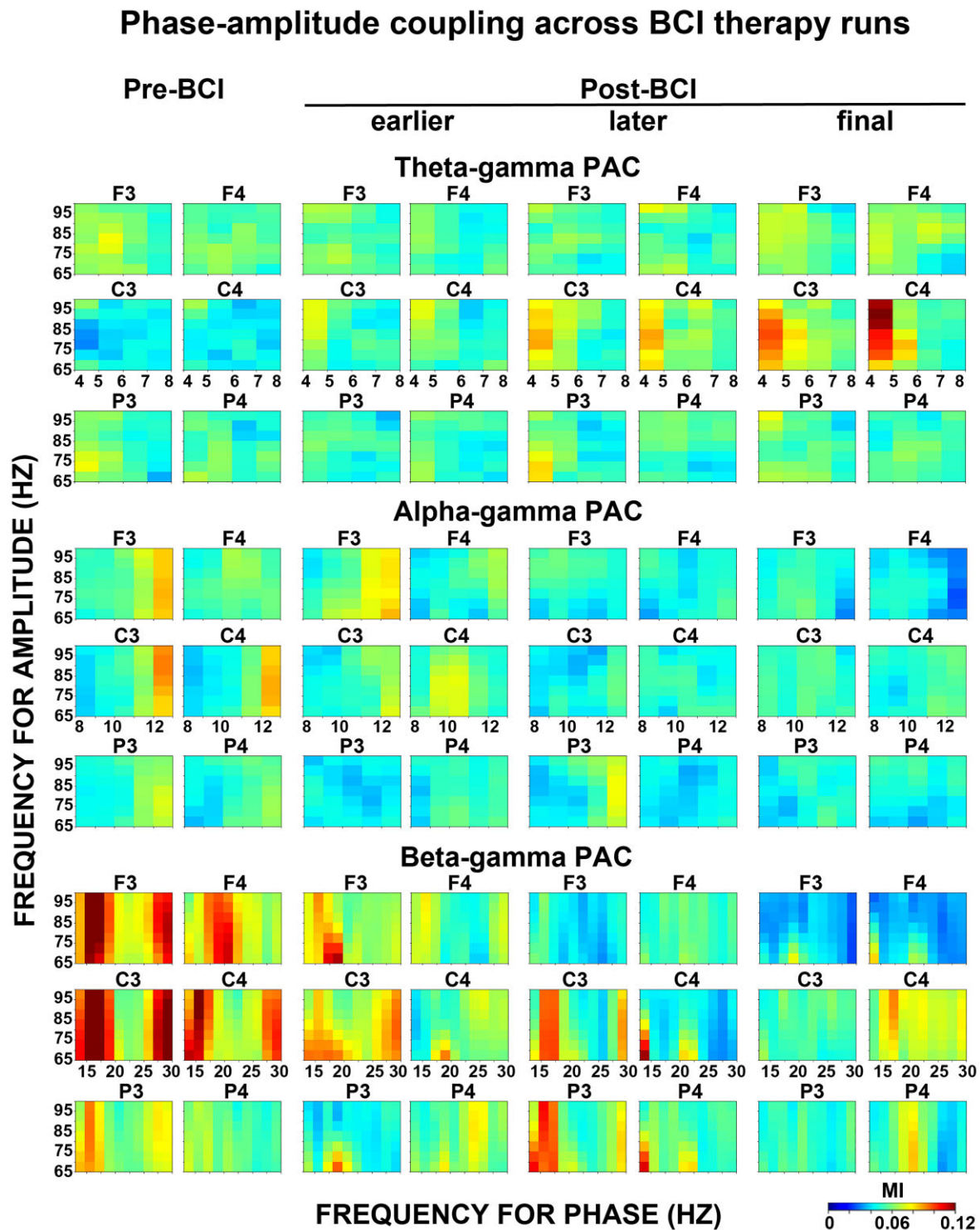


Figure 4 PAC across BCI therapy runs. Modulation of the amplitude of gamma oscillations by phase of theta, alpha or beta oscillations (top panels: theta–gamma PAC; middle panels: alpha–gamma PAC; bottom panels: theta–gamma PAC). PAC plots were shown for each electrode. Pre-BCI, before initiating therapy; earlier Post-BCI, 4th week; later Post-BCI, 8th week; final Post-BCI, 12th week. Y-axis, frequency for amplitude (gamma range); X-axis, frequency for phase (theta, alpha or beta range); MI, modulation index.

Post-BCI contrasts were not significant ($P = 0.47$ and 0.91 , respectively). The second Helmert contrast revealed the only significant difference between earlier versus final Post-BCI

($P = 0.04$), but earlier versus later Post-BCI contrast was not significant ($P = 0.94$). The third Helmert contrast did not prove significant (later versus final Post-BCI, $P = 0.25$).

These effects have largely been replicated when electrodes over the frontal region were grouped together based on the lesion side (see [Supplementary Fig. 2A](#), right panels) indicating reduction of beta–gamma PAC over both ipsilesional and contralesional frontal cortices following BCI intervention.

C3, C4, P3 and P4 electrodes: the main effect of the stage did not prove significant, $F(1,38)=0.69, 1.45, 0.64$ and 0.03 , and $P=0.56, 0.24, 0.59$ and 0.81 , respectively, indicating that PACs at these electrodes were not significantly modulated with the use of a BCI therapy.

Cross-electrode theta/alpha/beta–gamma PAC

The same PAC findings have been replicated when neighbouring electrodes were used to generate the lower (theta, alpha and beta) and higher (high gamma) frequency signals to compute PAC (see [Supplementary Fig. 3A and B](#)). This excludes the possible effects of filtering on the PAC results reported above.

Spearman correlation analyses

Correlations between PAC values across BCI therapy runs

Correlations between PAC values across BCI therapy runs are shown in [Fig. 3B](#). Across-therapy run correlation coefficients for theta–gamma PAC at the C3 and C4 electrodes were 0.56 ($P=0.00008$) and 0.60 ($P=0.00004$), respectively, suggesting significant positive correlations. Theta–gamma PAC at the F3, F4, P3 and P4 electrodes showed poor correlations ($r=0.15, -0.05, -0.10, -0.09$, and $P=0.20, 0.65, 0.42, 0.43$, respectively) ([Fig. 3B](#), top row). Alpha–gamma PAC did not correlate significantly across therapy runs (F3, F4, C3, C4, P3 and P4 electrodes: $r=-0.08, -0.19, -0.03, -0.07, -0.16, 0.02$, and $P=0.51, 0.11, 0.77, 0.58, 0.18, 0.86$, respectively) ([Fig. 3B](#), middle row). Beta–gamma PAC showed significant correlations at the F3 and F4 electrodes, with across-therapy run correlation coefficients of -0.34 ($P=0.01$) and -0.33 ($P=0.02$), respectively. Beta–gamma PAC at the C3, C4, P3 and P4 electrodes showed poor correlations ($r=0.06, -0.12, -0.03, 0.10$ and $P=0.62, 0.32, 0.82, 0.43$, respectively) ([Fig. 3B](#), bottom row). These results have been replicated when electrodes over the right and left hemispheres were grouped together based on lesion side (see [Supplementary Fig. 2B](#)).

Correlations between motor recovery and theta–gamma PAC

Correlations between changes in motor scores and theta–gamma PACs across BCI therapy runs relative to Pre-BCI are shown in [Fig. 5A](#) (also see [Fig. 3C](#)). Correlation coefficients between UEFM score change and PAC change at the C3 and C4 electrodes were 0.51 ($P=0.0001$) and 0.49 ($P=0.0002$), respectively, suggesting significant positive correlations. Similarly, AMAT score change showed significant correlation with PAC change at the C3 and C4

electrodes, with correlation coefficients of 0.52 ($P=0.0001$) and 0.39 ($P=0.004$), respectively. Theta–gamma PAC increase at both ipsilesional and contralesional motor electrodes showed significant correlations with UEFM and AMAT score changes (see [Supplementary Fig. 2C](#), left panels). MI score change and PAC change at the C3 electrode correlated significantly 0.33 ($P=0.02$), while PAC change at the C4 showed poor correlation with MI score change 0.02 ($P=0.88$). Grip, elbow MAS and wrist MAS changes did not correlate significantly with PAC change at the C3 and C4 electrodes ($r=0.06, 0.13$ and $P=0.68, 0.35$; $r=0.03, 0.15$ and $P=0.84, 0.28$; $r=-0.22, 0.23$ and $P=0.12, 0.10$, respectively).

No correlation between motor recovery and beta–gamma PAC

Correlations between changes in motor scores and beta–gamma PACs across BCI therapy runs relative to Pre-BCI are shown in [Fig. 5B](#). UEFM, AMAT, MI, Grip, elbow MAS and wrist MAS changes correlated poorly with PAC change at the F3 and F4 electrodes (F3 electrode, $r=-0.07, -0.15, -0.22, -0.16, -0.17, 0.07$ and $P=0.62, 0.29, 0.12, 0.26, 0.23$ and 0.62 , respectively; F4 electrode, $r=-0.10, -0.19, 0.12, 0.21, -0.13$ and -0.04 , and $P=0.48, 0.16, 0.42, 0.14, 0.38$ and 0.80 , respectively). The lack of correlation effects was not dependent on the lesion side (see [Supplementary Fig. 2C](#), right panels).

Sources of theta–gamma PAC increase following BCI therapy

To examine the sources of theta–gamma PAC increase during motor recovery relative to baseline, source estimation was calculated. Compared with Pre-BCI, the final Post-BCI resulted in significant foci of theta–gamma PAC increase ([Fig. 3D](#)). These foci were located in the cortical areas representing hand regions of the primary motor cortex on the left and right cerebral hemispheres (left-hand M1, MNI: $-36, -19, 48$, $P=0.001$; right-hand M1, MNI: $38, -18, 45$, $P=0.004$).

Power spectral density

[Figure 6](#) shows PSD plots for Post-BCI conditions relative to Pre-BCI baseline. The same confirmatory ANOVA (see theta–gamma PAC results) was applied to each frequency band examining the possible PSD modulation with the use of a BCI therapy. In the *Stage* \times *Electrode* ANOVA, the main effect of the stage did not prove significant, $F(3,240)=1.35, 1.22, 1.03$ and 0.85 , and $P=0.21, 0.29, 0.43$ and 0.56 , for theta, alpha, beta and gamma band PSDs, respectively. Likewise, the interaction *Stage* \times *Electrode* was not significant, $F(3,240)=0.73, 1.07, 1.13$ and 0.95 , and $P=0.66, 0.41, 0.38$ and 0.45 , for theta, alpha, beta and gamma band PSDs, respectively. These findings indicate that BCI therapy did not have significant effects on PSDs across any frequency band or electrode, and found PAC modulation effects were not driven by underlying PSD changes.

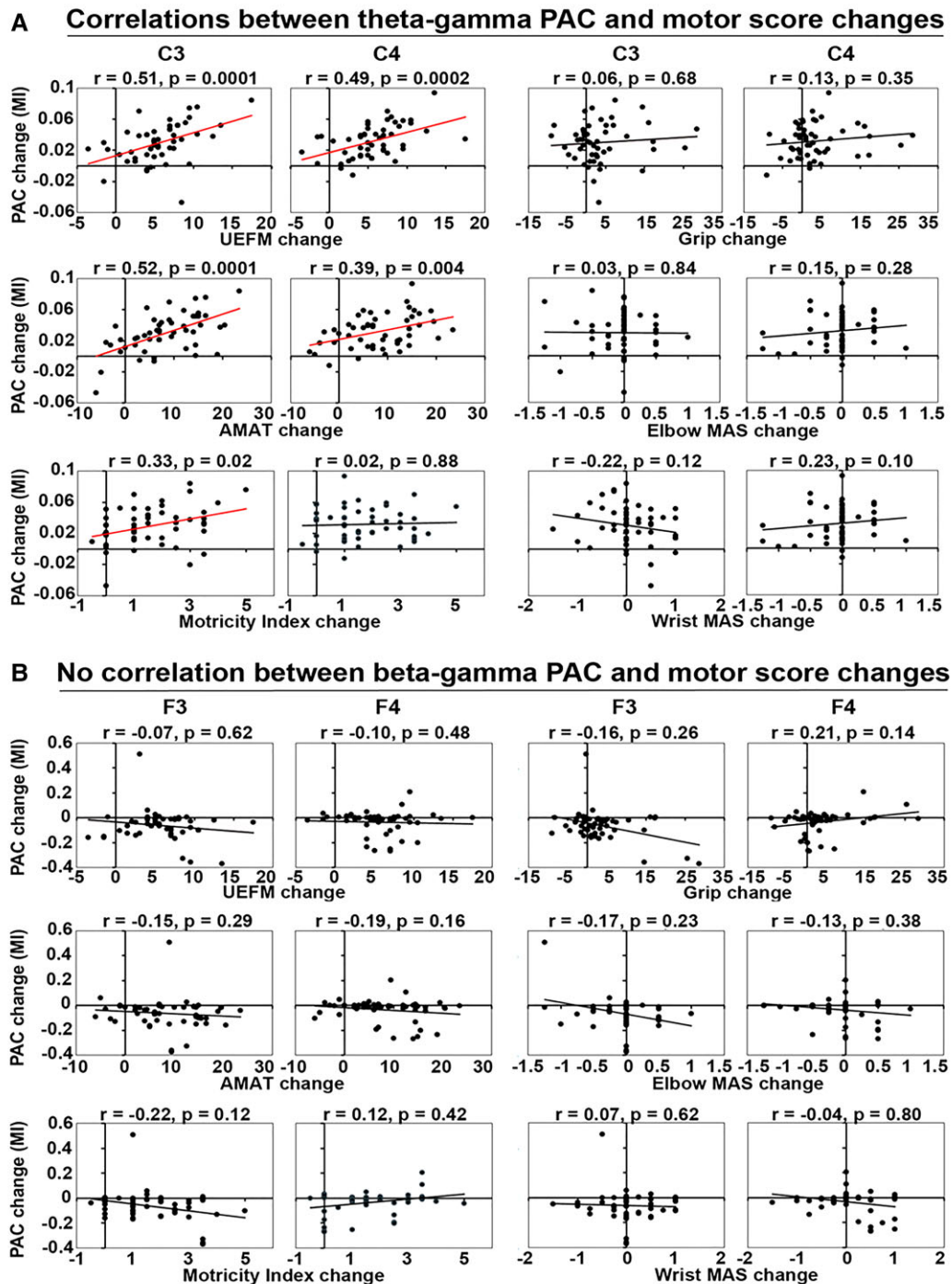


Figure 5 Relationships between motor recovery and PAC change. Spearman rank correlations were run between changes in motor scores and theta-, beta-gamma PAC values across BCI therapy runs relative to Pre-BCI baseline ($N = 51$). Significance thresholds were set at $P \leq 0.05$. **(A)** Significant correlations between motor recovery and theta-gamma PAC changes at the C3 and C4 electrodes (UEFM: $r = 0.51$, 0.49 and $P = 0.0001$, 0.0002 ; AMAT: $r = 0.52$, 0.39 and $P = 0.0001$, 0.004 ; MI: $r = 0.33$ and $P = 0.02$). Other measures showed no significant correlations (MI: $r = 0.02$ and $P = 0.88$; Grip: $r = 0.06$, 0.13 and $P = 0.68$, 0.35 ; Elbow MAS: $r = 0.03$, 0.15 and $P = 0.84$, 0.28 ; Wrist MAS: $r = -0.22$, 0.23 , and $P = 0.12$, 0.10). **(B)** No significant correlations have been detected between motor recovery and beta-gamma PAC changes at the F3 and F4 electrodes (UEFM: $r = -0.07$, -0.10 , and $P = 0.62$, 0.48 ; AMAT: $r = -0.15$, -0.19 , and $P = 0.29$, 0.16 ; MI: $r = -0.22$, 0.12 and $P = 0.12$, 0.42 ; Grip: $r = -0.16$, 0.21 and $P = 0.26$, 0.14 ; Elbow MAS: $r = -0.17$, -0.13 , and $P = 0.23$, 0.38 ; Wrist MAS: $r = 0.07$, -0.04 , and $P = 0.62$, 0.80). Y-axis, PAC change; X-axis, motor score change. MI, modulation index; UEFM, upper extremity Fugl-Meyer; AMAT: Arm Motor Ability Test; MAS: modified Ashworth Scale.

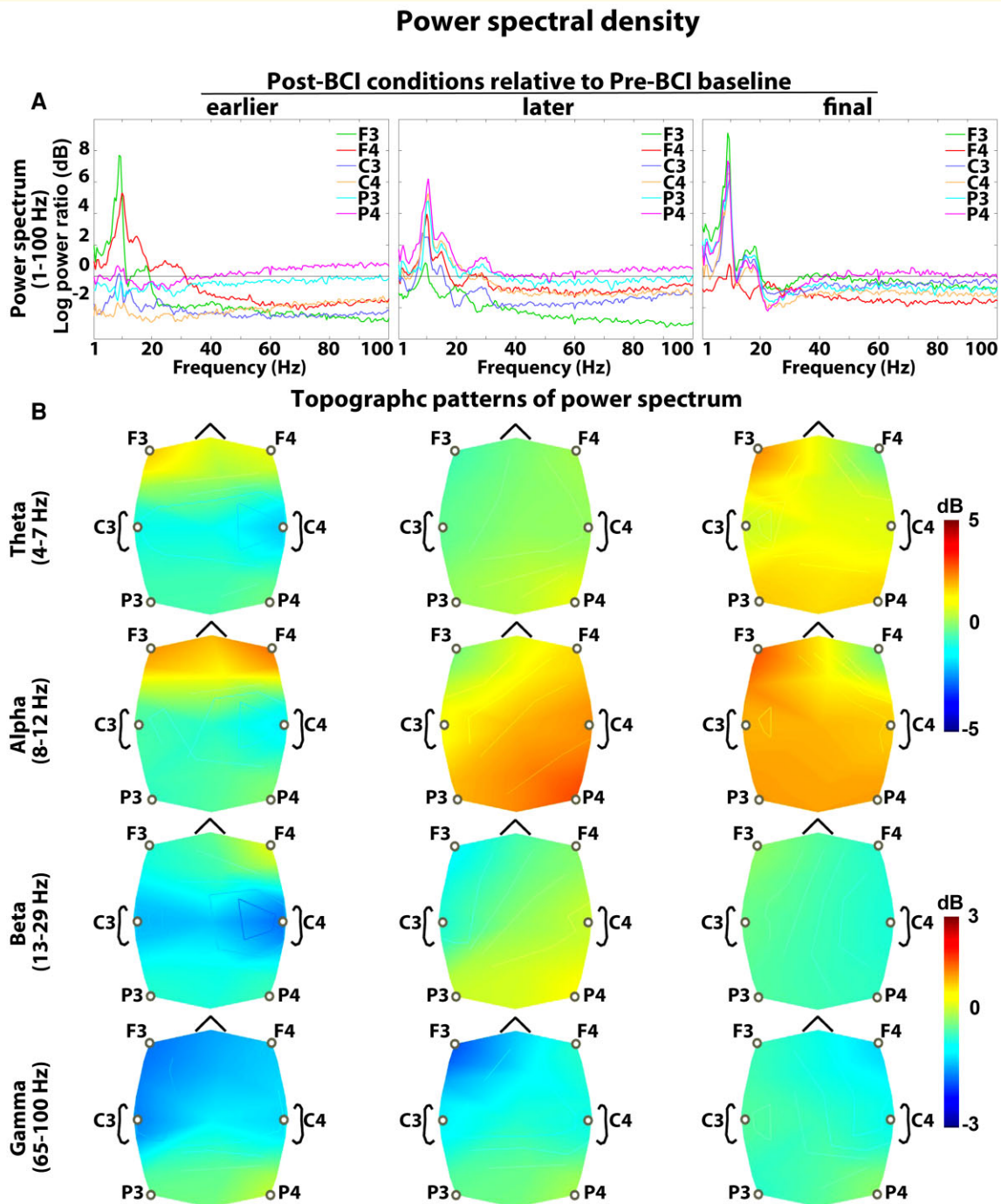


Figure 6 Power spectral density. (A) Average power spectra across all patients. EEG electrodes were depicted in six different colours. (B) Topographic representation of PSD for theta, alpha, beta and gamma frequency bands. The power spectra for Post-BCI runs were contrasted with Pre-BCI baseline. Pre-BCI, before initiating therapy; earlier Post-BCI, 4th week; later Post-BCI, 8th week; final Post-BCI, 12th week. Changes in PSD values across BCI therapy runs were assessed by repeated-measures ANOVA ($N = 17$; Bonferroni corrected). BCI intervention did not result in significant modulation of power spectrum in any frequency band.

Discussion

In the setting of chronic stroke, this study demonstrates that motor rehabilitation using contralesionally controlled BCI training for 12 weeks induced cortical changes reflected in resting-state PAC measures. A key electrophysiological

finding is the bilateral amplification of theta–gamma PAC at the C3 and C4 motor electrodes over the course of rehabilitation. Chronic stroke patients achieved clinically significant upper extremity motor recovery despite being over 6 months post-stroke. Importantly, there were significant positive correlations between theta–gamma PAC at the C3

and C4 motor electrodes, and motor assessment scores across BCI therapy runs. The sources of theta–gamma PAC increase following BCI therapy were mostly located in the hand regions of M1 on the left and right cerebral hemispheres. We also observed a bilateral decrease in beta–gamma PAC at the F3 and F4 frontal electrodes following the therapy. However, these effects did not show significant correlations with motor recovery. Moreover, alpha–gamma PAC was not modulated by BCI. Taken together, these findings support the notion that theta–gamma PAC amplification over the motor cortex is associated with functional motor improvement, and this may represent a mechanism for motor learning with the use of a BCI in chronic stroke patients.

CFC, interaction between neuronal oscillations at different frequency bands, has been gaining growing interest in the recent years.^{45,55,69,94,95} It has been described in animals,^{46,47,57,96,97} and humans,^{55,69,95} and in multiple brain regions, including hippocampus,^{46,50,66} subcortical nuclei^{45,95} and neocortex.^{55,69} Although the exact functional significance of CFC remains unclear, it has been found to manifest in response to sensory inputs and cognitive or motor tasks, and it is believed to be a major mechanism of information processing by which brain areas spatially and temporally coordinate their activity.^{44,51,98} The best-known example of CFC, namely the theta–gamma PAC, has consistently been demonstrated in relation to learning in the rodent hippocampus,^{46,65–67,99} linking this phenomenon to hippocampal function in learning and memory.^{100–102} The magnitude of theta–gamma coupling during learning of item–context associations was correlated with the high accuracy of behavioural performance, which increased during the course of learning.⁵⁴ Studies adopting short- and working-memory paradigms have shown that theta–gamma coupling is associated with encoding and retrieval of verbal and visual information.^{103,104} These findings support the view that the theta–gamma interaction contributes to memory and learning processes. However, very little is known about the role of theta–gamma PAC in non-hippocampal-dependent learning (e.g. motor learning). It has been suggested that M1 gamma activity has pro-kinetic role that is further supported by its increase within M1 in the hyperkinetic states experienced by patients with Parkinson's disease.¹⁰⁵ Physiologically, M1 gamma activity is locked to the peaks of ongoing theta activity and thus simultaneous theta and gamma oscillatory activities in M1 show PAC.⁶⁹ A decrease in M1 gamma-aminobutyric acid-ergic (GABAergic) activity predicts motor learning ability¹⁰⁶ and represents a central mechanism for motor plasticity.^{107–111} Interestingly, theta–gamma coupling within M1 emerged spontaneously when GABA activity is blocked.¹¹² Given the role of decreased GABAergic activity in motor learning and plasticity, and its relationship with theta–gamma coupling, it may be suggested that synchronization of gamma and theta oscillations represents an important signature of motor learning.

In this study, we tested a hypothesis about the role of theta–gamma PAC in motor learning. The current study is the

first to characterize the dynamic changes in EEG oscillatory synchronization associated with the improvement of motor skills throughout BCI training. Our main novel finding is that the motor recovery was associated with enhanced gamma–theta coupling in the motor areas. Enhancement of theta–gamma coupling throughout BCI therapy, and most importantly, its positive correlation with motor recovery indices suggests that theta–gamma coupling is involved in the processing of motor learning. This conclusion is in agreement with the role of theta power and theta–gamma interaction in spatial and motor learning.^{70,113,114} We also found that theta–gamma PAC synchronously and constantly increased in the later therapy sessions compared with the early ones. This might reflect mechanisms promoting the development of new and more efficient motor plans and the integration of this information into a new internal model. Our findings support previous studies showing learning-related involvement of the primary sensory-motor cortex.^{114–117}

In order to demonstrate the exclusive role of theta–gamma coupling in motor learning, we tested couplings between other frequency bands as well. Theta– and beta–gamma PAC both enhanced significantly following the treatment, yet only theta–gamma coupling amplification showed a significant correlation with motor recovery. Moreover, no significant effects were found with regard to alpha–gamma PAC. The lack of significant correlation of alpha– and beta–gamma PAC modulation with motor recovery emphasizes their important distinction from theta–gamma PAC in the context of BCI-driven motor recovery. It is important to note, however, that alpha– and beta–gamma PAC modulation have been associated with other motor and non-motor phenomenon. Exaggerated coupling between beta and gamma oscillations has been detected in basal ganglia, as well as motor and frontal cortices of patients with Parkinson's disease.^{118,119} Relationship of beta–gamma PAC with motor symptoms of Parkinson's disease is not fully understood. Nevertheless, reductions in the beta–gamma PAC through deep brain stimulation correlated with symptom improvement in Parkinson's disease,^{118,120–122} suggesting that enhanced beta–gamma coupling might be implicated in bradykinesia and rigidity. In our study, chronic stroke patients showed enhanced beta–gamma PAC over the frontal areas which was reduced significantly following BCI intervention. The lack of correlation between bifrontal beta–gamma PAC decrease and motor recovery can be explained by the fact that the frontal cortex is predominantly involved in executive and other cognitive functions rather than motor functions.^{123,124} Thus, reduced beta–gamma coupling in frontal areas may be involved in the mechanism underlying behavioural domains outside of motor control.

In healthy humans, brief periods of low-frequency oscillations (LFOs) below 4 Hz appear at motor cortices prior to movement onset.^{125,126} Recent work has shown the role of transient movement-related LFOs in the delta and lower theta band over the motor cortical areas during skilled upper-limb tasks.^{125,127–129} Cortical circuit dysfunction after stroke led to substantially diminished LFOs in proportion to the motor

deficit. The re-emergence of LFOs paralleled motor recovery, with a stronger increase in patients who showed a better recovery.^{130,131} Thus, LFOs were identified as an important neurophysiological marker of skilled motor control. In this study, we explored possible changes in resting cortical oscillatory activity following BCI intervention. It was important to establish whether coupling between neuronal oscillations at two different frequency bands was more functionally important than either of those underlying rhythms alone. We found that BCI produced modest non-significant changes in the resting power spectrum across different frequency bands. This implies that theta–gamma PAC amplification effects were driven by synchronization of underlying resting gamma and theta powers rather than changes in their magnitude. Our findings extend the body of previous work by linking the amplification of resting theta–gamma PAC dynamics in the motor cortex to motor recovery.

Limitations

This study has several limitations worth noting. First, our sample size was limited to 17 participants. Therefore, further studies with a larger sample size to validate these preliminary results are warranted. Those studies should also include fMRI assessment to assess the effect of contralesionally driven BCI therapy on motor system functional organization. Secondly, the study was conducted under the assumption that motor deficits were stable in the chronic stage of stroke and thus we did not have a separate BCI control group. Indeed, motor deficits have been shown to improve poorly in the chronic stage of stroke.^{6–8,132} Moreover, sham BCI therapy in a different study of motor recovery in stroke patients failed to promote recovery comparable to BCI therapy.¹⁹ Taken together, we therefore attribute motor function improvement and associated electrophysiological changes found in this study primarily to BCI intervention. Carefully designed external multicentre studies are needed to validate the constructed model. Thirdly, our EEG recording system had a limited number of electrodes negatively affecting the spatial specificity of our findings. Finally, while the phenomenon of theta–gamma coupling was a strong finding in this study with the use of BCI, we cannot say at this time whether it is specific to BCI techniques or whether this is a more generalized phenomenon with other rehabilitation methods in the chronic phase of stroke.

Conclusion

This study investigated the electrophysiological correlates of motor recovery in chronic stroke patients using a contralesionally controlled BCI therapy. Specifically, we tested whether theta–gamma PAC was associated with motor recovery. Concomitant with the BCI-induced functional improvement, we found enhanced theta–gamma PAC over motor regions correlated positively with these gains in motor function. These findings support the notion that specific CFC dynamics in the brain likely play a mechanistic role in mediating motor

recovery in the chronic phase of stroke recovery. Further research into these neural correlates of stroke recovery will be required to define the specificity and generalizability of these frequency interactions to different therapy strategies.

Acknowledgements

The authors thank study participants for their time and effort.

Funding

This work was supported by National Institutes of Health (NIH) R21NS102696 (E.C.L. and A.C.) and National Institute of Biomedical Imaging and Bioengineering (NIBIB) P41-EB018783 (E.C.L.).

Competing interests

E.C.L. owns stock in Neuroolutions, Inner Cosmos and Sora Neuroscience. Washington University owns stock in Neuroolutions. This work and E.C.L. have had their conflict of interest rigorously evaluated and managed throughout this study and with creation of this manuscript. Other authors have nothing to disclose.

Supplementary material

Supplementary material is available at *Brain Communications* online.

References

1. Lawrence ES, Coshall C, Dundas R, *et al.* Estimates of the prevalence of acute stroke impairments and disability in a multiethnic population. *Stroke*. 2001;32:1279–1284.
2. Sunderland A, Tinson D, Bradley L, Hewer RL. Arm function after stroke. An evaluation of grip strength as a measure of recovery and a prognostic indicator. *J Neurol Neurosurg Psychiatry*. 1989;52:1267–1272.
3. Wade DT, Langton-Hewer R, Wood VA, Skilbeck CE, Ismail HM. The hemiplegic arm after stroke: Measurement and recovery. *J Neurol Neurosurg Psychiatry*. 1983;46:521–524.
4. Jørgensen HS, Nakayama H, Raaschou HO, Vive-Larsen J, Stoier M, Olsen TS. Outcome and time course of recovery in stroke. Part II: Time course of recovery. The Copenhagen stroke study. *Arch Phys Med Rehabil*. 1995;76:406–412.
5. Lloyd-Jones D, Adams R, Carnethon M, *et al.* Heart disease and stroke statistics—2009 update: A report from the American heart association statistics committee and stroke statistics subcommittee. *Circulation*. 2009;119:480–486.
6. Hatem SM, Saussez G, Della Faille M, *et al.* Rehabilitation of motor function after stroke: A multiple systematic review focused on techniques to stimulate upper extremity recovery. *Front Hum Neurosci*. 2016;10:442.
7. Kwakkel G, Kollen B, Lindeman E. Understanding the pattern of functional recovery after stroke: Facts and theories. *Restor Neurol Neurosci*. 2004;22:281–299.

8. Langhorne P, Bernhardt J, Kwakkel G. Stroke rehabilitation. *Lancet*. 2011;377:1693–1702.
9. Rodgers H, Bosomworth H, Krebs HI, et al. Robot assisted training for the upper limb after stroke (RATULS): A multicentre randomised controlled trial. *Lancet*. 2019;394:51–62.
10. Levy RM, Harvey RL, Kissela BM, et al. Epidural electrical stimulation for stroke rehabilitation: Results of the prospective, multicenter, randomized, single-blinded everest trial. *Neurorehabil Neural Repair*. 2016;30:107–119.
11. Harvey RL, Edwards D, Dunning K, et al. Randomized sham-controlled trial of navigated repetitive transcranial magnetic stimulation for motor recovery in stroke. *Stroke*. 2018;49:2138–2146.
12. Dawson J, Liu CY, Francisco GE, et al. Vagus nerve stimulation paired with rehabilitation for upper limb motor function after ischaemic stroke (VNS-REHAB): A randomised, blinded, pivotal, device trial. *Lancet*. 2021;397:1545–1553.
13. Dawson J, Pierce D, Dixit A, et al. Safety, feasibility, and efficacy of vagus nerve stimulation paired with upper-limb rehabilitation after ischemic stroke. *Stroke*. 2016;47:143–150.
14. Kimberley TJ, Pierce D, Prudente CN, et al. Vagus nerve stimulation paired with upper limb rehabilitation after chronic stroke. *Stroke*. 2018;49:2789–2792.
15. Engineer ND, Kimberley TJ, Prudente CN, Dawson J, Tarver WB, Hays SA. Targeted vagus nerve stimulation for rehabilitation after stroke. *Front Neurosci*. 2019;13:280.
16. Hays SA, Rennaker RL, Kilgard MP. Targeting plasticity with vagus nerve stimulation to treat neurological disease. *Prog Brain Res*. 2013;207:275–299.
17. Ang KK, Chua KS, Phua KS, et al. A randomized controlled trial of EEG-based motor imagery brain-computer interface robotic rehabilitation for stroke. *Clin EEG Neurosci*. 2015;46:310–320.
18. Ono T, Shindo K, Kawashima K, et al. Brain-computer interface with somatosensory feedback improves functional recovery from severe hemiplegia due to chronic stroke. *Front Neuroeng*. 2014;7:19.
19. Ramos-Murguialday A, Broetz D, Rea M, et al. Brain-machine interface in chronic stroke rehabilitation: A controlled study. *Ann Neurol*. 2013;74:100–108.
20. Soekadar SR, Birbaumer N, Slutzky MW, Cohen LG. Brain-machine interfaces in neurorehabilitation of stroke. *Neurobiol Dis*. 2015;83:172–179.
21. Várkuti B, Guan C, Pan Y, et al. Resting state changes in functional connectivity correlate with movement recovery for BCI and robot-assisted upper-extremity training after stroke. *Neurorehabil Neural Repair*. 2013;27:53–62.
22. Bundy DT, Wronkiewicz M, Sharma M, Moran DW, Corbetta M, Leuthardt EC. Using ipsilateral motor signals in the unaffected cerebral hemisphere as a signal platform for brain-computer interfaces in hemiplegic stroke survivors. *J Neural Eng*. 2012;9:036011.
23. Bundy DT, Souders L, Baranyai K, et al. Contralesional brain-computer interface control of a powered exoskeleton for motor recovery in chronic stroke survivors. *Stroke*. 2017;48:1908–1915.
24. Cervera MA, Soekadar SR, Ushiba J, et al. Brain-computer interfaces for post-stroke motor rehabilitation: A meta-analysis. *Ann Clin Transl Neurol*. 2018;5:651–663.
25. Cramer SC, Nelles G, Benson RR, et al. A functional MRI study of subjects recovered from hemiparetic stroke. *Stroke*. 1997;28:2518–2527.
26. Weiller C, Ramsay SC, Wise RJ, Friston KJ, Frackowiak RS. Individual patterns of functional reorganization in the human cerebral cortex after capsular infarction. *Ann Neurol*. 1993;33:181–189.
27. Takeuchi N, Chuma T, Matsuo Y, Watanabe I, Ikoma K. Repetitive transcranial magnetic stimulation of contralesional primary motor cortex improves hand function after stroke. *Stroke*. 2005;36:2681–2686.
28. Hoyer EH, Celnik PA. Understanding and enhancing motor recovery after stroke using transcranial magnetic stimulation. *Restor Neurol Neurosci*. 2011;29:395–409.
29. Matsuura A, Karita T, Nakada N, Fukushima S, Mori F. Correlation between changes of contralesional cortical activity and motor function recovery in patients with hemiparetic stroke. *Phys Ther Res*. 2017;20:28–35.
30. Buetefisch CM. Role of the contralesional hemisphere in post-stroke recovery of upper extremity motor function. *Front Neurol*. 2015;6:214.
31. Diedrichsen J, Kornysheva K. Motor skill learning between selection and execution. *Trends Cogn Sci*. 2015;19:227–233.
32. Krakauer JW, Hadjiosif AM, Xu J, Wong AL, Haith AM. Motor learning. *Compr Physiol*. 2019;9:613–663.
33. Sanes JN, Donoghue JP. Plasticity and primary motor cortex. *Annu Rev Neurosci*. 2000;23:393–415.
34. Maruyama S, Fukunaga M, Sugawara SK, Hamano YH, Yamamoto T, Sadato N. Cognitive control affects motor learning through local variations in GABA within the primary motor cortex. *Sci Rep*. 2021;11:18566.
35. Hamano YH, Sugawara SK, Fukunaga M, Sadato N. The integrative role of the M1 in motor sequence learning. *Neurosci Lett*. 2021;760:136081.
36. Kantak SS, Stinear JW, Buch ER, Cohen LG. Rewiring the brain: Potential role of the premotor cortex in motor control, learning, and recovery of function following brain injury. *Neurorehabil Neural Repair*. 2012;26:282–292.
37. Buzsáki G, Draguhn A. Neuronal oscillations in cortical networks. *Science*. 2004;304:1926–1929.
38. Buzsáki G. *Rhythms of the brain*. Oxford University Press; 2006
39. Ray S, Maunsell JH. Do gamma oscillations play a role in cerebral cortex? *Trends Cogn Sci*. 2015;19:78–85.
40. Sohal VS. How close are we to understanding what (if anything) γ oscillations do in cortical circuits? *J Neurosci*. 2016;36:10489–10495.
41. Tsanov M, Wright N, Vann SD, Erichsen JT, Aggleton JP, O'Mara SM. Hippocampal inputs mediate theta-related plasticity in anterior thalamus. *Neuroscience*. 2011;187:52–62.
42. Schreckenberger M, Lange-Asschenfeldt C, Lochmann M, et al. The thalamus as the generator and modulator of EEG alpha rhythm: A combined PET/EEG study with lorazepam challenge in humans. *NeuroImage*. 2004;22:637–644.
43. Basha D, Dostrovsky JO, Lopez Rios AL, Hodaie M, Lozano AM, Hutchison WD. Beta oscillatory neurons in the motor thalamus of movement disorder and pain patients. *Exp Neurol*. 2014;261:782–790.
44. Jensen O, Colgin LL. Cross-frequency coupling between neuronal oscillations. *Trends Cogn Sci*. 2007;11:267–269.
45. Tort AB, Kramer MA, Thorn C, et al. Dynamic cross-frequency couplings of local field potential oscillations in rat striatum and hippocampus during performance of a T-maze task. *Proc Natl Acad Sci USA*. 2008;105:20517–20522.
46. Bragin A, Jandó G, Nádasdy Z, Hetke J, Wise K, Buzsáki G. Gamma (40–100Hz) oscillation in the hippocampus of the behaving rat. *J Neurosci*. 1995;15:47–60.
47. Buzsáki G, Buhl DL, Harris KD, Csicsvari J, Czéh B, Morozov A. Hippocampal network patterns of activity in the mouse. *Neuroscience*. 2003;116:201–211.
48. Rustamov N, Sharma L, Chiang SN, Burk C, Haroutounian S, Leuthardt EC. Spatial and frequency-specific electrophysiological signatures of tonic pain recovery in humans. *Neuroscience*. 2021;465:23–37.
49. Canolty RT, Knight RT. The functional role of cross-frequency coupling. *Trends Cogn Sci*. 2010;14:506–515.
50. Axmacher N, Henseler MM, Jensen O, Weinreich I, Elger CE, Fell J. Cross-frequency coupling supports multi-item working memory in the human hippocampus. *Proc Natl Acad Sci USA*. 2010;107:3228–3233.

51. Fell J, Axmacher N. The role of phase synchronization in memory processes. *Nat Rev Neurosci.* 2011;12:105–118.
52. Lega B, Burke J, Jacobs J, Kahana MJ. Slow-theta-to-gamma phase-amplitude coupling in human hippocampus supports the formation of new episodic memories. *Cereb Cortex.* 2016;26:268–278.
53. Maris E, van Vugt M, Kahana M. Spatially distributed patterns of oscillatory coupling between high-frequency amplitudes and low-frequency phases in human iEEG. *NeuroImage.* 2011;54:836–850.
54. Tort AB, Komorowski RW, Manns JR, Kopell NJ, Eichenbaum H. Theta-gamma coupling increases during the learning of item-context associations. *Proc Natl Acad Sci USA.* 2009;106:20942–20947.
55. Cohen MX, Elger CE, Fell J. Oscillatory activity and phase-amplitude coupling in the human medial frontal cortex during decision making. *J Cogn Neurosci.* 2009;21:390–402.
56. Szczepanski SM, Crone NE, Kuperman RA, Auguste KI, Parvizi J, Knight RT. Dynamic changes in phase-amplitude coupling facilitate spatial attention control in fronto-parietal cortex. *PLoS Biol.* 2014;12:e1001936.
57. Wang J, Li D, Li X, *et al.* Phase-amplitude coupling between θ and γ oscillations during nociception in rat electroencephalography. *Neurosci Lett.* 2011;499:84–87.
58. Liu CC, Chien JH, Kim JH, *et al.* Cross-frequency coupling in deep brain structures upon processing the painful sensory inputs. *Neuroscience.* 2015;303:412–421.
59. Voytek B, Canolty RT, Shestyuk A, Crone NE, Parvizi J, Knight RT. Shifts in gamma phase-amplitude coupling frequency from theta to alpha over posterior cortex during visual tasks. *Front Hum Neurosci.* 2010;4:191.
60. Combrisson E, Perrone-Bertolotti M, Soto JL, *et al.* From intentions to actions: Neural oscillations encode motor processes through phase, amplitude and phase-amplitude coupling. *NeuroImage.* 2017;147:473–487.
61. Daume J, Gruber T, Engel AK, Frieze U. Phase-amplitude coupling and long-range phase synchronization reveal frontotemporal interactions during visual working memory. *J Neurosci.* 2017;37:313–322.
62. Soto JL, Jerbi K. Investigation of cross-frequency phase-amplitude coupling in visuomotor networks using magnetoencephalography. *Annu Int Conf IEEE Eng Med Biol Soc.* 2012;2012:1550–1553.
63. von Nicolai C, Engler G, Sharott A, Engel AK, Moll CK, Siegel M. Corticostriatal coordination through coherent phase-amplitude coupling. *J Neurosci.* 2014;34:5938–5948.
64. Yanagisawa T, Yamashita O, Hirata M, *et al.* Regulation of motor representation by phase-amplitude coupling in the sensorimotor cortex. *J Neurosci.* 2012;32:15467–15475.
65. Lasztóczy B, Klausberger T. Layer-specific GABAergic control of distinct gamma oscillations in the CA1 hippocampus. *Neuron.* 2014;81:1126–1139.
66. Colgin LL. Theta-gamma coupling in the entorhinal-hippocampal system. *Curr Opin Neurobiol.* 2015;31:45–50.
67. Lopes-Dos-Santos V, van de Ven GM, Morley A, Trouche S, Campo-Urriza N, Dupret D. Parsing hippocampal theta oscillations by nested spectral components during spatial exploration and memory-guided behavior. *Neuron.* 2018;100:940–952.e7.
68. Fries P. Neuronal gamma-band synchronization as a fundamental process in cortical computation. *Annu Rev Neurosci.* 2009;32:209–224.
69. Canolty RT, Edwards E, Dalal SS, *et al.* High gamma power is phase-locked to theta oscillations in human neocortex. *Science.* 2006;313:1626–1628.
70. Akkad H, Dupont-Hadwen J, Frese A, *et al.* Increasing motor skill acquisition by driving theta-gamma coupling. *Elife.* 2021;10:e6735.
71. Sanford J, Moreland J, Swanson LR, Stratford PW, Gowland C. Reliability of the Fugl-Meyer assessment for testing motor performance in patients following stroke. *Phys Ther.* 1993;73:447–454.
72. Sullivan KJ, Tilson JK, Cen SY, *et al.* Fugl-Meyer assessment of sensorimotor function after stroke: Standardized training procedure for clinical practice and clinical trials. *Stroke.* 2011;42:427–432.
73. Gladstone DJ, Danells CJ, Black SE. The Fugl-Meyer assessment of motor recovery after stroke: A critical review of its measurement properties. *Neurorehabil Neural Repair.* 2002;16:232–240.
74. Delorme A, Makeig S. EEGLAB: An open source toolbox for analysis of single-trial EEG dynamics including independent component analysis. *J Neurosci Methods.* 2004;134:9–21.
75. Welch PD. The use of fast Fourier transform for the estimation of power spectra: A method based on time averaging over short, modified periodograms. *IEEE Trans Audio Electroacoust.* 1967;2:70–73.
76. Brovelli A, Lachaux JP, Kahane P, Boussaoud D. High gamma frequency oscillatory activity dissociates attention from intention in the human premotor cortex. *NeuroImage.* 2005;28:154–164.
77. Grützner C, Wibral M, Sun L, *et al.* Deficits in high- (>60Hz) gamma-band oscillations during visual processing in schizophrenia. *Front Hum Neurosci.* 2013;7:88.
78. Tan LL, Oswald MJ, Heintz C, *et al.* Gamma oscillations in somatosensory cortex recruit prefrontal and descending serotonergic pathways in aversion and nociception. *Nat Commun.* 2019;10:983.
79. Darvas F, Scherer R, Ojemann JG, Rao RP, Miller KJ, Sorensen LB. High gamma mapping using EEG. *NeuroImage.* 2010;49:930–938.
80. Rustamov N, Northon S, Tessier J, Leblond H, Piché M. Integration of bilateral nociceptive inputs tunes spinal and cerebral responses. *Sci Rep.* 2019;9:7143.
81. Rustamov N, Wagenaar-Tison A, Doyer E, Piché M. Electrophysiological investigation of the contribution of attention to altered pain inhibition processes in patients with irritable bowel syndrome. *J Physiol Sci.* 2020;70:46.
82. Northon S, Rustamov N, Piché M. Cortical integration of bilateral nociceptive signals: When more is less. *Pain.* 2019;160:724–733.
83. Heid C, Mouraux A, Treede RD, Schuh-Hofer S, Rupp A, Baumgärtner U. Early gamma-oscillations as correlate of localized nociceptive processing in primary sensorimotor cortex. *J Neurophysiol.* 2020;123:1711–1726.
84. Miller KJ, Leuthardt EC, Schalk G, *et al.* Spectral changes in cortical surface potentials during motor movement. *J Neurosci.* 2007;27:2424–2432.
85. Lemaire N, Hernandez LF, Hu D, Kubota Y, Howe MW, Graybiel AM. Effects of dopamine depletion on LFP oscillations in striatum are task- and learning-dependent and selectively reversed by L-DOPA. *Proc Natl Acad Sci USA.* 2012;109:18126–18131.
86. Gramfort A, Papadopoulos T, Olivi E, Clerc M. OpenMEEG: Opensource software for quasistatic bioelectromagnetics. *Biomed Eng.* 2010;9:45.
87. Baillet S, Mosher JC, Leahy RM. Electromagnetic brain mapping. *IEEE Signal Process Mag.* 2001;18:14–30.
88. Pantazis D, Nichols TE, Baillet S, Leahy RM. A comparison of random field theory and permutation methods for the statistical analysis of MEG data. *NeuroImage.* 2005;25:383–394.
89. Maris E, Oostenveld R. Nonparametric statistical testing of EEG- and MEG-data. *J Neurosci Methods.* 15 2007;164:177–190.
90. Hülsemann MJ, Naumann E, Rasch B. Quantification of phase-amplitude coupling in neuronal oscillations: Comparison of phase-locking value, mean vector length, modulation index, and generalized-linear-modeling-cross-frequency-coupling. *Front Neurosci.* 2019;13:573.
91. Höller Y, Uhl A, Bathke A, *et al.* Reliability of EEG measures of interaction: A paradigm shift is needed to fight the reproducibility crisis. *Front Hum Neurosci.* 2017;11:441.
92. Salinsky MC, Oken BS, Morehead L. Test-retest reliability in EEG frequency analysis. *Electroencephalogr Clin Neurophysiol.* 1991;79:382–392.
93. Page SJ, Fulk GD, Boyne P. Clinically important differences for the upper-extremity Fugl-Meyer Scale in people with minimal to moderate impairment due to chronic stroke. *Phys Ther.* 2012;92:791–798.

94. Sirota A, Montgomery S, Fujisawa S, Isomura Y, Zugaro M, Buzsáki G. Entrainment of neocortical neurons and gamma oscillations by the hippocampal theta rhythm. *Neuron*. 2008;60:683–697.
95. Cohen MX, Axmacher N, Lenartz D, Elger CE, Sturm V, Schlaepfer TE. Good vibrations: Cross-frequency coupling in the human nucleus accumbens during reward processing. *J Cogn Neurosci*. 2009;21:875–889.
96. Hentschke H, Perkins MG, Pearce RA, Banks MI. Muscarinic blockade weakens interaction of gamma with theta rhythms in mouse hippocampus. *Eur J Neurosci*. 2007;26:1642–1656.
97. Wulff P, Ponomarenko AA, Bartos M, et al. Hippocampal theta rhythm and its coupling with gamma oscillations require fast inhibition onto parvalbumin-positive interneurons. *Proc Natl Acad Sci USA*. 2009;106:3561–3566.
98. Gray CM, König P, Engel AK, Singer W. Oscillatory responses in cat visual cortex exhibit inter-columnar synchronization which reflects global stimulus properties. *Nature*. 1989;338:334–337.
99. Reinhart RMG, Nguyen JA. Working memory revived in older adults by synchronizing rhythmic brain circuits. *Nat Neurosci*. 2019;22:820–827.
100. Jensen O, Lisman JE. Theta/gamma networks with slow NMDA channels learn sequences and encode episodic memory: Role of NMDA channels in recall. *Learn Mem*. 1996;3:264–278.
101. Lisman J. The theta/gamma discrete phase code occurring during the hippocampal phase precession may be a more general brain coding scheme. *Hippocampus*. 2005;15:913–922.
102. Lisman J, Buzsáki G. A neural coding scheme formed by the combined function of gamma and theta oscillations. *Schizophr Bull*. 2008;34:974–980.
103. Cowan N. The magical number 4 in short-term memory: A reconsideration of mental storage capacity. *Behav Brain Sci*. 2001;24:87–114; discussion 114–185.
104. Sauseng P, Klimesch W, Heise KF, et al. Brain oscillatory substrates of visual short-term memory capacity. *Curr Biol*. 2009;19:1846–1852.
105. Swann NC, de Hemptinne C, Miocinovic S, et al. Gamma oscillations in the hyperkinetic state detected with chronic human brain recordings in Parkinson's disease. *J Neurosci*. 2016;36:6445–6458.
106. Nowak M, Hinson E, van Ede F, et al. Driving human motor cortical oscillations leads to behaviorally relevant changes in local GABA(A) inhibition: A tACS-TMS study. *J Neurosci*. 2017;37:4481–4492.
107. Stagg CJ, Bachtiar V, Johansen-Berg H. The role of GABA in human motor learning. *Curr Biol*. 2011;21:480–484.
108. Stagg CJ, Best JG, Stephenson MC, et al. Polarity-sensitive modulation of cortical neurotransmitters by transcranial stimulation. *J Neurosci*. 2009;29:5202–5206.
109. Clarkson AN, Huang BS, Macisaac SE, Mody I, Carmichael ST. Reducing excessive GABA-mediated tonic inhibition promotes functional recovery after stroke. *Nature*. 2010;468:305–309.
110. Blicher JU, Near J, Næss-Schmidt E, et al. GABA levels are decreased after stroke and GABA changes during rehabilitation correlate with motor improvement. *Neurorehabil Neural Repair*. 2015;29:278–286.
111. Bachtiar V, Near J, Johansen-Berg H, Stagg CJ. Modulation of GABA and resting state functional connectivity by transcranial direct current stimulation. *eLife*. 2015;4:e08789.
112. Johnson NW, Özkan M, Burgess AP, et al. Phase-amplitude coupled persistent theta and gamma oscillations in rat primary motor cortex in vitro. *Neuropharmacology*. 2017;119:141–156.
113. Caplan JB, Madsen JR, Schulze-Bonhage A, Aschenbrenner-Scheibe R, Newman EL, Kahana MJ. Human theta oscillations related to sensorimotor integration and spatial learning. *J Neurosci*. 2003;23:4726–4736.
114. Gentili RJ, Bradberry TJ, Oh H, Hatfield BD, Contreras-Vidal JL. Cerebral cortical dynamics during visuomotor transformation: Adaptation to a cognitive-motor executive challenge. *Psychophysiology*. 2011;48:813–824.
115. Contreras-Vidal JL, Kerick SE. Independent component analysis of dynamic brain responses during visuomotor adaptation. *NeuroImage*. 2004;21:936–945.
116. Anguera JA, Seidler RD, Gehring WJ. Changes in performance monitoring during sensorimotor adaptation. *J Neurophysiol*. 2009;102:1868–1879.
117. Bradberry TJ, Gentili RJ, Contreras-Vidal JL. Reconstructing three-dimensional hand movements from noninvasive electroencephalographic signals. *J Neurosci*. 2010;30:3432–3437.
118. de Hemptinne C, Ryapolova-Webb ES, Air EL, et al. Exaggerated phase-amplitude coupling in the primary motor cortex in Parkinson disease. *Proc Natl Acad Sci USA*. 2013;110:4780–4785.
119. Kondylis ED, Randazzo MJ, Alhourani A, et al. Movement-related dynamics of cortical oscillations in Parkinson's disease and essential tremor. *Brain*. 2016;139(Pt 8):2211–2223.
120. de Hemptinne C, Swann NC, Ostrem JL, et al. Therapeutic deep brain stimulation reduces cortical phase-amplitude coupling in Parkinson's disease. *Nat Neurosci*. 2015;18:779–786.
121. van Wijk BC, Beudel M, Jha A, et al. Subthalamic nucleus phase-amplitude coupling correlates with motor impairment in Parkinson's disease. *Clin Neurophysiol*. 2016;127:2010–2019.
122. Malekmohammadi M, AuYong N, Ricks-Oddie J, Bordelon Y, Pouratian N. Pallidal deep brain stimulation modulates excessive cortical high β phase amplitude coupling in Parkinson disease. *Brain Stimul*. 2018;11:607–617.
123. DeLong MR, Wichmann T. Basal ganglia circuits as targets for neuromodulation in Parkinson disease. *JAMA Neurol*. 2015;72:1354–1360.
124. Magrinelli F, Picelli A, Tocco P, et al. Pathophysiology of motor dysfunction in Parkinson's disease as the rationale for drug treatment and rehabilitation. *Parkinson's Dis*. 2016;2016:9832839.
125. Bansal AK, Vargas-Irwin CE, Truccolo W, Donoghue JP. Relationships among low-frequency local field potentials, spiking activity, and three-dimensional reach and grasp kinematics in primary motor and ventral premotor cortices. *J Neurophysiol*. 2011;105:1603–1619.
126. Mollazadeh M, Aggarwal V, Davidson AG, Law AJ, Thakor NV, Schieber MH. Spatiotemporal variation of multiple neurophysiological signals in the primary motor cortex during dexterous reach-to-grasp movements. *J Neurosci*. 2011;31:15531–15543.
127. Churchland MM, Cunningham JP, Kaufman MT, et al. Neural population dynamics during reaching. *Nature*. 2012;487:51–56.
128. Hall TM, de Carvalho F, Jackson A. A common structure underlies low-frequency cortical dynamics in movement, sleep, and sedation. *Neuron*. 2014;83:1185–1199.
129. Ganguly K, Secundo L, Ranade G, et al. Cortical representation of ipsilateral arm movements in monkey and man. *J Neurosci*. 2009;29:12948–12956.
130. Ramanathan DS, Guo L, Gulati T, et al. Low-frequency cortical activity is a neuromodulatory target that tracks recovery after stroke. *Nat Med*. 2018;24:1257–1267.
131. Bönstrup M, Krawinkel L, Schulz R, et al. Low-frequency brain oscillations track motor recovery in human stroke. *Ann Neurol*. 2019;86:853–865.
132. Krakauer JW. Motor learning: Its relevance to stroke recovery and neurorehabilitation. *Curr Opin Neurol*. 2006;19:84–90.

Contralesional Brain–Computer Interface Control of a Powered Exoskeleton for Motor Recovery in Chronic Stroke Survivors

David T. Bundy, PhD; Lauren Souders, MOT; Kelly Baranyai, MOT; Laura Leonard, MOT; Gerwin Schalk, PhD; Robert Coker, MS; Daniel W. Moran, PhD; Thy Huskey, MD*; Eric C. Leuthardt, MD*

Background and Purpose—There are few effective therapies to achieve functional recovery from motor-related disabilities affecting the upper limb after stroke. This feasibility study tested whether a powered exoskeleton driven by a brain–computer interface (BCI), using neural activity from the unaffected cortical hemisphere, could affect motor recovery in chronic hemiparetic stroke survivors. This novel system was designed and configured for a home-based setting to test the feasibility of BCI-driven neurorehabilitation in outpatient environments.

Methods—Ten chronic hemiparetic stroke survivors with moderate-to-severe upper-limb motor impairment (mean Action Research Arm Test=13.4) used a powered exoskeleton that opened and closed the affected hand using spectral power from electroencephalographic signals from the unaffected hemisphere associated with imagined hand movements of the paretic limb. Patients used the system at home for 12 weeks. Motor function was evaluated before, during, and after the treatment.

Results—Across patients, our BCI-driven approach resulted in a statistically significant average increase of 6.2 points in the Action Research Arm Test. This behavioral improvement significantly correlated with improvements in BCI control. Secondary outcomes of grasp strength, Motricity Index, and the Canadian Occupational Performance Measure also significantly improved.

Conclusions—The findings demonstrate the therapeutic potential of a BCI-driven neurorehabilitation approach using the unaffected hemisphere in this uncontrolled sample of chronic stroke survivors. They also demonstrate that BCI-driven neurorehabilitation can be effectively delivered in the home environment, thus increasing the probability of future clinical translation.

Clinical Trial Registration—URL: <http://www.clinicaltrials.gov>. Unique identifier: NCT02552368. (*Stroke*. 2017;48:1908-1915. DOI: 10.1161/STROKEAHA.116.016304.)

Key Words: arm ■ brain-computer interface ■ hand ■ rehabilitation ■ stroke

A significant challenge in the treatment of stroke survivors is the rehabilitation of chronic motor disabilities. Although behavioral therapies such as constraint-induced movement therapy¹ or robot-aided sensorimotor stimulation² can improve upper-limb motor function, they require some level of peripheral motor function to engage with the therapy. This residual function is variable across patients and absent in the setting of complete hemiplegia. An alternative to behavioral therapies is to engage with the patient's central nervous system directly. Specifically, a brain–computer interface

(BCI) system can measure movement-related signals from the central nervous system and provide meaningful feedback to the central nervous system to direct plasticity.

BCIs have recently emerged as novel and potentially powerful tools to restore function in chronic stroke survivors.³ Early results present promising demonstrations that BCI-controlled orthoses or functional electric stimulators can lead to improvements in motor function in chronic stroke survivors.³⁻⁸ These stroke-specific BCI systems for rehabilitation have focused on signals stemming from perilesional cortex, contralateral to the

Received July 3, 2016; final revision received March 22, 2017; accepted April 18, 2017.

From the Department of Rehabilitation Medicine, University of Kansas Medical Center, Kansas City (D.T.B.); Departments of Biomedical Engineering (D.T.B., R.C., D.W.M., E.C.L.), Neurology (L.S., K.B., L.L., T.H.), Neurological Surgery (E.C.L.), Mechanical Engineering and Material Sciences (E.C.L.), and Neuroscience (E.C.L.), Washington University, St. Louis, MO; and National Center for Adaptive Neurotechnologies, Wadsworth Center, NYS Department of Health, Albany, NY (G.S.).

*Drs Huskey and Leuthardt contributed equally.

The online-only Data Supplement is available with this article at <http://stroke.ahajournals.org/lookup/suppl/doi:10.1161/STROKEAHA.116.016304/-/DC1>.

Correspondence to Eric C. Leuthardt, MD, Department of Neurological Surgery, Washington University School of Medicine, St. Louis, MO 63110. E-mail LeuthardtE@wudosis.wustl.edu

© 2017 The Authors. *Stroke* is published on behalf of the American Heart Association, Inc., by Wolters Kluwer Health, Inc. This is an open access article under the terms of the [Creative Commons Attribution](https://creativecommons.org/licenses/by/4.0/) License, which permits use, distribution, and reproduction in any medium, provided that the original work is properly cited.

Stroke is available at <http://stroke.ahajournals.org>

DOI: 10.1161/STROKEAHA.116.016304

affected hand for BCI control. Because the ability to modulate perilesional cortical activity decreases with increasing cortical damage,⁹ it may be particularly important for neurorehabilitation systems to focus on the ipsilateral, contralesional cortex in those patients who are most severely affected.

Although movement-related neural activity occurs in the ipsilateral and the contralateral cortices,^{10,11} the role of the unaffected hemisphere in stroke recovery is uncertain. Specifically, decreases in contralesional activity are associated with optimal recovery in some studies.^{12,13} Other studies show that increases in contralesional activity may be related to motor recovery,^{14,15} particularly in patients with incomplete recovery.¹⁶ As motor recovery is inversely correlated with the extent of corticospinal tract transection,¹⁷ we hypothesized that using contralesional hemisphere activity to drive a BCI-controlled exoskeleton may lead to functional improvements. Previously, we demonstrated that chronic stroke survivors can control BCIs using electroencephalographic (EEG) signals from the contralesional hemisphere associated with the intention to move the affected limb.¹⁸ However, it was uncertain whether emphasizing the relationship between activation of ipsilateral cortex and resultant sensory feedback would be beneficial.

This feasibility study tested an EEG-BCI system that used signals related to affected hand motor imagery, recorded from the unaffected hemisphere, to control the affected hand via a powered exoskeleton. This study is the first to specifically focus on the unaffected hemisphere with a BCI rehabilitation system and the first to provide BCI-driven therapy in the patients' homes. This setting is important because it increases the likelihood that this approach can be scaled more widely across the stroke-affected population.

Methods

To determine whether a BCI-controlled exoskeleton using EEG signals from the unaffected hemisphere can lead to functional rehabilitation, we created a novel home-based system called the IpsiHand. We then examined whether a 12-week training period led to functional improvements in chronic, hemiparetic stroke survivors.

Patient Characteristics

Ten chronic hemiparetic stroke survivors with moderate-to-severe upper-limb hemiparesis, enrolled at least 6 months after first-time hemispheric stroke, completed the study. Because motor recovery plateaus after 3 months,¹⁹ the study was designed as a self-controlled study comparing motor function before and after the intervention to establish the feasibility of the BCI-driven therapy studied. The Table contains patient demographics and baseline motor function. The [online-only Data Supplement](#) contains detailed inclusion and exclusion criteria. Moderate-to-severely impaired patients were specifically targeted because they are less likely to recover through other methods and therefore require an alternative rehabilitation strategy, such as a BCI. The Washington University School of Medicine Institutional Review Board approved the study protocol, and all patients provided written informed consent.

BCI System Design

The BCI system (Figure 1A) combined a novel powered exoskeleton with a commercial EEG amplifier and active electrodes. The exoskeleton opened and closed the patient's hand in a 3-finger pinch grip (1 degree of freedom). A detailed description of the system is contained in the Methods in the [online-only Data Supplement](#). Consistent with

our previous work,¹⁸ the system used spectral power changes to control hand position. Because stroke patients typically have difficulty extending their extremities, BCI control associated motor imagery with opening the affected hand. Each trial began with the hand fully closed, and spectral power at the control feature was used to update the hand position, providing visual and proprioceptive feedback. During rest trials, patients were instructed to try to keep the exoskeleton closed by imagining that they were resting. During movement trials, patients were instructed to try to open their hand via motor imagery.

EEG Screening

After meeting the inclusion criteria, patients underwent an EEG screening protocol to ensure that a consistent control signal was present for device control. Each patient completed 3 separate screenings to assess the stability of potential BCI control signals. EEG electrodes were applied by a trained biomedical engineer, and EEG signals were collected while patients performed a visually cued motor screening task consisting of trials of (1) rest, (2) unaffected hand movements, (3) affected hand motor imagery, and (4) bilateral motor imagery. Spectral power, or the power in the EEG signal as a function of frequency, was calculated using an autoregressive spectral estimation method. The coefficient of determination (r^2), the percent of variance in spectral power that was accounted for by the difference between affected hand motor imagery and rest trials, was calculated for each channel and frequency. After completing 3 EEG screenings, the EEG data were examined for the presence of consistent spectral power changes during affected hand motor imagery. BCI control features were required to be associated with imagined movements of the affected hand and located in unaffected hemisphere motor regions. These sessions were not designed to achieve BCI mastery but to identify patients with consistent cortical activations (ie, μ [8–12 Hz] or β [12–30 Hz] power decreases) in at least 2 of 3 sessions. The feature in the unaffected hemisphere with the strongest r^2 value was chosen as the patient-specific BCI control feature. Patients without consistent spectral power changes were unable to continue in the study.

Outcome Measures

The primary outcome measure was the Action Research Arm Test (ARAT).²⁰ Secondary outcome measures included: (1) the Canadian Occupational Performance Measure,²¹ (2) the Motricity Index, (3) the modified Ashworth Scale at the elbow joint, (4) grip strength, (5) pinch strength, and (6) the active range of motion (AROM) at the metacarpophalangeal joint of digits 2 to 5. As this study was the first to use a BCI system for stroke rehabilitation in the home setting, we measured the BCI control quality by comparing the topographies of spectral power changes in the laboratory and home-based sessions. We assessed compliance by recording the total number of days and time that each patient used the system.

Study Protocol

The study timeline is shown in Figure 1B. After completing the EEG screenings, patients completed 2 pretherapy motor evaluations in which all primary and secondary outcome measures were measured by an occupational therapist. On these days, the exoskeleton was also fit to the patient's hand. In addition, patients and their caregivers were trained to use the system. This included (1) donning the exoskeleton and EEG cap, (2) examining the EEG readouts to verify that physiological signals were collected, (3) software operation, and (4) system maintenance. After the baseline motor evaluations and training, each patient was sent home with a BCI system to complete 12 weeks of training. Patients were instructed to use the BCI system on a minimum of 5 days per week. Patients completed 1 to 12 10-minute runs of the BCI task per day depending on their stamina and time constraints. At 2-week intervals, patients came to the laboratory for follow-up motor evaluations consisting of the ARAT and Canadian Occupational Performance Measure. At these follow-up sessions and as needed, an occupational therapist or a biomedical engineer communicated with the patients to ensure compliance with the study,

Table. Patient Characteristics and ARAT Scores

Patient	Age, y	Time Post-Stroke, mo	Hand Dominance	Clinical Cause/Location	Affected UE	Baseline ARAT	Completion ARAT	ARAT Change
1	63	49	L	L Ischemic CVA	R	16.5	29	12.5
2	41	18	L	R ICA/MCA Dissection leading to a R basal ganglia/internal capsule stroke	L	6.5	7	0.5
3	72	7	R	L Hemorrhagic CVA	R	4	12	8
4	57	29	R	L Thalamic Hemorrhage	R	10	16	6
5	65	12	R	L Periventricular cystic encephalomalacia	R	32	34	2
6	67	283	R	R Ischemic CVA	L	15	21	6
7	62	35	R	R Ischemic CVA	L	5	6	1
8	48	6	R	R Ischemic MCA CVA	L	5	12	7
9	46	42	R	L Ischemic CVA	R	29.5	43	13.5
10	65	255	R	R AVM	L	10.5	16	5.5
Mean	58.6	73.6				13.4	19.6	6.20
Median	62.5	32				10.25	16	6.00
SD	10.3	104.2				10.1	12.2	3.81

ARAT indicates Action Research Arm Test; AVM, arteriovenous malformation; CVA, cerebrovascular accident; ICA, internal carotid artery; L, left; MCA, middle cerebral artery; R, right; and UE, upper extremity.

answer questions about the device, fix any malfunctions, and discuss EEG signal quality, which was assessed regularly by a biomedical engineer. After 12 weeks, patients were again tested on all primary

and secondary outcome measures. Different occupational therapists collected baseline and completion outcome measures, and all occupational therapists were blinded to observed EEG changes.

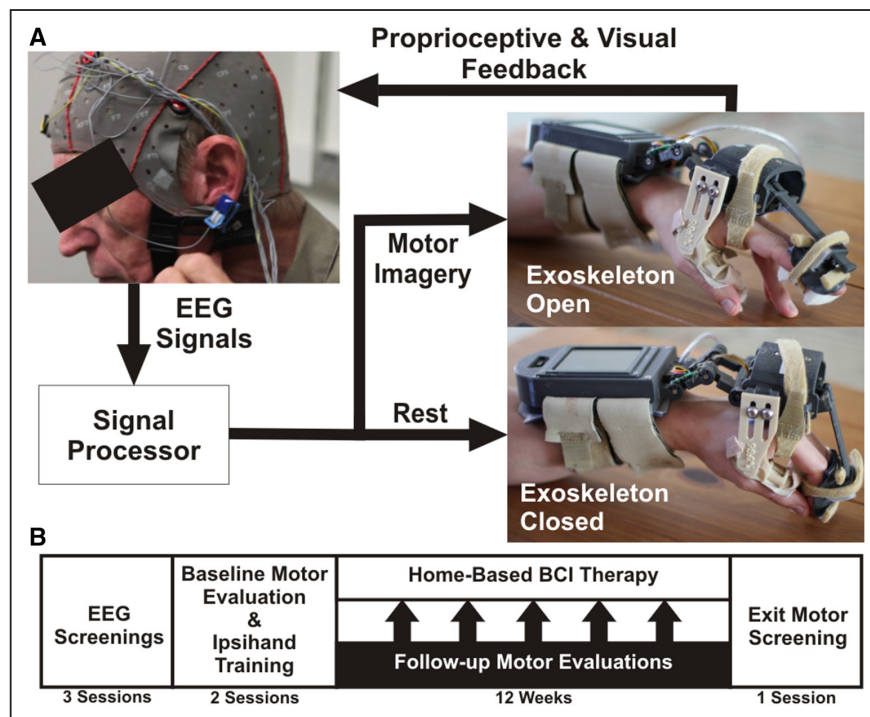


Figure 1. Study methodology. **A**, The exoskeleton used attached to a patient’s affected hand via straps on the forearm, palm of the hand, and intermediate phalanges of the index and middle finger, whereas the thumb was held stationary. The exoskeleton was controlled by a microprocessor in the forearm assembly that processed electroencephalographic (EEG) signals. A linear actuator drove hand movements in a 3-finger pinch grip based on the decoded EEG. **B**, The study tested whether training with the brain-computer interface (BCI)-controlled exoskeleton would lead to functional improvements. Patients that met the inclusion criteria completed 3 EEG screenings. Patients with consistent movement-related EEG activations then completed baseline motor evaluations and BCI system training. Finally, patients completed a 12-wk home-based BCI protocol with follow-up motor evaluations at 2-wk intervals.

Analysis of Outcome Measures

A paired-sample *t* test was used to evaluate the statistical significance of ARAT changes and continuous secondary outcome measures (grip strength, pinch strength, and AROM). Signed-rank tests were used for all other outcome measures because their measurement scales were ordinal. Because the exoskeleton drove extension of the second and third digits, AROM values for the second and third digits and fourth and fifth digits were averaged separately. Changes were examined for both the overall and subcomponents of the ARAT and Motricity Index.

Neurophysiological Correlates

To examine potential mechanisms of action, we calculated the correlation between the change in ARAT and changes in BCI control accuracy, total usage time, and EEG modulation changes. To quantify BCI performance, we calculated the average hand position in the second half of each trial. The BCI accuracy for each run of the BCI task was calculated by taking the difference in this average position between movement and rest trials. EEG modulation was determined by calculating the coefficient of determination (r^2 value) quantifying the difference in EEG spectral power between motor imagery and rest trials. The change in BCI accuracy and EEG modulation was defined as the slope of a robust multilinear regression representing the change per run of the BCI task. The relationship between the ARAT change and change in both BCI control accuracy and EEG modulation was measured with Spearman *r*. To control for the location and frequency used for BCI control, we performed 3 control analyses: (1) change in EEG modulation at the same frequency but at the location contralateral to the control site (ipsilesional motor cortex), (2) change in EEG modulation at the same frequency used for control but at a nonmotor electrode site (F3), and (3) change in EEG modulation at the location used for BCI control (contralesional motor cortex) but at a different frequency (50 Hz). Because patients performed the BCI task at home, poor-quality EEG activity was observed on some days. Thus, we included only those runs in which BCI control signals significantly ($P < 0.01$) differed between movement and rest trials.

Results

Ten patients completed the study. Patient characteristics are summarized in the Table, and the [online-only Data Supplement](#) contains a detailed description of patient recruitment. In short, of the 22 patients who completed EEG screenings, 18 (81%) were suitable for further BCI therapy, 13 (59%) began the therapy, and 10 (45%) completed the study. The drop off was

because of a variety of causes, including unrelated medical diagnoses, inability to comply with the time commitment, and poor orthosis fit.

BCI Control

After initial training, patients and their caregivers were able to apply EEG electrodes in the home setting to record physiological EEG signals. Figure 2 shows exemplary movement-related EEG activity observed in the laboratory and while at home. The patient demonstrated bilateral μ - and β -band power decreases in both settings. Furthermore, the patient had very similar spatial and spectral patterns of movement-related EEG activity during both sessions. The significant decrease in power during motor imagery in the BCI control task led to a high level of accuracy with discriminable patterns of exoskeleton movement during rest and motor imagery.

Because our hypothesis focused on the contralesional hemisphere, the features used to drive the BCI system were from electrodes over the contralesional motor cortex. Movement-related EEG activations were also observed from the ipsilesional hemisphere in 8 of the 10 patients. Although the frequency used for BCI control varied across patients, all BCI control features were μ - and β -band power suppressions, also referred to as event-related desynchronization.²² Patients used the device on 37 to 72 days. Patients performed 74 to 465 10-minute runs of the BCI task for a total of 740 to 4650 minutes of online BCI control in addition to the daily screening task. Details of the patient-specific BCI control are included in the [online-only Data Supplement](#).

Functional Outcomes

The 2 baseline motor assessments were averaged to determine each patient's baseline motor function. ARAT changes throughout the study protocol are shown in Figure 3A. Patients had a statistically significant mean ARAT increase of 6.2 points. Importantly, 5.7 points has been estimated to represent the minimal clinically important difference in chronic stroke survivors.²³ Specifically, 6 of the 10 patients

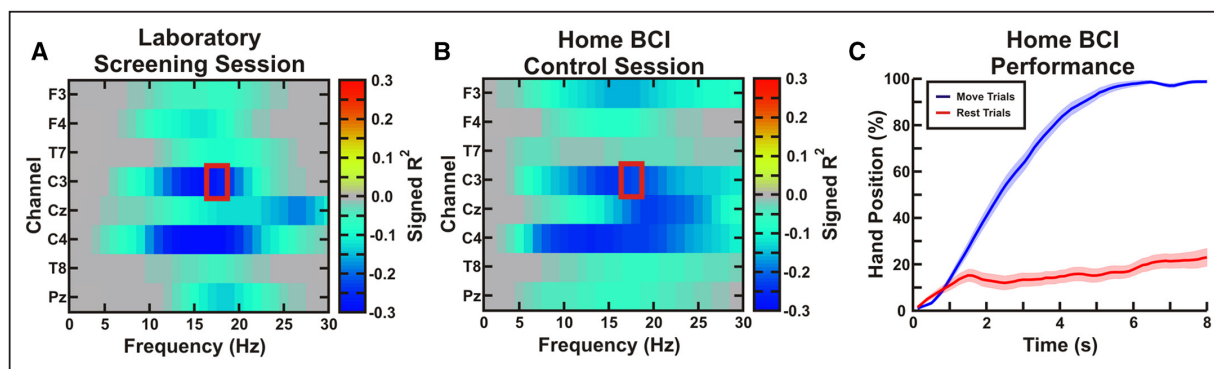


Figure 2. Exemplar electroencephalographic (EEG) activity and brain-computer interface (BCI) control. **A**, During an exemplar laboratory-based screening session, the patient (patient 10, left affected) demonstrated significant decreases in μ - and β -band spectral power bilaterally. The color scale shows signed r^2 values indicating increases (positive values) and decreases (negative values) in spectral power during motor imagery. A BCI control feature (red box) ipsilateral to the affected hand was chosen (contact C3). **B**, During a home-based BCI control session, a similar spatio-spectral pattern of movement-related EEG activity was observed. **C**, The mean (\pm SE) of the hand position in movement and rest trials shows that the patient achieved a high level of BCI control (0% fully closed, 100% fully open).

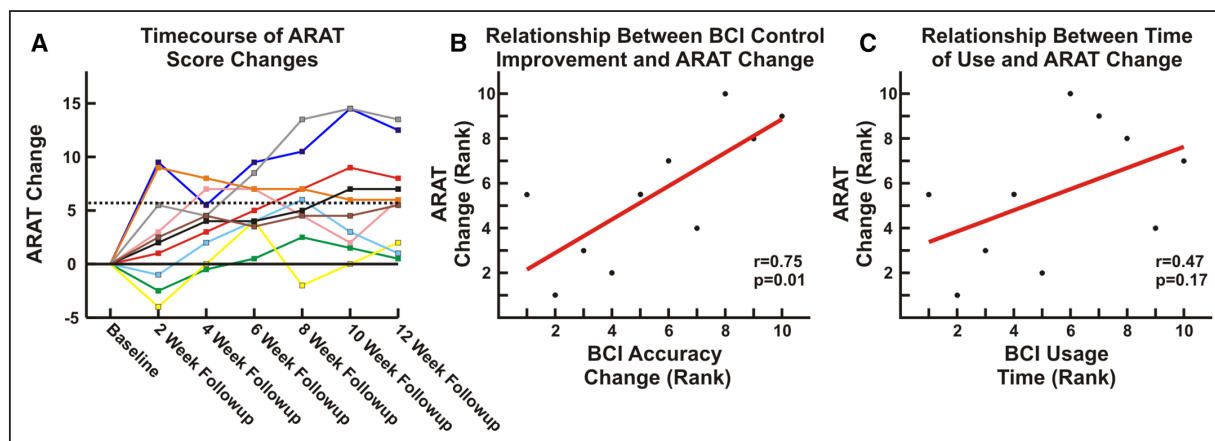


Figure 3. Improvement in motor function. **A**, Each line shows the change in Action Research Arm Test (ARAT) during the study. At completion, 6 of 10 patients had ARAT increases surpassing the minimal clinically important difference (MCID; 5.7 points). **B**, ARAT increases were related to the rate of change in brain–computer interface (BCI) accuracy (Spearman $r=0.75$, $P=0.013$). **C**, ARAT increases were not related to the time of device use (Spearman $r=0.47$, $P=0.17$).

had ARAT improvements above this level. In addition to this per-protocol analysis, a significant increase in ARAT score was also found using an intention-to-treat analysis as described in the [online-only Data Supplement](#). Grasp strength, Motricity Index, the grip and grasp ARAT subscores, and Canadian Occupational Performance Measure performance and satisfaction ratings were also significantly increased after therapy, whereas pinch strength, AROM, and the pinch and gross ARAT subscores were not changed. Figure 4 and Table II in the [online-only Data Supplement](#) summarize changes across outcomes. Other than minor fatigue, no negative effects were observed.

Neurophysiological Correlates

Across patients, there was a significant correlation between the change in ARAT score and the change in BCI accuracy (defined as the difference between the hand position in the movement and rest trials) per BCI task run (Figure 3B; Spearman $r=0.75$, $P=0.013$). There was not a significant relationship between the change in ARAT score and the total device usage time (Figure 3C; Spearman $r=0.47$, $P=0.17$).

Finally, we sought to determine whether there was a relationship between ARAT and EEG changes (Figure 5). There was a trend toward a positive relationship between ARAT

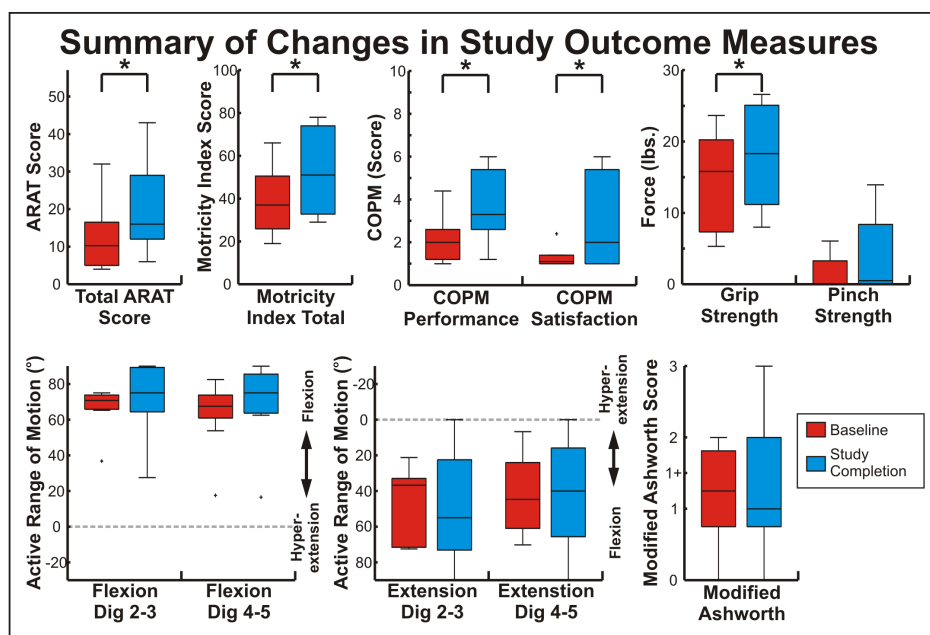


Figure 4. Summary of outcome measures. Each box shows the distribution of each outcome measurement at baseline and study completion. Boxes show the 25th percentile, median, and 75th percentile; bars indicate the range of values; and outliers >2.7 SDs from the mean are marked with a +. Measures with statistically significant ($P<0.05$) changes are indicated with an *. ARAT indicates Action Research Arm Test; and COPM, Canadian Occupational Performance Measure.

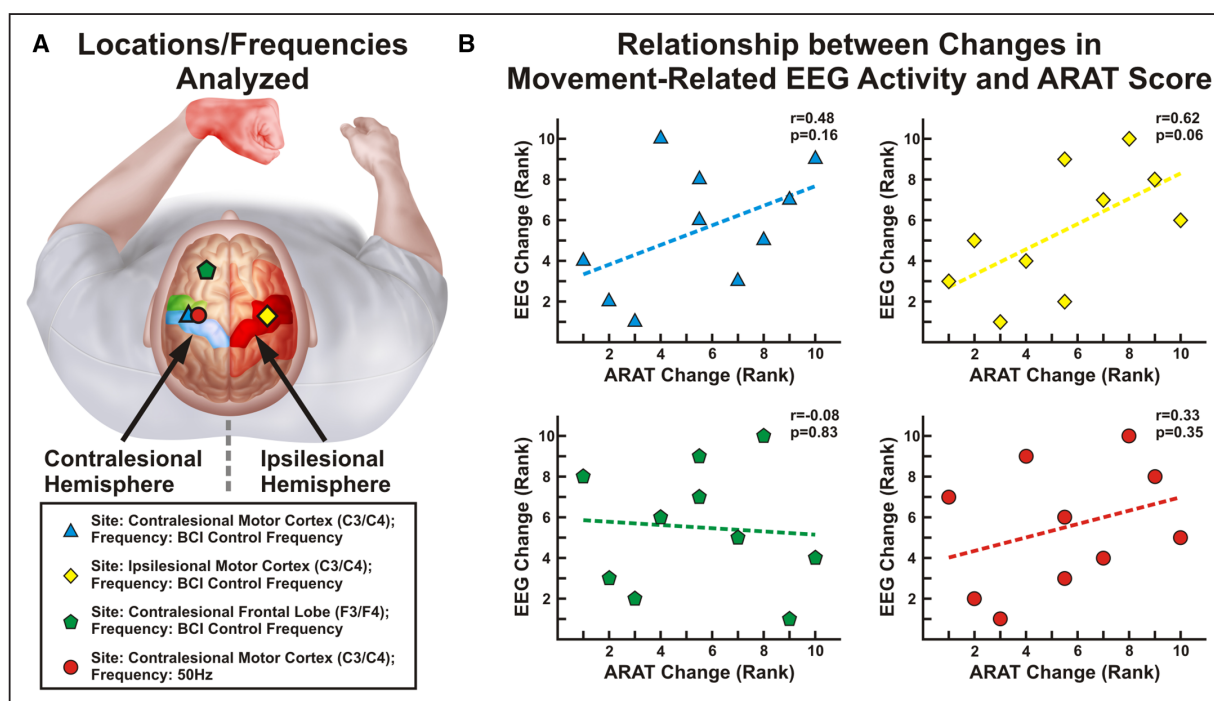


Figure 5. Relationship between changes in electroencephalographic (EEG) activity and Action Research Arm Test (ARAT) improvements. Ranked changes in motor function (ARAT) and changes in EEG activations (r^2 value) per brain-computer interface (BCI) run are shown. **A**, Analyses were performed using EEG activity at the site and frequency used for BCI control, at the frequency used for BCI control but an electrode in the contralateral hemisphere, at the frequency used for BCI control but an electrode in the frontal lobe (F3; serving as a spatial control), and at the site used for BCI control but at 50 Hz (serving as a spectral control). **B**, There was a positive relationship that trended toward significance at both the BCI control feature (**top left**) and in the contralateral motor cortex (**top right**) but not at a location outside the motor cortex (**bottom left**) or a task-irrelevant frequency (**bottom right**).

score changes and the change in the EEG modulation per run of the BCI task at the location and frequency used for BCI control and in a site in the contralateral motor cortex (BCI control feature: Spearman $r=0.48$, $P=0.16$, contralateral motor cortex: Spearman $r=0.62$, $P=0.06$).

Discussion

This study provides evidence for the potential role of the unaffected hemisphere in rehabilitation via a BCI-controlled exoskeleton. Specifically, patients had an average ARAT improvement surpassing the minimal clinically important difference.²³ In addition, improvements were observed in some, but not all, objective secondary measures of function. Although pinch strength, AROM, and the ARAT pinch subcomponent did not change, these measures are less sensitive in more severely impaired patients and were likely affected by a qualitative increase in spasticity observed, particularly in patients who had received botox 90 to 120 days before study onset. Furthermore, the grasp and grip ARAT subcomponents and grip strength, which all involve distal hand function, significantly improved. It is uncertain whether observed improvements in general distal hand function that did not localize to pinch were because of the poor spatial specificity of EEG or the sensitivity of pinch-specific subcomponents. Finally, we also observed statistically significant increases in a self-scored subjective measure of each patient's use of their affected arm in functional tasks (Canadian Occupational

Performance Measure). These findings build on previous evidence that BCI-controlled rehabilitation systems can facilitate motor recovery.⁴⁻⁸ There are several features that distinguish this work from previous studies. First, this study was the first to focus exclusively on using the unaffected hemisphere in a BCI rehabilitation system. Second, the BCI drove the velocity of the exoskeleton, providing a closer temporal pairing between brain activity and proprioceptive feedback than previous systems.^{4,6}

The choice of a BCI control signal for poststroke motor rehabilitation requires careful consideration, particularly given the conflicting evidence on the unaffected hemisphere after stroke.^{12-15,24-28} By pairing cortical activations with peripheral feedback, we hypothesized that we would induce plasticity in the remaining (ipsilateral) central nervous system pathways. As noted, there was a significant relationship between the change in ARAT scores and the rate of change in BCI control accuracy that could not be explained by the volume of device use. Further, there was a trend toward a significant relationship between the rate of change in EEG activity and ARAT score specific to the bilateral motor system, but not in the frontal lobe or at task-irrelevant frequencies. Therefore, although what can be asserted from a mechanistic standpoint is somewhat limited, the results indicate that the choice of a BCI control feature in the unaffected hemisphere may have played an important role in the benefits of the intervention.

There are many potential explanations that could account for the functional improvements observed. Specifically, although postrecovery increases in activity have been found in both the affected and unaffected hemispheres,^{16,24,26,29} the reorganization of interhemispheric connectivity between the contralesional and ipsilesional motor cortices may also play a role in functional recovery.^{17,28} Further studies designed to better define the mechanism of action will be beneficial to better understand the characteristics of patients who will benefit optimally from BCIs controlled from the unaffected hemisphere. Because the integrity of the ipsilesional corticospinal tract is strongly correlated with motor recovery,¹⁷ we would hypothesize that the corticospinal tract integrity is essential in determining what role the contralesional hemisphere will play in recovery. Specifically, in patients with the greatest corticospinal tract damage, we would expect recovery to require an alternative pathway, such as fibers descending ipsilateral to the contralesional motor cortex.

This study was also unique in that the system was used in the home setting without daily oversight. Traditional BCI systems for rehabilitation have been used in a laboratory setting with trained experts operating them.^{4–8} The ability to provide therapy in a patient's home without constant supervision would likely reduce the cost of therapy, increase the time of therapy, and give patients flexibility in scheduling therapy. For this approach to achieve large-scale implementation, several practical aspects will need to be addressed, including building the system in a cost-effective fashion, optimizing the orthosis and EEG headset design for enhanced user experience and compliance, and integrating the hardware and software to enable seamless remote maintenance and minimize the need for EEG quality checks.

There are also several limitations to note. Because of the home-based setting, it was impossible to ensure that data were free from artifacts. Although the majority of patients had good-quality EEG recordings in the majority of sessions, a few patients met this standard in <50% of sessions. In addition, because the study sample is small in size and was restricted to those with enough motivation to complete the study protocol, the scope and generalizability of the results is uncertain. Also, pinch strength, all Motricity Index subcomponents, ARAT pinch and gross subcomponents, and AROM did not improve. Whether this was because of the poorer sensitivity of these subcomponents combined with the small sample size, the poor spatial resolution of the EEG signals used, or a limitation of the therapy is uncertain. Finally, the study was uncontrolled. Previous work has shown ARAT improvements can be achieved in chronic stroke patients after interventions such as constraint-induced movement therapy or standard physical therapy,³⁰ but patients in these studies began with a much higher baseline ARAT score than the current cohort. Also of note, while shorter in duration (2 weeks), a randomized controlled trial of a BCI-controlled hand orthosis in patients with a similar baseline motor function showed no improvement in a control group receiving a sham therapy.⁶ Taken together, there remains an open question of whether more severely affected chronic stroke patients benefit from a BCI intervention exclusively versus prolonged physical therapy; a question that will ultimately be answered with a randomized clinical trial. However, this work provides important early evidence

that training with a BCI-driven orthosis can be implemented in the home environment and is associated with a meaningful functional improvement.

Conclusions

This feasibility study shows a statistically significant and clinically meaningful improvement in the motor function of chronic stroke survivors after using a home-based BCI-controlled exoskeleton. The use of control features in the contralesional hemisphere shows evidence of the potential relevance of the unaffected hemisphere for functional rehabilitation. Collectively, although this study represents an important step toward developing and translating BCI-driven rehabilitation protocols for chronic stroke survivors, the effectiveness of BCI-driven therapies must be proven in large randomized controlled trials before full acceptance.

Sources of Funding

This study was funded by Neuroolutions, Inc.

Disclosures

Dr Bundy, Dr Schalk, R. Coker, Dr Moran, and Dr Leuthardt own stock in Neuroolutions, Inc. Study data were reviewed by an unaffiliated neurologist before submission as part of a comprehensive conflict of interest management plan. The other authors report no conflicts.

References

1. Wolf SL, Thompson PA, Winstein CJ, Miller JP, Blanton SR, Nichols-Larsen DS, et al. The EXCITE stroke trial: comparing early and delayed constraint-induced movement therapy. *Stroke*. 2010;41:2309–2315. doi: 10.1161/STROKEAHA.110.588723.
2. Volpe BT, Krebs HI, Hogan N, Edelstein OTR L, Diels C, Aisen M. A novel approach to stroke rehabilitation: robot-aided sensorimotor stimulation. *Neurology*. 2000;54:1938–1944.
3. Soekadar SR, Silvoni S, Cohen LG, Birbaumer N. Brain-machine interfaces in stroke neurorehabilitation. In: Kansaku K, Cohen LG, Birbaumer N, eds. *Clinical Systems Neuroscience*. Tokyo, Japan: Springer; 2015:3–14.
4. Ang KK, Chua KS, Phua KS, Wang C, Chin ZY, Kuah CW, et al. A randomized controlled trial of EEG-based motor imagery brain-computer interface robotic rehabilitation for stroke. *Clin EEG Neurosci*. 2015;46:310–320. doi: 10.1177/1550059414522229.
5. Ono T, Tomita Y, Inose M, Ota T, Kimura A, Liu M, et al. Multimodal sensory feedback associated with motor attempts alters BOLD responses to paralyzed hand movement in chronic stroke patients. *Brain Topogr*. 2015;28:340–351. doi: 10.1007/s10548-014-0382-6.
6. Ramos-Murguialday A, Broetz D, Rea M, Laer L, Yilmaz O, Brasil FL, et al. Brain-machine interface in chronic stroke rehabilitation: a controlled study. *Ann Neurol*. 2013;74:100–108. doi: 10.1002/ana.23879.
7. Varkuti B, Guan C, Pan Y, Phua KS, Ang KK, Kuah CW, et al. Resting state changes in functional connectivity correlate with movement recovery for BCI and robot-assisted upper-extremity training after stroke. *Neurorehabil Neural Repair*. 2013;27:53–62. doi: 10.1177/1545968312445910.
8. Young BM, Nigogosyan Z, Remsik A, Walton LM, Song J, Nair VA, et al. Changes in functional connectivity correlate with behavioral gains in stroke patients after therapy using a brain-computer interface device. *Front Neuroeng*. 2014;7:25. doi: 10.3389/fneng.2014.00025.
9. Buch ER, Modir Shanechi A, Fourkas AD, Weber C, Birbaumer N, Cohen LG. Parietofrontal integrity determines neural modulation associated with grasping imagery after stroke. *Brain*. 2012;135(pt 2):596–614. doi: 10.1093/brain/awr331.
10. Kawashima R, Roland PE, O'Sullivan BT. Activity in the human primary motor cortex related to ipsilateral hand movements. *Brain Res*. 1994;663:251–256.
11. Wisneski KJ, Anderson N, Schalk G, Smyth M, Moran D, Leuthardt EC. Unique cortical physiology associated with ipsilateral hand movements

- and neuroprosthetic implications. *Stroke*. 2008;39:3351–3359. doi: 10.1161/STROKEAHA.108.518175.
12. Ward NS, Brown MM, Thompson AJ, Frackowiak RS. Neural correlates of motor recovery after stroke: a longitudinal fMRI study. *Brain*. 2003;126(pt 11):2476–2496. doi: 10.1093/brain/awg245.
 13. Ward NS, Brown MM, Thompson AJ, Frackowiak RS. Neural correlates of outcome after stroke: a cross-sectional fMRI study. *Brain*. 2003;126(pt 6):1430–1448.
 14. Cramer SC, Nelles G, Benson RR, Kaplan JD, Parker RA, Kwong KK, et al. A functional MRI study of subjects recovered from hemiparetic stroke. *Stroke*. 1997;28:2518–2527.
 15. Weiller C, Ramsay SC, Wise RJ, Friston KJ, Frackowiak RS. Individual patterns of functional reorganization in the human cerebral cortex after capsular infarction. *Ann Neurol*. 1993;33:181–189. doi: 10.1002/ana.410330208.
 16. Tecchio F, Zappasodi F, Tombini M, Oliviero A, Pasqualetti P, Vernieri F, et al. Brain plasticity in recovery from stroke: an MEG assessment. *Neuroimage*. 2006;32:1326–1334. doi: 10.1016/j.neuroimage.2006.05.004.
 17. Carter AR, Patel KR, Astafiev SV, Snyder AZ, Rengachary J, Strube MJ, et al. Upstream dysfunction of somatomotor functional connectivity after corticospinal damage in stroke. *Neurorehabil Neural Repair*. 2012;26:7–19. doi: 10.1177/1545968311411054.
 18. Bundy DT, Wronkiewicz M, Sharma M, Moran DW, Corbetta M, Leuthardt EC. Using ipsilateral motor signals in the unaffected cerebral hemisphere as a signal platform for brain-computer interfaces in hemiplegic stroke survivors. *J Neural Eng*. 2012;9:036011. doi: 10.1088/1741-2560/9/3/036011.
 19. Duncan PW, Goldstein LB, Matchar D, Divine GW, Feussner J. Measurement of motor recovery after stroke. Outcome assessment and sample size requirements. *Stroke*. 1992;23:1084–1089.
 20. Yozbatiran N, Der-Yeghiaian L, Cramer SC. A standardized approach to performing the action research arm test. *Neurorehabil Neural Repair*. 2008;22:78–90. doi: 10.1177/1545968307305353.
 21. Bodiam C. The use of the Canadian Occupational Performance Measure for the assessment of outcome on a neurorehabilitation unit. *Br J Occup Ther*. 1999;62:123–126.
 22. Pfurtscheller G, Lopes da Silva FH. Event-related EEG/MEG synchronization and desynchronization: basic principles. *Clin Neurophysiol*. 1999;110:1842–1857.
 23. van der Lee JH, Beckerman H, Lankhorst GJ, Bouter LM. The responsiveness of the Action Research Arm test and the Fugl-Meyer Assessment scale in chronic stroke patients. *J Rehabil Med*. 2001;33:110–113.
 24. Green JB, Bialy Y, Sora E, Ricamato A. High-resolution EEG in post-stroke hemiparesis can identify ipsilateral generators during motor tasks. *Stroke*. 1999;30:2659–2665.
 25. Johansen-Berg H, Rushworth MF, Bogdanovic MD, Kischka U, Wimalaratna S, Matthews PM. The role of ipsilateral premotor cortex in hand movement after stroke. *Proc Natl Acad Sci USA*. 2002;99:14518–14523. doi: 10.1073/pnas.222536799.
 26. Levy CE, Nichols DS, Schmalbrock PM, Keller P, Chakeres DW. Functional MRI evidence of cortical reorganization in upper-limb stroke hemiplegia treated with constraint-induced movement therapy. *Am J Phys Med Rehabil*. 2001;80:4–12.
 27. Lotze M, Markert J, Sauseng P, Hoppe J, Plewnia C, Gerloff C. The role of multiple contralesional motor areas for complex hand movements after internal capsular lesion. *J Neurosci*. 2006;26:6096–6102. doi: 10.1523/JNEUROSCI.4564-05.2006.
 28. Murase N, Duque J, Mazzocchio R, Cohen LG. Influence of interhemispheric interactions on motor function in chronic stroke. *Ann Neurol*. 2004;55:400–409. doi: 10.1002/ana.10848.
 29. Rossiter HE, Eaves C, Davis E, Boudrias MH, Park CH, Farmer S, et al. Changes in the location of cortico-muscular coherence following stroke. *Neuroimage Clin*. 2012;2:50–55. doi: 10.1016/j.nicl.2012.11.002.
 30. Page SJ, Sisto S, Levine P, McGrath RE. Efficacy of modified constraint-induced movement therapy in chronic stroke: a single-blinded randomized controlled trial. *Arch Phys Med Rehabil*. 2004;85:14–18.